UNIVERSITÀ DI PISA

Dipartimento di Farmacia

Corso di Laurea Specialistica in Chimica e Tecnologia Farmaceutiche

Tesi di Laurea

Design, Synthesis, X-ray analysis and preliminary Biological evaluation of Powerful Dual inhibitors for MMP homodimerization

Relatori: *Prof. Armando Rossello*

Dott.ssa Elisa Nuti

Dott. Enrico A. Stura

Candidata: *Claudia Antoni*

Settore Scientifico Disciplinare: **CHIM/08**

ANNO ACCADEMICO 2012 – 2013

Secretazione dell'elaborato scritto della Tesi di Laurea

"Il contenuto di questa Tesi di Laurea è strettamente riservato, essendo presenti argomenti tutelati dalla legge come segreti. Pertanto tutti coloro che ne prendono conoscenza sono soggetti all'obbligo, sanzionato anche penalmente dagli articoli 325 e 623 del codice penale, di non divulgare e di non utilizzare le informazioni acquisite." *

Clause Secret

The contents of this report is strictly confidential, as arguments protected by law as confidential. Therefore all those who take knowledge are required, even sanctioned fees to Articles 325 and 623 of the Criminal Code, and not to disclose not use the information gained.
(These terms are in accordance with regulations of the University of Pisa in relation to the protection of intellectual property patents.)

Identificazione per presa visione *

Nome	Cognome	Estremi Documento	note

To Mum and Dad,
who have always believed in me,
To my Sister,
for her comprehension and affection,
To Stefano,
with whom I began and finished my University studies,
for his love and his encouragement.

To my Teachers,
for their dedication in their teachings.

Summary

Chapter IV

SYNTHETIC INHIBITORS OF MMPs

Chapter V

INTRODUCTION TO THE EXPERIMENTAL PART

Chapter VI

EXPERIMENTAL PROCEDURES

Abstract

In humans, the family of matrix metalloproteinases (MMPs) is composed by 24 closely related proteins that share a catalytic zinc ion, responsible for their catalytic activity and a typical metzincin fold. Their ability to cleave the extracellular matrix allows them to remodel the extracellular space, and change connections from cell to cell through the release of ligands present on the cell surface. These changes affect cellular signalization, leading to cellular phenotype modification, extending the role of MMPs far beyond that of mere enzymes. The alteration of MMPs expression is related to the manifestation of a series of severe diseases such as autoimmune pathologies, cancer, myocardial infarction, rheumatoid arthritis, Alzheimer's disease. Moreover, MMPs are involved in the control of physiological processes such as ovulation, wound healing and growth. For these reasons, it is important that their activity at both the transcriptional and post-transcriptional level is finely regulated. The regulatory mechanisms are at several different levels: i) induction or inhibition of the transcription process, mediated by cytokines, hormones, growth factors, and factors which promote tumor growth. ii) regulation and endocytosis of the propeptide. iii) activation of the zymogen by the suitable protease. iv) inhibition by physiological mediators, such as α2-macroglobulin and TIMPs (tissue inhibitors of MMPs). For this reason, in recent years the pharmaceutical research has dedicated many efforts to the discovery of zinc-protease inhibitors. In particular, the subject of this thesis has been the study of a way of signalization which involves MMPs: the homodimerization process. In order to obtain structural information useful for the design of molecules able to control the signalization pathways, the involved proteins should be crystallized in complex with ligands that induce dimerization. Bi-functional drugs have been generated by linking two ligands together chemically and the relative crystallizability[1] of complexes with mono-functional and bi-functional ligands have been evaluated. At the very beginning, crystallographic studies of some ligands previously synthesized in Prof. Rossello's laboratory (EN238, LC20 and LC29) have been conducted using MMP-12 and MMP-9 as model proteins. These compounds were characterized by carboxylate or hydroxamate as zinc binding group (ZBG) and by the presence or absence of a linker (**Fig.1**).

[1] Antoni, C .; *et al.* Crystallization of bi-functional ligand protein complexes. *J. Struct. Biol.* **2013**, *182*, 246-254.

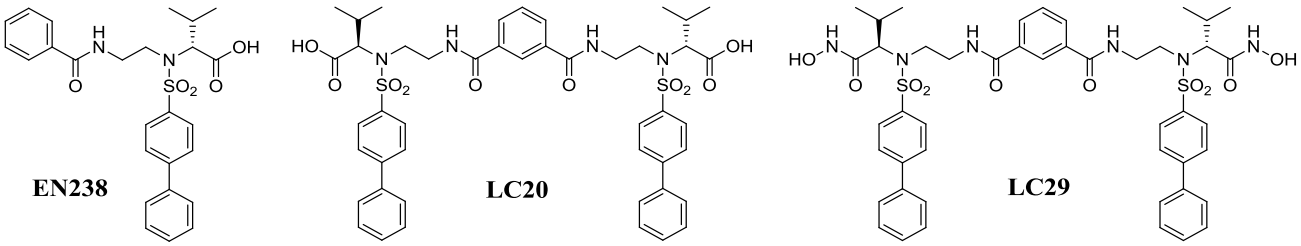

Figure 1. *Chemical structure of compounds used for crystallographic studies.*

These analyses have allowed to verify the formation of homodimeric structures when bi-functional ligands were used (LC20 and LC29) with both MMP-12 and MMP-9. Moreover, the formation of a different homodimer was obtained when two molecules of the mono-ligand EN238 were crystallized with MMP-12. On the basis of these first results during my thesis I carried out:

- The design and synthesis of a new dual carboxylate inhibitor (SA001, **Fig. 2**) that would enable the formation of a precise homodimer of MMP-12 (previously obtained in the presence of two molecules of EN238 with two MMP -12)**.**
- The synthesis of the hydroxamate analogue of EN238 (LR32, **Fig. 2**).
- The synthesis of two additional dual inhibitors with a short ureidic linker, bearing a carboxylic acid (CA11) and a hydroxamate (CA14) as ZBG (**Fig. 2**).

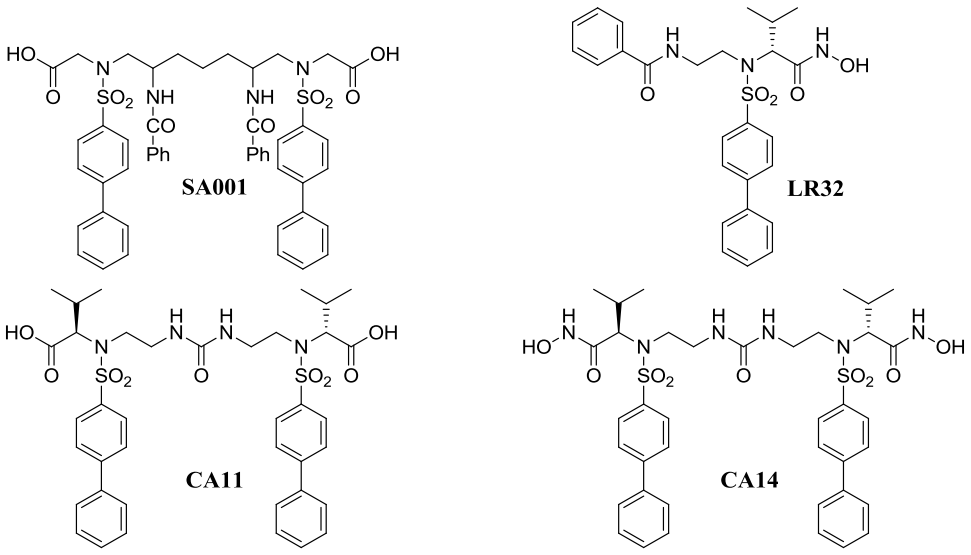

Figure 2. *Chemical structure of the newly synthesized compounds.*

All the new inhibitors were tested in vitro on human recombinant MMPs (MMP-1; MMP-2, MMP-8, MMP-9, MMP-12, MMP-13, MMP-14) by fluorometric assay. Results are

reported in Table 1, together with those obtained for the previously described analogues (EN238, LC20 and LC29). All compounds showed a nanomolar activity against MMP-9 and MMP-12 with the carboxylate dual inhibitors (CA11 and LC20) being more selective over the other tested MMPs with respect to their hydroxamate analogues.

Table 1. *In vitro* activity (IC_{50}, nM) on MMPs.

Compd	MMP9	MMP12	MMP1	MMP2	MMP8	MMP13	MMP14
EN238	508	35	16000	170	115	152	1830
LR32	2.5	1.5	13	0.16	2.0	0.24	23
LC20	26	1.3	11800	63	89	35	2200
LC29	5.5	7.1	280	10	8.9	8.2	250
CA11	175	4.6	8300	145	134	200	1700
CA14	26	15	3100	42	15	9	4900

The preliminary crystallographic analysis conducted with CA11 on MMP-9 and on MMP-12, showed the formation of dimers which, in both cases, appear to be different from those formed with LC20. Moreover, CA14 has been crystallized with MMP-8, providing a not previously observed dimer.

Aims of the thesis

This work aims to investigate the role of the linker when used to join two different or identical chemical entities in a biological context. The chemical structure of the linker has been given little importance and the possible interaction that it makes with proteins overlooked. The difficulty in going beyond the consideration of length and branch point is given by the difficulty in obtaining structural information. In this work we have been able to overcome these difficulties and by employing crystallization and X-ray structure determination to understand how linker length and branch point influences the inhibition of MMPs, our model enzyme system. The results presented here can be used to pursue a more detailed structure-guided spacer design.

Preface

In the first chapter the development of selective inhibitors of Matrix Metalloproteinases (MMPs) is summarized. The presence of a zinc atom in the catalytic domain of MMPs has been exploited to design inhibitors. The first MMP inhibitors relied on recognized peptide sequences with the addition of a zinc-binding chemical function. Most MMPs inhibitors have been designed with a hydroxamic acid, a strong zinc-binding moiety when negatively charged. Non-peptidic, non-hydroxamate based inhibitors with improved inhibitor selectivity profile followed.

Chapter two reviews the use of linkers in biology. They are used to join two functionalities to create probes, contrast agents for medical purposes or to add tags for affinity purification. In the third chapter the experimental work carried out in preparation for the linker study is reported. The methodology to obtain crystals of complexes between an inhibitor and a MMPs is detailed and the results obtained reported. The work looks at the use of linkers to produce MMP homodimers based on the work with twin hydroxamic acids. The fourth chapter describes the chemical synthesis of a bi-functional inhibitor.

Chapter I
THE METALLOPROTEINASIS

1.1 *Introduction.*

In the body, the main role of connective tissue is to support other tissues by means of a complex organization of cells, fibrils and extracellular matrix (ECM). It participates dynamically to maintain the functionality of tissues (blood and lymph) through the degradation of connective tissue and is often at the base of diseases of various kinds. The remodeling and turnover of connective tissue is regulated by some endoproteases that operate by identifying and hydrolyzing peptide bonds. These proteases are classified as:

- aspartate proteases,
- cysteine proteases,
- serine proteases,
- threonine proteases
- and metalloproteases.

The system of matrix regulation as a functional unit consists of the capillary bed, connective tissue cells and autonomic nerve endings. It supports and maintains the structure of cells under physical load and during locomotion. The extracellular fluid can be reckoned as common area of the three elements listed above. The ECM is also essential for morphogenesis and regenerative capacity. This fluid pervades the entire organism, connects the lymphatic organs and is the defining feature of connective tissue in animals. The ECM includes the interstitial matrix localized in the intercellular space where gels of polysaccharides and fibrous proteins create a system able to sustain the cell structure under physical load. It is composed by basement membranes that represent a subtle deposition of EMC on top of which the epithelial cells rest (**Fig.3**).

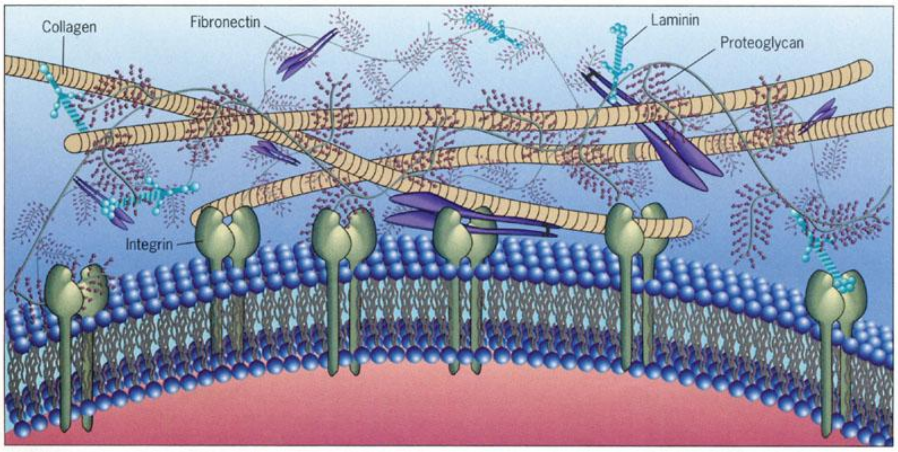

Figure 3. *Representation of ECM*[2].

This control system regulates the nutrition of the cells (inner circulation) and is responsible for the elimination of waste products. It is involved in inflammatory and immune processes fundamental for all basic vital processes [1]. Domains of ECM proteins are widely altered by different chemical modifications, such as proline hydroxylation to hydroxyproline which is necessary for cells, proteolytic removal of the N-terminal and C-terminal domains of interstitial collagens, required on membrane cell [2].

The principal components of ECM are: collagen, non-collagen proteins and proteoglycans. Collagens are a super-family of fibrous proteins that contribute to the structural integrity of the cell. They represent 25% of all proteins. Composed by three polypeptide chains with a repetitive sequence, the typical structure of collagens is a triple helix. The molecular aggregation of collagens with glycoproteins of matrix and proteoglycans leads to a supramolecular structure that provides the three-dimensional scaffold from which the extracellular matrix is built.

Among the non-collagen glycoproteins we find laminins, tenascin, thrombospondin, vitronectin, elastin. These proteins fold into specific domains that bond together cells, matrix glycoproteins, proteoglycans, growth factors, proteases and their inhibitors. The increase of one type of non-collagen glycoprotein can influence the activity of other.

Proteoglycans: These form a complex family; each member is composed of an amino acid core and various polysaccharide chains. These multi-functional proteins are capable of promoting or inhibiting growth factors, with adhesive and anti-adhesive properties, to

[2] Image available at:
http://cc.scu.edu.cn/G2S/Template/View.aspx?courseType=1&courseId=17&topMenuId=113299& action menuType =1& =view&type=&name=&linkpageID=113468.

promote angiogenic processes, control storage, release growth factors and condition cellular differentiation. Proteoglycans are divided into two groups: leucine-rich proteoglycans and modular proteoglycans. The first type are formed by an alternation of hydrophilic and hydrophobic amino acids. Modular proteoglycans are glycosilated proteins composed of domains homologous to proteins involved in cell growth, lipid metabolism or in adhesion processes such as immunoglobulins and protease inhibitors [18].

Tissue remodeling is a complex multi-phase process implicated in pathologic reactions and required for physiologic activities. The control of proteolytic activity is extremely important for the maintenance of homeostasis. ECM is degraded by several enzymes, metalloproteinases, serine-proteases, cysteine-proteases and aspartate-proteinases. High turnover and displacement of ECM due to an excessive activity of MMPs leads to an intensive degradation of collagen and other ECM components. This unbalancing is the cause of inception of several pathology such as tumor invasion and metastasis. [19-20].

1.2 *Metalloproteinases (MMPs).*

MMPs were chosen as model system to to study whether protein homodimerization using synthetic twin inhibitors can be used to increase inhibitor selectivity. MMPs were first discovered during a study of tissue remodeling during tadpole metamorphosis. The study detected the proteolytic activities of MMP-1 (an interstitial collagenase) on collagen, a major representative component of the extra cellular matrix (ECM). MMP-1 is able to cleave the collagen native triple helix composed of three polypeptide chains. The triple helical structure makes collagen particularly resistant to most other proteases. MMP-1 can induce a conformational change in the collagen leading to triple helix opening so that one of the three chains positions itself in the active site of MMP-1 [14]. The collagen unwinding ability requires the full form of the enzyme because the catalytic domain alone is unable to degrade full-length collagen.

MMP-1 is composed by three essential parts: the pro-domain, the catalytic domain and the C-terminal hemopexin domain. The pro-domain, located at N-terminus, is needed to ensure cellular release. The association between catalytic and hemopexin domains is required for collagen degradation. The hemopexin domain is believed to play a role in the local unfolding of collagen triple helix [15]. Metalloproteinases are enzymes that contain a metal ion cofactor responsible for their catalytic activity. Matrix Metalloproteinases (MMPs) are zinc endopeptidases. These proteolytic peptidases are capable of breaking amino acid

stretches within a protein sequence but may also act as signalization molecules. Their ability to cleave the ECM allows them to remodel the extracellular space, and change connections from cell to cell and those between cells and the ECM. These changes affect cellular signalization, leading to cellular phenotype modification, extending the role of MMPs beyond that of mere enzymes. The metal ion is typically coordinated by three amino acids. In MMPs three histidines coordinate a zinc ion while in other metalloproteinases other metals and other amino acids such as Glu, Asp, or Lys may be present. When the pro-peptide is removed, the fourth coordination bond provided by the thiol group is assured by a water molecule.

1.2.1 *Regulation of MMPs.*

MMPs are secreted and expressed by cells as inactive pro-enzymes: some MMP can be directly activated by furine. Since the active site in the pro-peptide form is filled and any access to substrates is denied, MMP activation requires cleavage of the pro-peptide. Many proteases can cleave the pro-peptide of MMPs, these enzymes belong to the serine proteinase family (plasmin) or the MMP proteinase family. The pro-peptide is 80 residues long with a highly conserved sequence in most MMPs. In this domain is located a Cys that ligates the zinc ion to maintain the latent form of pro-enzyme. In particular, the sulfur atom of Cys interacts with the zinc atom present in the active site of MMPs. This interaction maintains the connection between the pro-peptide and the catalytic domain and prevents MMP activation. A chemical modification of the Cys sulfur atom destabilizes the pro-enzyme leading to auto-activation by proteolysis.

The catalytic domain is about 170 amino acids residue long, folds into five-stranded beta-sheets, three α-helices, and several bridging loops. This domain shows a zinc binding motif and one Met residue that forms a “Met-turn” structure. This particular conformation is similar to that of other members of matrixins, such as astacins, serralysins. The C-terminal hemopexin-like domain is about 210 amino acids, has an ellipsoidal disk shape and is necessary for enhanced collagenase activity [5]

MMPs are zinc and calcium dependent enzymes and these ions are required both for the stability and for enzymatic activity. They are able to degrade various extracellular matrix components in embryo development and growth, processes that requires several bioactive molecules and extensive tissue remodeling. Furthermore they play role in the cleavage of the cell surface receptors, release of apoptotic factors, activation or inactivation of

chemokines and cytokines. MMPs also can affect cell behaviors such as cell proliferation, migration, angiogenesis, apoptosis, differentiation, and host defense. MMPs are implicated in many physiological and pathological processes mainly associated with inflammatory reactions, in blastocyst implantation, ovulation, cervical dilatation, postpartum uterine involution, endometrial cycling and hair follicle cycling. MMPs role is complicated to define because they have a large spectrum of possible physiologic substrates.

MMPs act primarily on the cell surface or in the extracellular space and their activity is regulated by zymogen activation and their inhibition is operated by endogenous inhibitors such as α2-macroglobulin and Tissue Inhibitors of Metalloproteinases (TIMPs). The α2-macroglobulin has action in the fluid phase, whereas TIMPs are the inhibitors in tissue. The α2-macroglobulin is an endogenous glycoprotein of 725 kDa consisting of four identical subunits bound together by -SS-bonds [29].

TIMPs have high affinity to MMPs and they form a 1 to 1 complex with them. The molecular model of TIMP inhibition of MMPs was not understood until the first crystallographic structure of a MMP-TIMP complex was solved [16]. This structure showed that the contact between inhibitor and enzyme was located on N-terminal sequence of TIMP where two Cys are involved in two -S-S -bonds (Cys-X-Cys). The cysteine sulfur atom does not interact with the zinc atom of the enzyme active site in contrast to that from pro-peptide. The interaction is made by amine of N-terminal domain and with the carbonyl group of the first Cys.

TIMPs are composed of a C-terminal domain, an N-terminal domain, 6 loops and 12 Cys residues involved in 6 intramolecular -S-S-bonds. The N terminal domain docks in the MMP catalytic site where the carbonyl of Cys is able to chelate the catalytic zinc ion replacing the water molecule. The C-terminal domain preferentially binds to pro-MMP. It is known that TIMPs are able to promote the activation of some metalloproteinases trough the formation of tri-molecular complexes: such as pro-MMP-2, TIMP-2, MT-1-MMP. The N-terminal domain of TIMP-2 binds the active form of MT-1-MMP inhibiting it while its C-terminal domain binds the hemopexin domain of pro-MMP-2. The active form of MT-1-MMP can process the trimolecular complex by removing the pro-peptide sequence of pro-MMP-2 which is then fully activated by a second MMP-2. So, low to moderate levels of TIMP-2 promote the activation of MMP-2, whereas higher levels inhibit its activation because no free MT-MMP is available to remove the MMP-2 prodomain (**Fig.4**) [31].

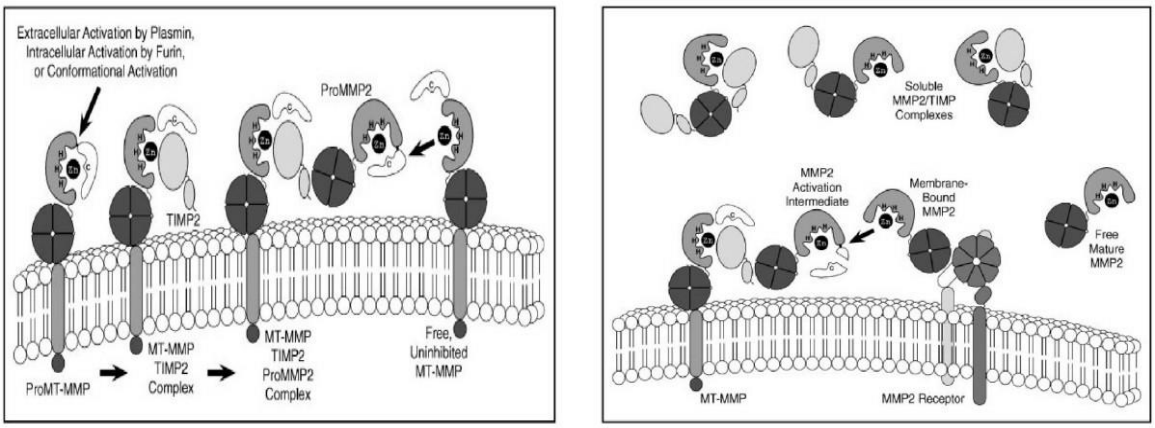

Figure 4. *Cell surface activation of MMP2. A ProMT-MMP is activated during transport to the cell surface by an intracellular furin-like serine proteinase, at the cell surface by plasmin or by non-proteolytic conformational changes. The activated MT-MMP is then inhibited by TIMP2 and the hemopexin domain of ProMMP2 binds to the C-terminal portion of TIMP2 to form a trimolecular complex. An uninhibited MT-MMP then partially activates the ProMMP2 by removing most of the MMP2 propeptide. The remaining portion of the propeptide is removed by a separate MMP2 molecule at the cell surface to yield fully active mature MMP2. Mature MMP2 can then be released from the cell surface or bound by another cell surface MMP2- docking protein. It can also be inhibited by another TIMP molecule or left in an uninhibited active state depending on local MMP: TIMP molar ratios*[3] *[31].*

TIMPs have additional functions, including promotion of cell growth, matrix binding, angiogenesis inhibition and induction of apoptosis. Certain MMPs activities are regulated at the transcription level, this includes activation of precursor zymogens, their interaction with specific ECM and inhibition by endogenous inhibitors.

[3] Image available at M. D. Sternlicht, Z. Werb, *"How matrix metalloproteinases regulate cell behavior", Annu Rev Cell Dev Biol*. 2009.

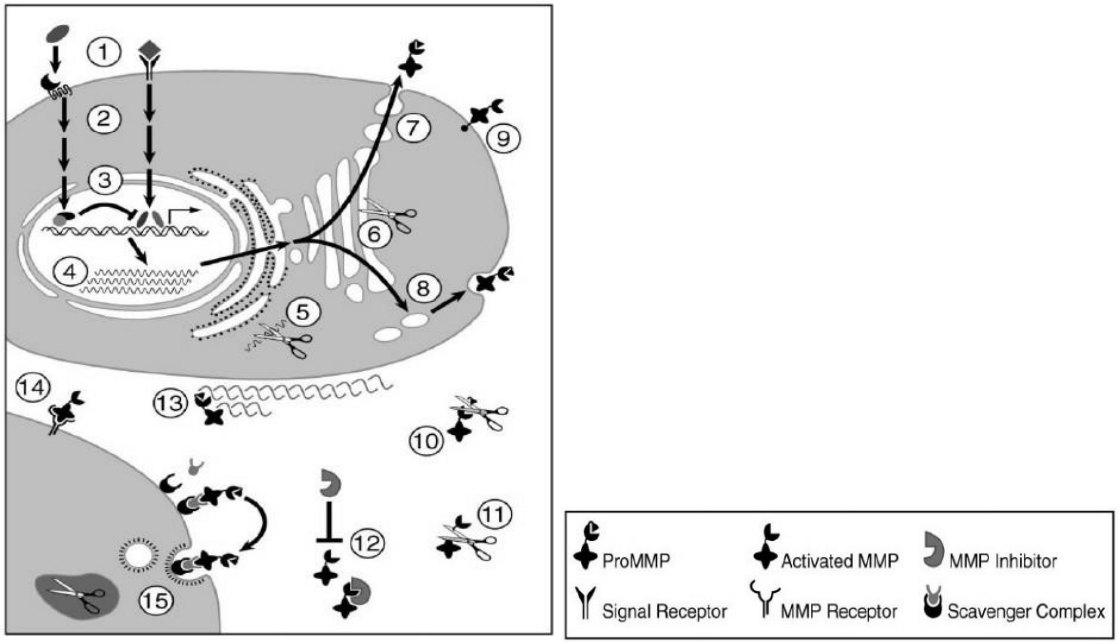

Figure 5. *Regulation of MMPs. MMP regulatory mechanisms include inductive and suppressive signaling (1), intracellular signal transduction (2), transcriptional activation and repression (3), post-transcriptional mRNA processing (4), mRNA degradation (5), intracellular activation of furin-susceptible MMPs (6), constitutive secretion (7), regulated secretion (8), cell surface expression (9), proteolytic activation (10), proteolytic processing and inactivation (11), protein inhibition (12), ECM localization (13), cell surface localization (14), and endocytosis and intracellular degradation (15)*[4].

The first step in MMPs regulation is at the transcription level. Many genes of MMPs are inducible by effectors such as growth factors, physical stress, cytokines and oncogenic cellular transformation. There are also suppressive agents such as growth factor beta, glucocorticoids (**Fig.5**) [5]. The second regulatory step involves post-translational modifications: most of MMPs are released as inactive zymogens and their activation is under control of several effector molecules.

MMPs were identified because of their involvement in homeostasis and turnover of the extracellular matrix (ECM), later they were found to act also on cytokines, chemokines and protein mediators to regulate various aspects of immunity and inflammation. Degradation products of matrix proteins involved in cellular behavior regulation, playing a key role in regulating extracellular matrix degradation, and MMPs are involved in numerous processes of tissue remodeling associated with cell growth and development and in various

[4] Image available at: M.D.Sternlicht, Z. Werb, *"How matrix metalloproteinases regulate cell behavior", Annu Rev Cell Dev Biol*. 2009.

pathologies.

1.2.2 *Classification and structure of MMPs.*

At the moment 24 types of MMPs have been identified in humans. Among the 23 genes in the human genome coding for these proteins, we can distinguish 17 MMPs secreted in the extracellular matrix and 7 Membrane-Type Metal Protease (MT-MMPs) anchored to the cell membrane through a trans-membrane domain and a cytoplasmic C-terminal extremity. Numerous are the homologies among the members of this family, so to allow a classification, the first discriminating factor is the type of substrate hydrolyzed. These proteases are expressed on cell surfaces (such as MT-MMPs) or are secreted by cells. MMPs are classified into six sub-groups according to their functionality; Gelatinases, Collagenases, Stromelysins, Matrilysins, Membrane-type MMPs and other MMPs. The most used MMPs classification is partly based on their cellular localization and on the historical assessment of substrate specificity.

1. *Collagenases*, namely MMP-1, MMP-8, MMP-13, and MMP-18, cleave interstitial collagens I, II, and III, and act on ECM and non-ECM molecules. Four types of collagenases were identified and only three of them are present in humans and have collagen I, II and III as substrate (this constitutes 90% of the total of collagen). Each one prefers a particular type of collagen, with Collagenase-1 (MMP-1; also called "interstitial collagenase") having greater affinity for the collagen type III, Collagenase-2 (MMP-8; also called "neutrophil collagenase") preferring type I collagen, while Collagenase-3 (MMP-13) favors collagen type II as a substrate.

2. *Gelatinases* (MMP-2 gelatinase-A, MMP-9 gelatinase-B) degrade collagen type IV, which is the constituent of basal laminae. Their role is to digest denaturated collagens and gelatins. These enzymes are different from the previous ones because of an additional domain spliced into the catalytic domain. In fact they have three repeats of a type II fibronectin domain inserted in their catalytic domain used to bind to gelatin, laminin and collagens. MMP-2 digests type I, II and III collagens, instead MMP-9 is not able to do so. Gelatinase B (MMP-9) is also capable of hydrolyzing the collagen type I, V, VII, X and XII and other proteins such as fibronectin, laminin and elastin. The collagen triple helix breaking-up mechanism involves binding collagen, followed by a triple helicase activity that liberates a

bound collagen that is then hydrolyzed. The ability to destabilize the collagen triple helix is a property shared by both collagenases and gelatinases.

3. *Stromelysins* (MMP-3 stromelysins-1, MMP-10 stromelysins-2). These two enzymes are able to cleave the ECM but are unable to cleave the triple-helical fibrillar collagens. MMP-3 has a proteolytic efficiency higher than MMP-10; stromelysins-1 is able to activate several pro-MMPs. MMP-11 is called stromelysin-3, but its sequence and substrate specificity is different from that of other stromelysins and is grouped with the "other MMPs". These do not have a helicase activity, but they degrade components of the extracellular matrix such as proteoglycans and proteins like laminin and fibronectin. While stromelysins -1 and -2 seem functionally related with similar roles and substrate preferences, the function of stromelysin-3 remains obscure. It is known that it is expressed in breast cancer, and that it is able to inactivate serine protease inhibitors (serpins). This last function, also typical of other MMPs, suggests that there may be an interplay between the enzyme cascades of serine proteases and metalloproteinases. [33]

4. *Matrilysins* (MMP-7 matrilysins-1) do not have a hemopexin domain. MMP-7, also known as PUMP-1, degrades fibronectin, laminin, some types of collagen that do not wind to form a helix and many elements of the ECM. MMP-26, is expressed in endometrium cells and operates on a large range of substrates including elastin, fibrin and fibrinogen. In contrast to other MMPs, MMP-7 is largely accumulated intracellularly.

5. *Membrane-Type* MMPs. There are four types of transmembrane proteins and the last two are glycosyl-phosphatidyl-inositol anchored proteins. They are able to activate pro-MMP-2. MT-MMPs and can also hydrolyze ECM components such as proteoglycans, gelatin, fibronectin and are involved in the front line in the Metallomatrix activation of the same proteases. They are numbered from 1 to 6, while the MMP-23 is defined CA-MMP (Cysteine Array MMP) because it has a free cysteine in the catalytic site.

6. Other MMPs are MMP-11, MMP-12, MMP19, MMP-20, MMP-22, MMP-23. Human macrophage elastase (MMP-12) is involved in the elastin destruction in the

lung alveolar wall in the pathogenesis of emphysema and is essential for macrophage migration. MMP-19 is known as RASI (Rheumatoid Arthritis Synovial Inflammation) because it was discovered in plasma of rheumatoid arthritis patients. MMP-20, identified in the enamel of the teeth, digests amelogenin. MMP-21, recently discovered in humans, has no known substrates. The function of MMP-22 is also not known. MMP-23 is mostly expressed in reproductive tissues (**Fig.6**), [3, 6, 34].

The three-dimensional structure of pro-MMP-2 was determined in 1999 by the group of K. Tryggvason showing the typical domain organization of MMPs family members, each presenting the autonomous structure and stability.

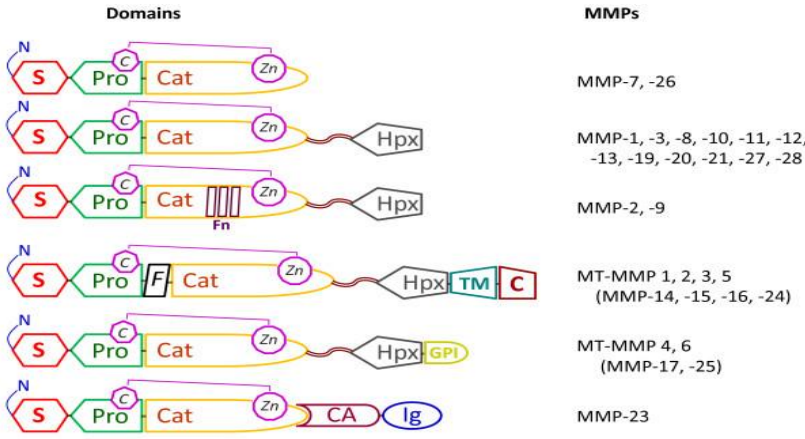

Figure 6. **Domain structures of secreted and membrane-anchored MMPs**. *The basic organizations of human MMP family members are depicted: S, signal peptide; Pro, pro-peptide; Cat, catalytic domain, containing cysteine group (C); Zn, zinc ion; Fn, fibronectin-II- like repeats; Hpx, hemopexin like domain; TM, transmembrane domain; GPI, glycol-phosphatidylinositol membrane anchor; C, cytoplasm tail; CA, cysteine array; Ig, immunoglobulin-like domain; the flexible linker or hinge region is represented by a wavy black ribbon. The domain structure includes the S, which guides the enzyme into the endoplasmic reticulum during synthesis, the Pro domain, which sustains the latency of MMPs, the Cat, which houses the* Zn^{2+} *region and is responsible for enzyme activity, the Hpx domain, which determines the substrate specificity, and a small hinge region. Additional transmembrane and intracellular domains are also present: the hinge region in MMP-9 is heavily O-glycosylated; the furin-activated MMPs and all of the membrane-anchored MMPs have a basic motif at the C-terminal end of their prodomains; the MMP-2 and -9 contain three fibronectin-II-like repeats; four of the six MT-MMPs are anchored to the cell membranes through a type I transmembrane domain and the other two through a glycosyl-phosphatidy-linositol moiety. The membrane-anchored MMP-23, has an N-terminal type II transmembrane domain. The two minimal domain MMPs and MMP-23 lack the HPX domain and, in the latter enzyme, this domain is replaced by a C-terminal cystein array (Ca) and an immunoglobulin-like (Ig) domain. MMPs are produced in a latent form and most are activated by*

extracellular proteolytic cleavage of the propeptide and finely regulated by (TIMP)[5].

The members of the MMP family share a primary structure with 40% similarity. Starting from the N-amino extremity, the structure of MMPs is composed by:

- signal peptide,
- N terminal pro-peptide,
- catalytic site,
- linker peptide,
- hemopexin domain.

MMPs are initially in form of zymogens and are accumulated inside the Golgi apparatus and then secreted outside the cell. In the cell, the hydrolysis of the signal peptide by membrane-type MMP or other proteases leads to the activation of these molecules. This hydrolysis is mediated by a "furin-like" convertase. The N-terminal pro-peptide is composed of approximately 80 amino acids and is the latency part. Its function is to fill the active site to prevent access of substrates. The peptide chain crosses the active site of MMPs from C-terminal to N-terminal, an orientation opposite compared to that for the substrate. The hydrogen bonding is stronger for pro-domain binding than that for the substrate, due to the different orientation. The cysteine has an important role because it interacts with the catalytic zinc ion *via* the thiol group. The pro-peptide sequence is highly conserved "Pro-Arg-Gly-Cys-X-Pro-Asp where X represents any amino acid". The presence of this part the MMPs characterizes the pro-MMP form [3]. When the pro-peptide is removed, the thiol group is replaced by a water molecule, which ensures the zinc fourth coordination bond. Similar structure to hemopexin proteins family, has the catalytic domain: it has indeed a spheric surface as tertiary structure, allowing protein-protein interactions. The catalytic domain contains two or three calcium and two zinc ions. One of these zinc ions is directly involved in the catalytic process, while the other and the three calcium ions are involved in stabilizing the structure.

[5] Image available at: F. Manello. What does matrix metalloproteinase-1 expression in patients with breast cancer really tell us*? BMC Medicine*, **2011**.

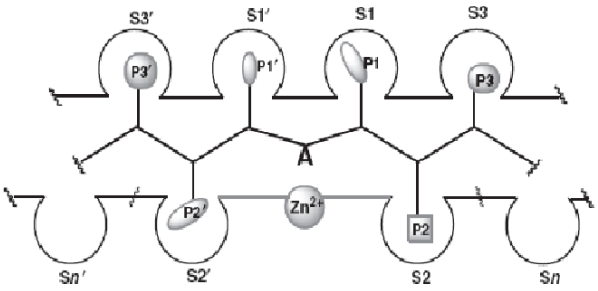

Figure 7. *Catalytic site of MMPs*[6].

The catalytic domain is composed by 170 amino acids folded into one β-sheet composed of 4 parallel and one antiparallel strands, three α-helices and connecting loops. Within the catalytic site various subsites that determine substrate specificity are present. These subsites are numbered: S1, S2, S3, Sn, S1', S2', S3', Sn' and are fitted by portions of the substrate denominated P1, P2, P3, Pn, P1', P2', P3', Pn' (**Fig.7)**. The active site of MMPs appears as a series of shallow cavities, except the S1' subsite that is able to accept six amino acid residues positioned from S3 to S3'. S1' is considered the most important subsite for MMP specificity. It is the deepest in most MMPs except in MMP-1, MMP-7 and MMP-11 where large side chains such as Arg, Tyr, Glu restrict the size of the cavity. The variability in the amino acid sequence of S1' loop, called the specificity loop is responsible for the tailoring of the cavity. This characteristic is exploited in the design of specific inhibitors for the different MMPs. However, its high flexibility makes developing selective inhibitors difficult. The pockets S2 and S3 are similar in various MMP and are shallow, whereas S2 prefers hydrophobic groups.

1.2.3 *Mechanism of action.*

The catalytic domain is connected to the hemopexin domain by a linker region. This hemopexin domain is formed by four blades and its role is in substrate recognition. The center of the hemopexin domain contains a pocket which accepts Ca(III?) ions [28]. The peptide linker connecting the catalytic domain to the hemopexin domain is rich in proline residues. The zinc ion in the catalytic domain is stabilized by three histidine residues. Two of them are from an α-helix present in catalytic domain. They are separated by three highly conserved residues with a HEXXH motif. These two His residues are situated on the same face of the α-helix to achieve an ideal orientation to chelate the catalytic zinc atom. The

[6] Image available at*:* Nuti, E.; Tuccinardi, T.; Rossello, A. *Current Pharmaceutical Design*, **2007**, 13, *2087-2100*, [40].

third His residue is located on a loop within the active site. These three residues belong to a highly conserved sequence in the MMP family, HEXXHaaGaaH. The conserved Gly residue is important for the correct folding of the structure. In this way three His are able to interact with zinc atom present in the active site. The zinc atom is tetra-coordinated where three bonds are made with the three His and the fourth bond is with a Cys residue of the pro-domain in the pro-form. Instead, in active form, a water molecule occupies that position and participates in hydrolysis. The α-helix of active site propeptide chain progresses from right to left in the standard representation of catalytic domain structure of MMPs where the zinc atom is to the left of the P1' pocket. After the first His there is one Glu: this residue is orientated towards the zinc ion and interacts with a water molecule. The role of the Glu is to act as an acceptor/donor of protons in the enzymatic reaction. In the hydrolysis mechanism, the interaction of the water oxygen atom with the zinc atom leads to a polarization of this molecule promoting a OH^- formation. The formation of this specie is favored by a proton release from the water molecule to the Glu residue; thus the COO^- group of the Glu side chain is able to pass to the COOH state. At the same time, the natural substrate is positioned in the pocket of active site and the carbonyl group of its peptide chain is orientated toward the zinc atom.

Thus the coordination state of the zinc atom shifts from the tetra- to the penta-coordinated state. This transitory structure favors the nucleophilic reaction. The carbon of carbonyl group is polarized because it makes an interaction with the zinc atom and is attacked by an OH^- ion. This reaction leads to a change of transition state; the carbon of peptide chain passes from sp2 state to sp3 state.

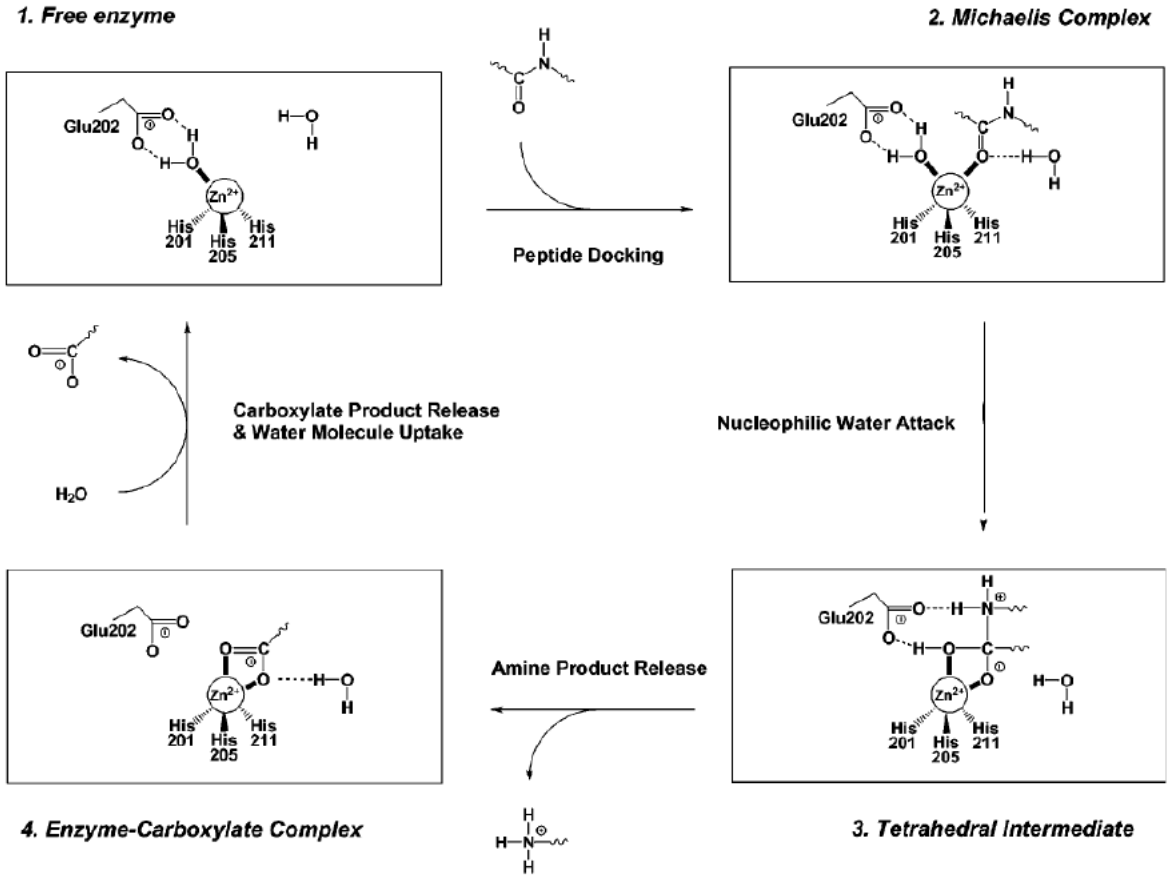

Figure 8. *Catalytic cycle for the proteolytic mechanism of stromelysin-1 (MMP-3)*[7].

This transition state is stabilized by an interaction between the glutamate residue and the zinc atom. After peptide chain opening, on breakage of the C-N bond, the proton on the glutamate residue passes to the nitrogen, forming a free amine function (**Fig.8**) [17]. There are some structural and functional differences among MMP family members. Among the collagenases the presence of the hemopexin-like domain is important, because it is responsible for the specificity, determining which amino acids sequences of interstitial collagen are most efficiently degraded.

It is fundamental in activating pro-enzymes. Matrilysins do not have this domain, while in gelatinases it has a similar structure as matrix proteins. MMP-12, MMP-19, MMP-20 and MMP-27 are new group of MMPs. The physiological action of these new members of MMPs family regards collagen and elastin, fundamental in animal cells. MMPs operate through degradation and subsequently on reconstruction of connective tissues: these actions are implicated in various diseases such as cell migration, differentiation and

[7] Image available at: V. Pelmenschikov, P.E.M. Siegbahn, *"Catalytic Mechanism of Matrix Metalloproteinases: Two-Layered ONIOM Study",* Inorg. Chem. 2002, 41, 5659-5666; [32].

growth, but also inflammatory process, neovascularization, wound healing, apoptosis, uterine cycle, embryonic development ovulation and in angiogenesis process. Indeed MMPs are produced by endothelial cells and several of those have the ability of stimulating the new blood vessels building [3].

1.2.4 *Implication of MMPs in pathologies.*

In the complex network of injury tissue response are involved proteinases, through their action on matrix remodeling and by their influence on cellular behavior. Plasminogen system is an enzymatic cascade involving many members of the serine proteinase family. Many experiments on mice with a plasminogen system component deficiency, have been reported in literature. In these experiments, it has been demonstrated that the plasminogen system is involved in many diseases, promoting tissue destruction or healing by direct or indirect activation of matrix metallo-proteinases. Proteinases influence diseases progression in different ways: examples are unusual cytokine activation, alteration of extracellular matrix turnover, growth factor availability and blood vessel formation. In homeostasis conditions all these functions are usually balanced: in fact the activity of all proteins is regulated by different factors such as expression and transcription of gene levels, levels of pro-enzymes and specific proteinases inhibitors. The dysfunction of interactions between the extracellular matrix and organs leads to the development of pathologies. [1] After cell stimulation, pathological levels of MMPs and TIMPs are detected in the inflammation area. An example that help us understand the relationship between TIMPs and pathologies is given by studies concerning the reduction of TIMP-3 expression which leads to an adverse matrix remodeling in a cardiomyopathic hamster model and in failing of human heart [6].

MMP-20 (enamelysin) digests amelogenin that is present within newly formed tooth enamel. The pathology called *amelogenin imperfect* is a genetic disorder, involving a mutation of MMP-20 cleavage sites, leads to imperfect enamel formation [6]. Experiments with mice deficient in MMP-12 (metalloelastase), did not develop emphysema in response to long time exposure to cigarette smoke compared to the wild type reference. Deficient in MMP-12, macrophages cannot penetrate the basement membrane neither *in vitro* nor *in vivo*. The various subtypes of MMPs have been implicated in the dissemination of cancer cells by breaking down ECM. This event might create a suitable starting environment able to support the initiation and maintenance of growth of primary and metastatic tumors [5]. Another example of MMP-12 involvement in pathologies comes from an animal model of

experimental autoimmune encephalomyelitis (EAE). These studies have shown in different ways which MMPs are implicated in the ability of leukocytes and T cells to penetrate ECM barriers and pass through the basement membrane of cerebral capillaries (**Fig.9**).

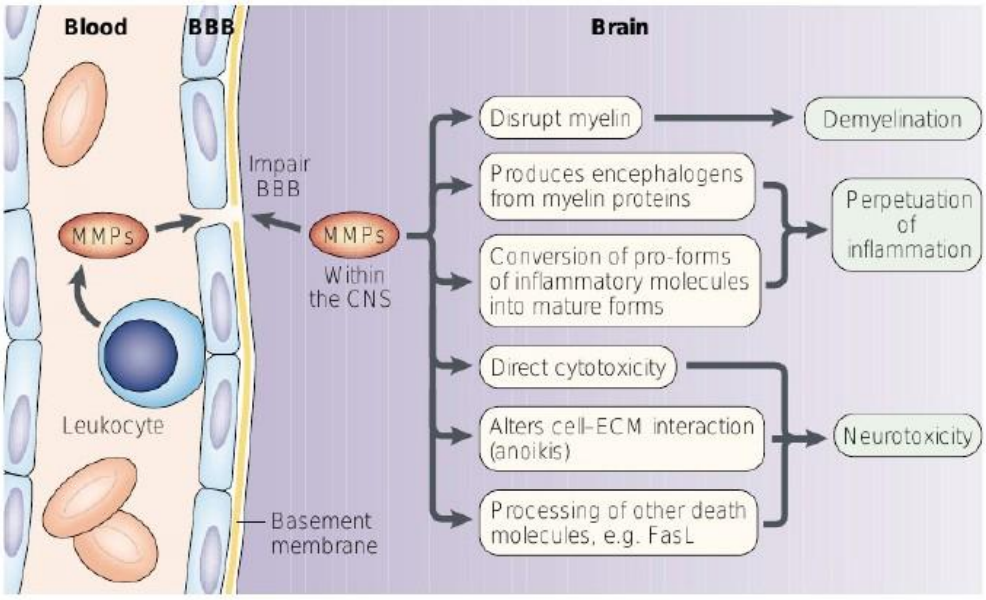

Figure.9 *Mechanisms by which MMPs contribute to neurophatology*[8].

Leukocytes express matrix metalloproteinases to facilitate their entry into the central nervous system. This process disrupts the basement membrane that surrounds the vasculature and results in blood-brain barrier impairment. In the central nervous system, high MMP content and its indiscriminate localization result in perpetuation of an inflammatory response, which contributes to demyelination and neuronal or oligodendrocyte death [7].

In other studies, mice with MMP-12-null have been used: they had in fact macrophages with a lower capacity of penetrating the basement membrane [7, 22]. Presence of ECM is essential for cells life, as previously mentioned, in cell growth processes. Several pathologies (tumor invasion and metastasis) often show degradation of ECM by different types of enzymes like serine, threonine proteases and matrix metalloproteinases. The degradation of ECM by MMPs may alter cellular behavior and phenotypes. Unbalanced levels of MMPs and their loss of activity control, are distinctive elements common in

[8] Image available at: V. W. Yong, C. Power, P. Forsyth and D. R. Edwards, Metalloproteinases in biology and pathology of the nervous system, *Macmillan Magazines Ltd*, **2001**, *502-511*; [7].

arthritis, cancer, atherosclerosis and aneurysms. TIMPs are specific natural inhibitors of MMPs, they act on MMPs present in tissues with 1:1 stoichiometry.

The TIMPs are glycoproteins with molecular weight of 21-34 kDa, denominated TIMP-1, -2, -3, -4. They differ from each other in their solubility, diffusion rate and their interaction with MMPs. TIMP-2 is constitutive and widely expressed in organisms. TIMP -1, -3, -4 are inducible and are found in different types of cells, among these, TIMP-4 is tissue specific, concentrated in brain and ovary cells, in adult cardiac cells and in skeletal muscle. TIMP-1 is a weak inhibitor of MT1-MMP, MT3-MMP, MT5-MMP and MMP-19. TIMP-2 and -4 are inhibitors of gelatinase, whereas TIMP-3 is an excellent inhibitor of ADAMs, especially TACE [38].

In pathological events MMPs levels are often altered. Such altered levels are matched by altered levels of TIMPs to control their activity. TIMPs contain an N-terminal and C-terminal domain with each containing three disulfide bonds. In the N-terminal domain there is a separate subunit responsible of inhibition of MMPs. An example that correlates TIMPs and pathology regards the reduction of TIMP-3 where it has an adverse effect on matrix remodeling in a cardiomyopathic hamster model and in humans is involved in heart failure. In an atherosclerosis mouse model an over-expression of TIMP-1 leads to a reduction in lesion extension [6].

1.2.5 *Target structure and functions.*

- ***MMP-8***

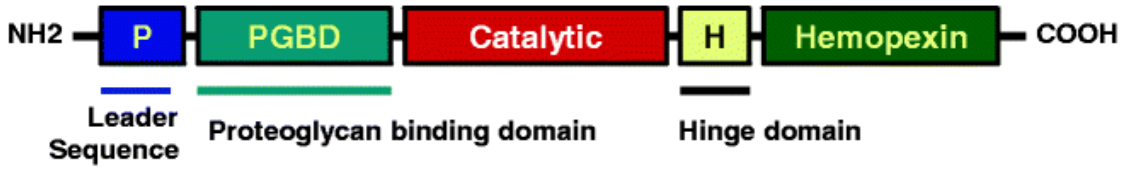

Figure 10. *Domain structure of MMP-8.*

Matrix metalloproteinase 8 (MMP-8) is also known as collagenase-2 or neutrophil collagenase. These alternative names highlight its two main functions. First MMP-8, member of the collagenases, can cleave the triple helix structure of native collagen. This lytic activity requires cooperation between its catalytic and hemopexin domain [89]. In

addition, MMP-8 is rapidly released upon activation of neutrophils, ensuring rapid availability in the site of inflammation. Only 15-20% of the cellular content of MMP-8 is freely released from polymorphonuclear cells (PMN), while most of MMP-8 is localized on the cell surface. The latter is a powerful "membrane-bound": about 90% of the PMN cell surface, in fact, processes the collagen type I, and is resistant to inactivation of TIMPs and might therefore be most important during inflammation, healing and other physiological process [90]. The MMP8 released by neutrophils is heavily glycosylated [91]. In addition to the PMN-derived full-length MMP-8 (80 kDa) form, other MMP-8 species with lower molecular mass (40-60 kDa), were identified. These poorly glycosylated forms derived from other cell types [92] and are secreted into the extracellular environment immediately after their synthesis. These proteases play a role in the development of an inflammatory response but it seems that they have also an anti-inflammatory action during the healing process [73]. MMP-8 is heavily involved in lung diseases: in fact, is the most potent collagenase that degrades type I collagen, the major ECM component of the lung [93]. MMP8 is also able to modulate numerous mediators of inflammation. Lung disorders are associated with a high degree of oxidative stress: MMP-8 is highly sensitive to the activation of ROS (reactive oxygen species) [94]. High levels of MMP-8 were found in adults [95] and children [67] suffering from acute lung injury in their lung secretion. Other involvement of this MMP is in obstructive lung disorders. Studies conducted on children showed that macrophages and eosinophiles, in particular, release high levels of MMP8 while in healthy persons, neutrophilis are the main source of MMP-8. In addition, this metalloprotease is expressed in a variety of cells involved in the development of atherosclerotic plaque, in particular in endothelial cells, vascular smooth, muscle cells, and macrophages [96-97].

- ***MMP-9***

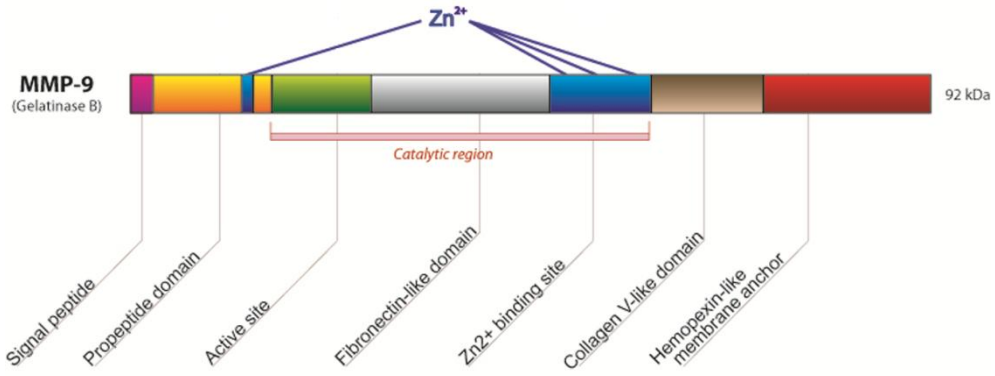

Figure 11. *Domain structure of MMP-9.*

The MMP-9 is a dependent Zn^{2+} endopeptidase, synthesized and secreted as a zymogen. The native form has a N-terminal sequence that allows to direct the protein to the endoplasmic reticulum. There is a "pro-domain" which allows to keep the enzyme in a latent form: this propetide of 80-90 residues contains a unique Cys of which sulfhydryl group coordinates the zinc ion in the active site to keep the enzyme in the inactive form. Moreover, there is a "catalytic domain", characterized by a conserved zinc-binding region. The activation of pro-MMP-9 is mediated by plasminogen activator/plasmin system. In addition, the hemopexin/vitronectin-like domain is connected to the catalytic domain through the linker region. This hemopexin domain is responsible for binding to some substrates, for membrane activation, is involved in some proteolytic activities and in the bond with TIMPs (TIMP-1 and 3). In particular, TIMP-3 is involved in the control of the MMP-9 activity [82], whereas its expression is controlled by cytokines, growth factors such as EGF (Epidermal Growth Factor), PDGF (Platelet Derived Growth), by interferons and interleukins. The main biological function of MMP-9 is the degradation of the proteins of ECM such as decorin, elastin, laminin, gelatin, and colagen type IV, V, XI, XVI. Physiologically, like other MMPs, MMP-9 is involved in tissue remodeling processes and therefore in embryonic development, neuronal growth, angiogenesis and ovulation. A high expression of MMP-9 was detected by Sakata *et al* [83] in the epithelial tumor of the ovary and in the lymph node metastases of ovarian carcinoma cells. Other studies show excessive levels of MMP-9 expression, in patients with pulmonary lymphangioleiomyomatosis [84]. An up regulation of MMPs, in association with a decrease of TIMPs in biological fluids, were found in multiple sclerosis (MS) patients and in animal models in which the disease was induced. The hypothesis of an involvement of MMPs in the treatment of MS was thus considered [85]. Indeed, significant levels of MMP-9 related to the various courses of MS were found [86]. A link between high levels of MMP-9 both in the cardiovascular risk [87] and with coronary artery disease [88] was also found.

- ***MMP-12***

Figura 12. *MMP-12 domain structure. S, signal peptide; Pro, propeptide; CAT, catalytic domain; PEX, hemopexin domain. The flexible, variable length linker or hinge region is depicted as a wavy black ribbon.*

MMP-12 is secreted in its inactive form (54 kDa) and subsequently processed to its active

form, following loss of the end N- and C-terminal domain (22 kDa). Both the mRNA and protein were detected in alveolar macrophages [81]. MMP-12 is mainly produced by macrophage, and involvement of this protein with skin diseases [99], atherosclerosis [100], aneurysms [98] and cancers [101], have been demonstrated. In addition, this metalloelastase seems to play a predominant role in the pathogenesis of chronic lung injury and, particularly, in emphysema. MMP-12 is able to degrade several substrates including elastin, which represents 2.5% of the dry weight of the lung and is widely distributed in these organs. This metalloprotease is very important for the elastic recoil of the small airways and their ability to resist to negative pressure collapse [27]. MMP-12 is the major enzyme that leads to the lysis of alveolar elastin magrophages [81]. Preclinical studies on COPD (Chronic obstructive pulmonary disease) / emphysema include the blocking of MMP-12 as a possible viable therapeutic approach.

Chapter II
LINKERS

2.1 *Linkers in biology: different techniques that use linker strategy.*

Linkers are used in many disciplines. In immunology, spacers are used to produce monoclonal antibodies against small compounds, referred to as haptens. Haptens are intrinsically non-immunogenic because of their small size and must be linked to a carrier protein to stimulate an immune response. The B-cells produced in response to the immunization, are then selected for their ability to produce antibodies that recognize the hapten. Linkers are also part of anticancer drugs such as camptothecin. This powerful anticancer is already in therapeutic use. *Camptothecin* is a natural molecule with cytotoxic activity. It is indeed capable in inhibiting topoisomerase I, inducing cell death. Several attempts have been made to develop clinical *camptothecin* analogues with comparable anti-tumor cytotoxic activity. Drugs conjugates were designed as powerful *camptothecin* analogues using monoclonal antibodies (mAbs). Antibodies were conjugated with the drug *via* either a dipeptide or a glucuronide-based linker. Aniline containing *camptothecin*-analogues have been used to create a site of linker attachment using carbamate bonds, which are stable in blood circulation. Dipeptide and glucuronide drug linkers were designed with self-immolative spacers for drug release through lysosomal degradation after internalization of the complex into antigen-positive cell lines. The *camptothecin* drug linkers were conjugated to three different antibodies [8].

In the peptide linker design, appropriate parameters, such as flexibility and length, were considered to be important to obtain a specific spacer to join the ligands together. The linker had to be flexible enough to permit the binding to the second site and long enough to separate the two receptors from each other. [35]

Linker-length influences the interaction between molecules. In the study of biotinylated compounds, the avidin affinity for biotin, decreases when a short linker arm is used in the structure of biotinylated compound. The decrease in affinity is due to steric hindrance and can be attenuated with longer spacers leading to an increase in detection sensitivity for avidin or streptavidin. The longer spacers facilitate the formation of the avidin-biotin complex [13]. The proteasome is a catalytic protease, able to degrade unfolded polypeptides with no particular substrate specificity and without a particular cleavage

pattern. For this reason the design of an ideal and specific class of inhibitors is extremely difficult. Through the X-ray structure of *Saccaromyces cerevisiae* proteasome, and the observation of the "*unique topography of the six active sites in the inner chamber of the protease"* has permitted the start of a project to construct a series of specific multivalent inhibitors. Taking into account the separation between the active sites, different homo/hetero-bivalent inhibitors based on a specific group were designed with polioxyethylene spacing elements, to create a structure that gives access to the active site. For spacer design, the proteasome-resistance and flexibility were taken into consideration to create a derived structure similar to that of unfolded polypeptide chains that able to enter the proteolytic chamber. The length of the spacer was chosen based on inter and intra-molecular interactions, avoiding steric hindrance, to link two monovalent binding head-groups to obtain homo- or hetero- bivalent inhibitors, with enhanced binding affinity. The inhibitory potency of the bivalent inhibitors is greater the monovalent parent, interpreted to be due to bivalent binding. With the idea that the spacer should mimic the polypeptide chain of unfolded proteins, following modeling experiments, different compounds were designed. The researchers suggest that "e*ven better results may be expected with homogeneous spacers of defined optimal length for the various interactive site distances. Furthermore, this general principle of bivalency is not at all restricted to the use of peptide aldehydes as binding head groups, but could, in combination with more potent and selective monovalent inhibitors, result in a new generation of highly specific proteasome inhibitors"*. [36]

2.2 *Linker design.*

The linker is an important part of the final coupled synthetic molecule composed of biological or chemical entities arranged in controlled spatial relationship. Two ligands, different or identical, are connected by the spacer to generate a single entity capable of interacting with two active sites from selected proteins. The linker length influences the spatial arrangement of the subunits, giving greater or less freedom to the resulting structure. In addition to spacing out the two domains to avoiding mutual steric interference, a longer linker adds flexibility and allows for more conformational diversity. Linkers composed of flexible components, often amino acids, allow movement between adjacent subunits. Shorter linkers, composed of a small number of atoms, restrict adjustment between subunits so as to be more target selective. Although, by restricting the freedom of

adaptation, a certain degree of selectivity can be achieved, the risk of steric hindrance increases. To avoid this problem, X-ray crystallography data are extremely important when designing a library of synthetic chemical molecules with restrictive properties. Based on X-ray data, chemical spacer groups of different size and length can be modeled, first starting with flexible linkers and systematically arriving at rigid spacers.
Another aspect of linkers use in biology, is their influence on the stability of single-chain proteins as was noted in the study of the single chain Arc-repressor to conclude that spacer length affects the equilibrium, folding kinetics and biological activity. The study of Robinson and Sauer on wild-type Arc and an Arc dimer composed identical subunits connected with an L1 linker of 15-residues to give Arc-L1-Arc. Other tests, which varied the spacer length and composition, obtained single chain variants with efficient concentrations in the range between μM and M. These data show that the linker affects protein stability by altering the free energy of native and denatured states. The linker length required to achieve a stable protein conformation, appears to be well defined and the adding or deleting of even a few atoms can have, *de facto,* a destabilizing effect. The decrease in linker length often accelerates folding [10].

The designing of the linker requires many considerations. Based only on modeling data, it is extremely difficult to create a rigid linker able to form a specific homodimer. At the very beginning, a good working strategy is to synthesize a variety of flexible linkers of variable length, capable of producing different subunit orientations. Subsequently, from information that define the nature of the interactions and the length of the spacer, the linker can be optimized to allow a better interaction between the two sides of the catalytic domains, minimizing steric strain and simultaneously favoring the stabilization of interactions that promote complex formation.

In this thesis, initial crystallography studies of inhibitor protein complexes, with particular attention to metal proteases, have been carried out to show the formation of a molecular complex in which two monomeric inhibitors assemble into a dimeric protein-inhibitor complex driven by the coupling with this ligand.
The monomeric ligand complex involves interactions that stabilize a ligand-enzyme dimeric conformation where the intermolecular surface includes two protein surfaces and the external moieties from two molecules of inhibitor that do not participate in P1' interactions (**Fig.13**).

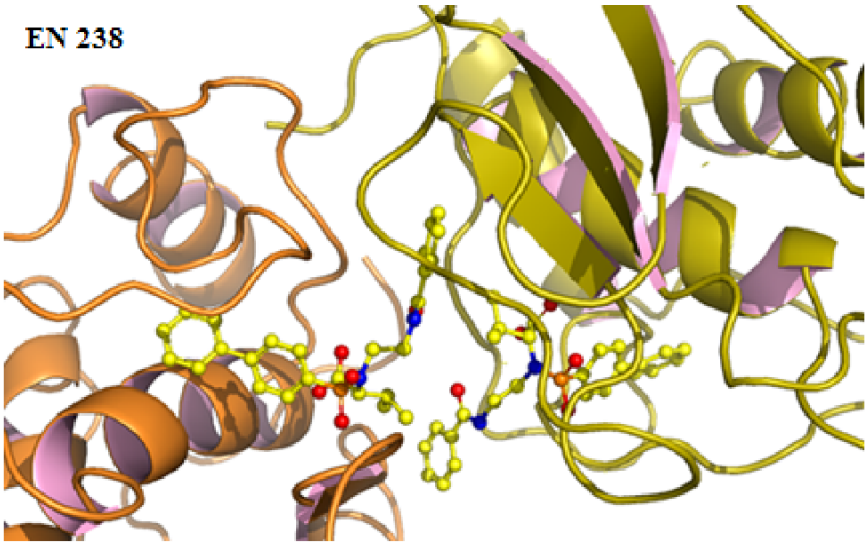

Figure 13. *The MMP-12 packing in the $P2_12_12_1$ space group observed for the complex with mono-ligand EN 238 (PDB entry 4H84; ligand code Y38)*[9].

This arrangement has inspired the design of a unique inhibitor that interacts in a classic way in the P1' pocket in order to guard the active site interactions and maintain the level of affinity and adding a linker that would allow dimer formation with the hydrophilic and hydrophobic interactions found in the spontaneously formed dimer. Modeling studies were performed to determine the amendments that could be made to the original monomer inhibitor to complete the linker structure. Length, flexibility and functional chemical groups, were all elements analyzed to arrive at the final structure. The point for linker insertion within the inhibitor and functional groups in the linker itself can be considered part of the design to increase the selectivity of the inhibitors for the various enzyme subtypes. The role of the linker can extend beyond structural innovation or simple "bridge" to become an active functional part of the inhibitor, able to increase the selectivity and affinity towards the protein studied. Small differences within members of the same proteins family may result in different quaternary associations guided by spacers do not act alone but recruit protein-protein interactions to modulate the geometry of the dimeric interaction [11].

Several biological studies are trying to find practical ways to induce dimerization. A

[9] C.Antoni, L.Vera, M. P.Catalani, B.Czarny, E.Cassar- Lajeunesse, E.Nuti, A.Rossello, V.Dive, E. A. Stura. Crystallization with bi-functional ligands, *J. Struct. Biol.* **2013**, 182, *246-254* [41].

specifically designed linker, may permit the formation of a precise dimer to simultaneously inhibit two molecules through the anchorage of two inhibitors present in two different pockets. Thus, a single molecule would interact with two biological structures stimulating the formation of homo- or hetero-dimers. The adding or deleting of even a single atom in the linker structure can have non-negligible consequences. A linker that is too short cannot force two proteins together, as steric hindrance becomes an unbridgeable obstacle, and only allow alternative monomeric inhibitor binding. On the other hand, a linker that is too long is less able to make use of contributory protein-protein interaction useful in the stabilization of the complex. An excessive level of freedom conferred by extravagant linker span fails to exploit the selectivity that could be provided by chemical groups within the linker. Failure to recruit protein-protein interactions from the external protein surface, is returning to the classical manner in which selectivity is based only on sequence differences among the various subtypes belonging to the same protein family in a limited region around the functionally conserved catalytic region. As linker length increases, only the closest chemical groups of the spacer are well positioned to influence affinity and stability, while the intermediate extensions add only to the randomization of the geometry.

Crystal formation, which is sensitive to entropic factors, is also promoted by rigid spacers and by dimerization but not by heterogeneity that could result from loss in affinity because of steric stress due to an inappropriate design. Crystallographic data needed to design a rigid linker that is able to control homodimerization must be acquired in successive steps with spacers that become progressively more rigid.

2.3 *MMPs as a model.*

MMPs have been used as model in this work to study the homo- and hetero-dimerization using synthetic twin inhibitors, characterized by different chemical groups and different spacer lengths. Protein-protein subunit interactions are to be found in catalysis processes, through hetero- and homodimerization. These interactions are of different types and only a few of the dimerization processes are involved in modulation of biological activity. The knowledge of three-dimensional structure of proteins, in association with the use of modeling studies, could help to define the possible interactions between them. In addition, the use of synthetic molecules could contribute to the discovery process, allowing identification of pathways in which protein homo- or heterodimerization have a functional role. An initial approach involves the testing a monomeric ligand to understand the specific interactions at the active site, then evolve towards spacer design finishing with a selective

bi-functional ligand. Crystallographic data and comparative modeling studies are extremely important because they may provide guidance for spacer design. Several types of synthetic ligand joined together by spacer could indeed be used to give a completely new approach of signal transduction involved in pathological process.

2.4 *Linker design and Twin inhibitors*

The objective of this study was directed towards the continuation of the design of new linkers, to obtain bifunctional ligands. Synthetic multivalent ligands, consisting of multiple receptor binding moieties joined together by linkers, can be effective to probe signal transduction and may be useful for pharmaceutical applications. With these considerations, it might be possible to design a library of linker, and therefore of the bifunctional ligands, which may subsequently be improved thanks to the data from both crystallographic analyzes and biological tests. The linker design is based on X-ray rationally oriented synthesis (X-ROS), thanks to which the various parts of the ligand are drawn in subsequent steps guided, precisely, from crystallographic data and comparative modeling. A rational discovery pathway could start with monomeric ligands, involve a spacer design step and finally lead to a bifunctional or self-dimerizing ligand. The choice of rather rigid linker may facilitate the crystallization, but its exact design requires the knowledge of the structural data obtained by crystallography. For this reason semi-rigid linkers were initially synthesized. Initial studies were based on a linker such as the *N*,*N*'-Bis-(3-ethylencarbamoyl-propyl)-isophthalamide (BEPI), which connected two units of monomeric inhibitor (S)-1-(([1,1'-biphenyl]-4-ylsulfonyl) (isopropoxy) methyl)-3-hydroxyurea in P1 position, providing the bifunctional ligand **MP24**.

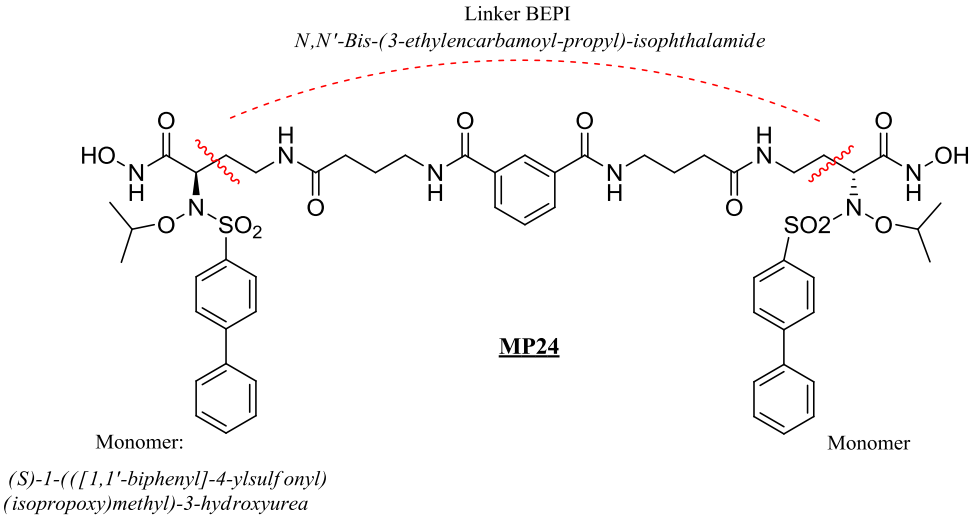

This study of linkers was enabled by the successful crystallization and structure determination of the complex between MP24 and MMP-9. In this homodimeric complex stood out the lack of significant interactions between protein and linker, and also the folding assumed by the spacer did hypothesize that a shorter linker would provide the correct distance and geometry of the twin inhibitor, capable to homo-dimer formation on MMPs. It is also necessary to consider that shortening the linker, another branch point must be used in the design of bifunctional ligand. Both computational and crystallographic studies, showed two exposed sites of linkage exploitable in sulfonamidic inhibitors, P1 and P2' sites, in order to obtain two kinds of twin inhibitors: type A (like MP24) and type B, respectively.

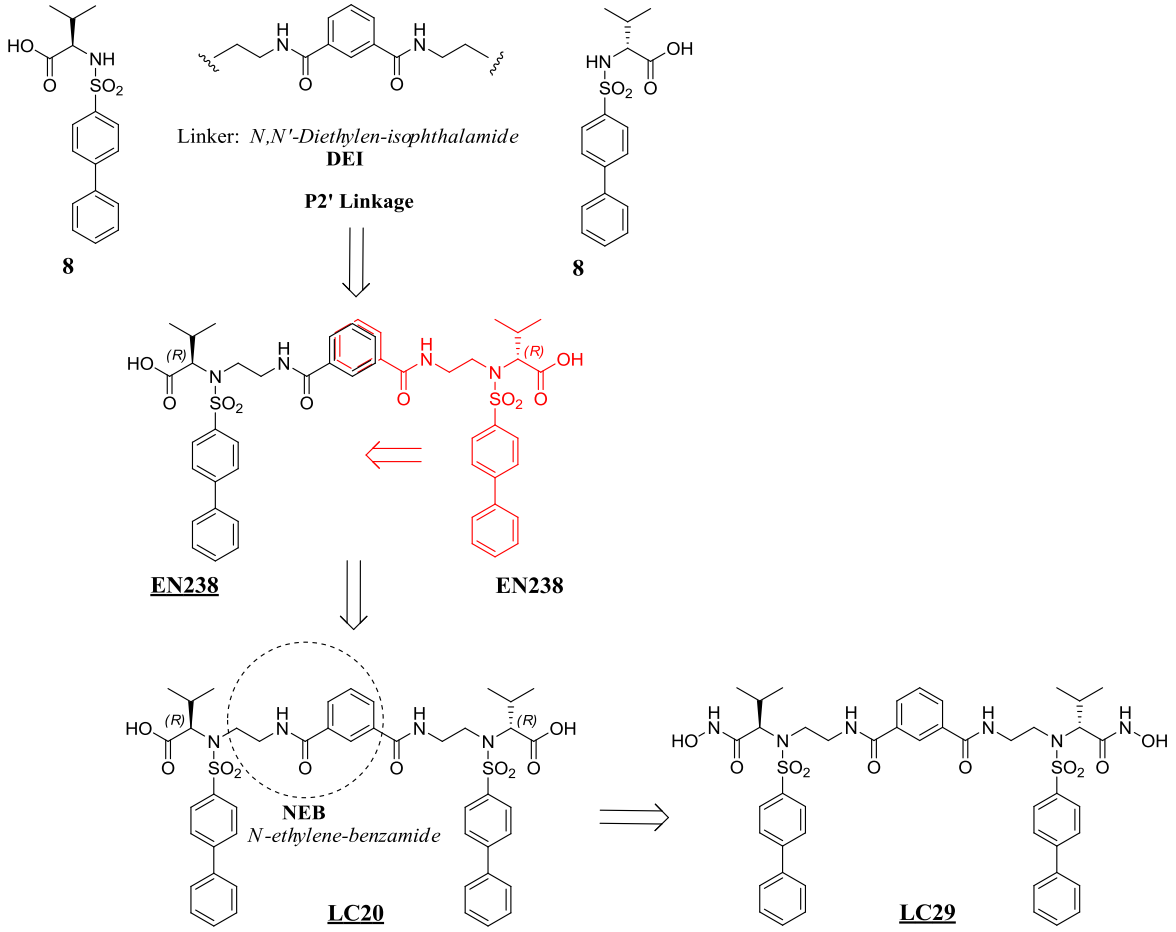

On these basis, new twin inhibitors of type B were synthesized, compounds **LC20** and **LC29**, which have been tested on MMPs and studied by X-ray crystallography. For type B inhibitors, the *N*,*N*'-Diethylen-isophthalamide (DEI) linker could be thought as obtained by the superimposition on phenyl ring of two molecules of inhibitor possessing on their P2' a *N*-ethylene-benzamide (NEB), as half linker (**EN238**).

Chapter III
CRYSTALLOGRAPHY, CRYSTALLOGENESIS AND CRYSTALLIZATION.

3.1 *Crystallography, crystallogenesis and crystallization.*

The X-ray crystallography is a method used for determining the atomic and molecular structures by collecting the intensities of X-rays diffracted from a crystal. Single crystals and a monochromatic (single wavelength) beam are used for data collection. The X-rays are scattered by the electron cloud of each atom in the crystal. The periodic assembly allow for an amplification of the signal proportional to the number of scattering atoms in the portion of the crystal irradiated by the X-ray beam. In a synchrotron n X-ray diffraction experiment, a single crystal is mounted on a goniometer head and rotated in the monochromatic X-ray beam, producing a diffraction pattern of regularly spaced spots known as reflections. The diffraction pattern is indexed and the intensity of each reflection extracted. Equivalent reflections are merged together to obtain the average recorded intensity so providing agreement statistics for the data set. Only the structure factors F (the intensity is F^2) can be calculated from the experimentally obtained intensities, the phases of the incident beam needed to calculate the electron density maps using a Fourier transform are lost. They can be obtained by various methods including molecular replacement where a related structure is used as a search model to determine the orientation and position of the molecules within the unit cell. The phases obtained this way are then used to generate electron density maps. Since the search model differs from the protein in the crystal the phases need to be improved by fitting the electron density with a new model that is progressively refined and completed, thus defining at the end, an accurate molecular structure for the components in the asymmetric unit responsible for the X-ray scattering.

The knowledge of the exact molecular structure of a biomolecules helps to guide the design and development of potential therapeutic agents. The crystallographic maps provide the means to elucidate how potential new drugs interact with their targets and so guide the design of specific ligands by revealing the nature of the ligand-enzyme interactions. To gain full advantage from a crystallographic analysis well formed, good ordered crystals are required. While technical progress in data collection equipment have helped reduce crystal size requirements, to achieve this objective a good knowledge about the complex system of

crystallization and the various dynamics that influence it are often essential.

3.1.1 *Introduction.*

Crystallization is the transition from the liquid state to an orderly solid state, controlled by complex kinetic laws. A crystal can be described as a regular arrangement repeated indefinitely in three spatial dimensions, called the crystal lattice. Protein crystallogenesis extends beyond spontaneous crystallization to involves extra design steps to obtain a well diffracting polymorph starting from a protein-inhibitor solution to arrive at a well defined crystalline solid state. The crystallization of biological macromolecules is complicated: biomolecules require indeed conditions similar to those physiological and their behavior is strongly influenced by some variable parameters such as purity, homogeneity (distribution of charge, site of glycosilation), pH (protein net charge), temperature (solubility of protein) and many other factors. Whatever the crystallization method used, the objective is to drive the protein solution into a metastable state of supersaturation, where crystals may form (**Fig. 14**). Crystallization needs conditions in which the transition from a disordered state of macromolecules to an ordered crystalline form is possible.

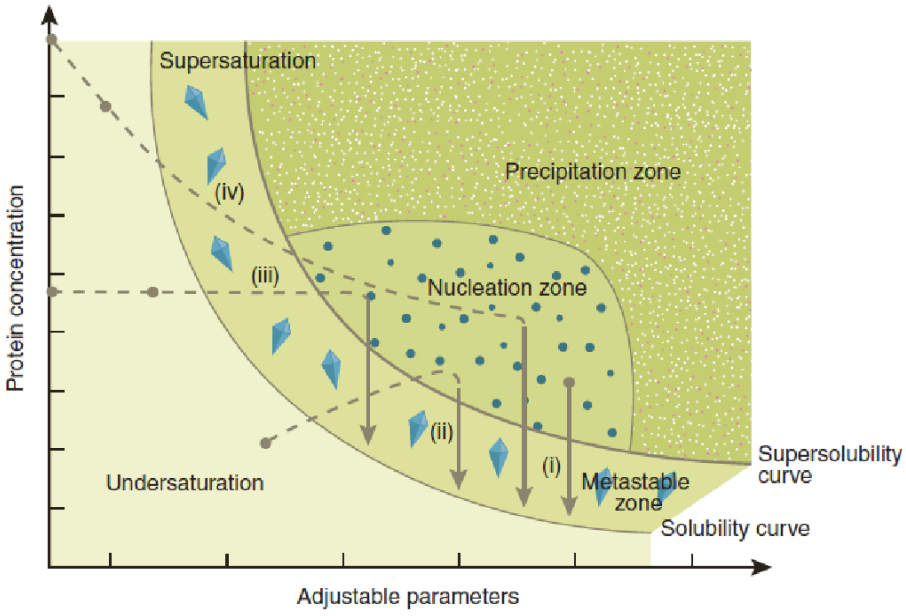

Figure 14. *Schematic illustration of a protein crystallization phase diagram. Adjustable parameters include the optimization of precipitant solution concentration, pH and temperature. The four major crystallization methods are represented: (i)micro-bath, (ii) vapor diffusion, (iii)dialysis and (iv) free interface diffusion (FID). Each involves a different route to reach the nucleation and the metastable zone, assuming as adjustable parameter, the concentration of precipitant solution. The filled black circles represent the starting condition. Two alternative starting points are shown for FID because the under-saturated protein solution can contain either protein alone or protein mixed with a low concentration of the precipitant agents. The*

solubility is defined as the concentration of protein in the solution, which is in equilibrium with crystals. The super-solubility curve is defined as the separating line conditions under which spontaneous nucleation occurs from those under which crystallization solution remains clear if left undisturbed[10] *[13]*.

A crystal can be simply defined as a set of protein molecules, assembled into a periodic lattice. To induce crystal formation, a fairly high protein concentration is often used together with substances that reduce its solubility. The dynamics of the method attempts to gradually arrive close to precipitation, so that within the drop, the solubility of the protein decreases promoting the formation of some nucleation sites and the subsequent growth of crystals. Often, several conditions must be tested before success is achieved. For this reason, initial screening involves testing a large array of conditions and then proceeding systematically to optimize those conditions that give crystalline particles.
The crystal formation can be divided into two steps:

- Nucleation: In various areas of the drop areas with a high concentration of macromolecules can be found. Such environment may be appropriate to create an ordered microscopic crystalline seed.
- Crystal growth: The organization of molecules follows that of the initial crystalline seed and the crystal dimensions increase.

Good nucleation conditions do not correspond to good crystallization conditions. Each of these two crystallization steps are important to get suitable crystals and must to be optimized. To reach the so-called supersaturated state, two aspects need to be considered: first of all, the rate of incrementation of the effective concentration of the protein and secondly the modulation of attractive (electrostatic, hydrophobic/ hydrophilic interactions) and repulsive forces [23]. For these reasons precipitant agents, with various properties, have been used: the salts have an effect on the ionic strength of the environment, while polymers have effect on the solvation layer of the protein and finally the organic solvents on the dielectric constant.
Crystallization is a multi-parameter process where, in order to obtain crystals, it is necessary to reach a supersaturation condition, while gradually balancing all the variables. The successful study of a crystal includes the definition of its space group and lattice packing.

[10]Image available at : N.E.Chain, E.Saridakis. Protein crystallization: from purified protein to diffraction-quality crystal, *Nature Methods*, **2008**, 5, *147-153*; [13].

Further aspects must also be taken into account to resolve more difficult problems:

- Protein sequence: Minimization of disordered zones to limit conformational heterogeneity during crystallization. Disordered zones are also more likely to be proteolyzed.
- Purity and homogeneity of sample: The concentration of impurities influences the crystallization process causing growth termination when impurity segregation is no longer possible.
- Temperature: Controlling the temperature of crystallization, allows for better macromolecule stability. It was observed that, at low ionic strength, most proteins are more soluble at room temperature than at lower temperature [24, 25].
- The nature and concentration of precipitant agents can be exploited to drive the proteins into the metastable zone. Precipitants can be grouped in three main sets:
    - Salts ($MgCl_2$, $CaCl_2$, Li_2SO_4...) affect the ionic strength of the medium;
    - Polymers (PEG) influence the solvation shell around macromolecules;
    - pH controls the net charge of macromolecules.

3.1.2 *Sitting drop and hanging drop vapor diffusion.*

During the course of this study, the sitting drop vapor diffusion (VD) method was used, practical for setting up rapidly many experiments, while using small amounts of proteins. In VD only volatile components equilibrate across the vapor phase that separates the reservoir solution from the crystallization drop. The drop consists of small volumes of precipitant solution with small volumes of protein solutions mixed together and positioned above a larger reservoir containing the precipitant solution. The VD method can be used either with a hanging drop or a sitting drop.

- In the hanging drop method, the drop is dispensed on a siliconized cover glass which is later reversed when closing the reservoir so that the drop is suspended at the top of the crystallization enclosure. The drop is composed of a few microliters of protein-inhibitor solution mixed with a similar amount of reservoir precipitant solution. A thread of vacuum silicon grease is added to the crystallization well to seal the reservoir by pressing on the cover glass to isolate the crystallization chamber from the external environment.

- In the sitting drop method, the precipitant solution is also situated in the reservoir, but a “tower” on which the drop is placed rises from the bottom of the well (**Fig.15**).

After an initial extensive screening by the sitting drop method with several conditions with different compositions of precipitant solutions those specific conditions (varying concentrations and type of precipitating agent) that showed a development potential of crystals are selected for refinement. The best hypothesis regarding the various parameters of crystallization solutions that might have influenced crystal formation, such as the precipitant concentration (polyethylene glycol, DMSO and other), pH of the solution, presence/absence of salt, are evaluated to design an optimization strategy. The optimization process, requires a basic understanding of the physical properties of the solvents. For volatile compounds, it is essential to consider the rate of equilibration which is affected by the vapor pressure of each of the compounds, while for non-volatile compounds, it is necessary to focus our attention on how they may influence vapor equilibration.

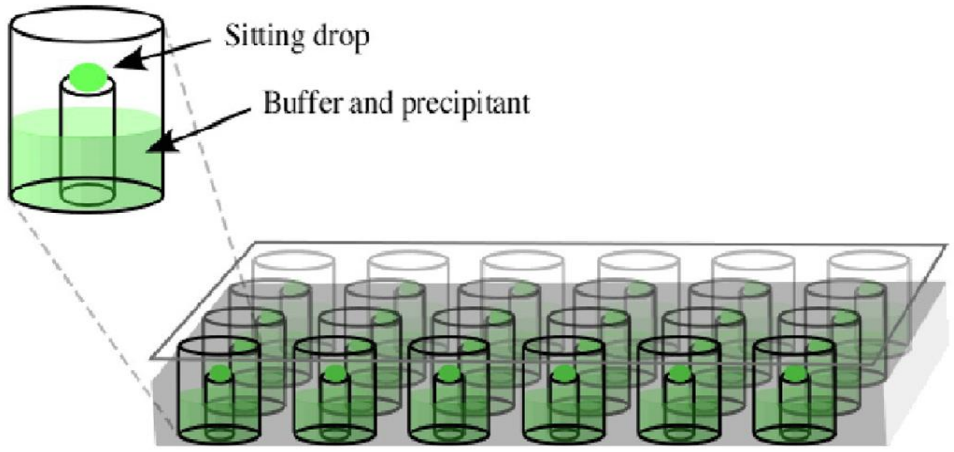

Figure.15 *CrysChem sitting drops.*

Hygroscopic compounds like glycerol if not in equilibrium on both sides of the vapor phase, can lead to an accumulation of water in the partition where its concentration is highest. Non-hygroscopic compounds also affect the chemical potential of water [21]. The protein-precipitant solution starts at a concentration of protein and precipitant agents where it is undersaturated (**Fig.14**), as water starts evaporating from the drop and moves into the reservoir, the protein enters the metastable zone allowing for the crystallization process to start. As the concentration of both protein and precipitant in the drop continues to increase,

crystals may form and grow (**Fig.16**). This condition is maintained, until the whole process of crystallization is complete.

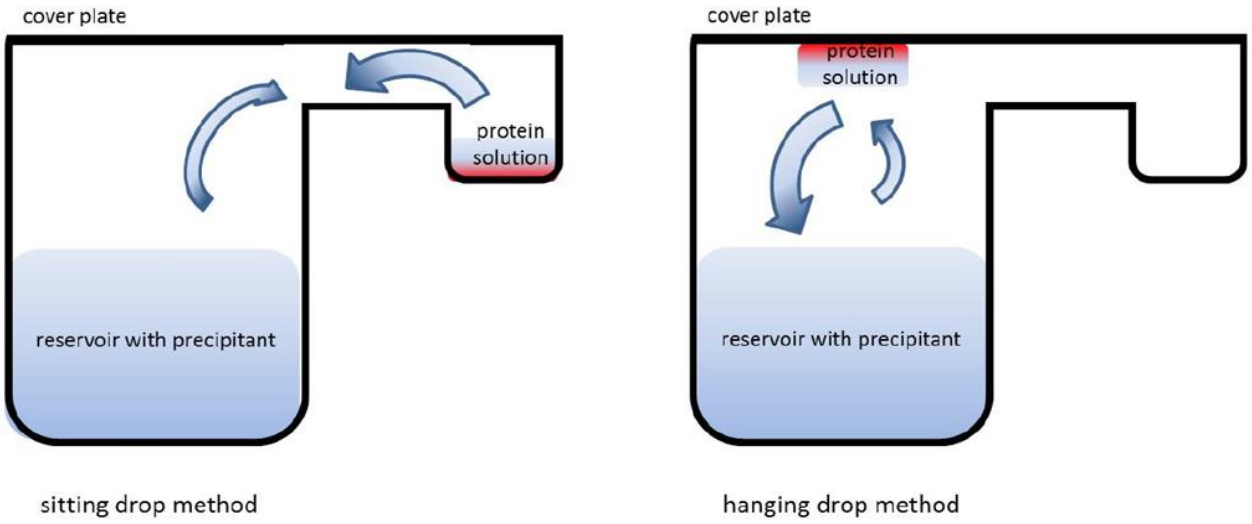

Figure.16 *Principe of vapor diffusion: Sitting drop and Hanging drop method*[11].

3.1.3 *Streak seeding.*

The sitting drop and vapor diffusion methods, allow the equilibration of the precipitating agents and the proteins in the drop. Those methods lead to a reduction of the solubility of proteins and under favorable conditions crystallization is induced. In order to improve the quality of the crystal, it is possible to combine the previously explained methods with the *streak seeding* technique (**Fig.17**). This technique consist in avoiding spontaneous nucleation by introducing microseeds extracted from previously grown crystals.

Figure 17. *Crystals grow along the path of the whisker*[12].

[11]Image available at: http://centeo.com/en/technical/sitting-and-hanging-drop.

[12] Image available at: http://upload.wikimedia.org/wikipedia/commons/2/2f/Streak-seeding.png.

This method uses a cat whisker to collect crystal seeds by touching a previously grown crystal in a different drop and then depositing them with the mustache in the new drop. The whisker releases seeds along its linear path (streak) across the crystallization drop stimulating crystal growth that grow along the length of the track.
The streak seeding technique has to be done in a particular moment, to introduce seeds into the drop within the metastable state. The number of seeds must be limited to allow for regular and slow growth. This consideration permits to obtain larger crystals, capable of diffracting to higher resolution.

3.2 *Crystallization*

> *"Crystals – familiar to all in gemstones, glittering snowflakes or grains of salt – are everywhere in nature. The study of their inner structure and properties gives us our deepest insights into the arrangement of atoms in the solid state - insights that advance the sciences of chemistry, solid-state physics and, perhaps surprisingly, biology and medicine. A century has passed since crystals first yielded their secrets to X-rays. In that time, crystallography has become the very core of structural science, showing us the structure of DNA, allowing us to understand ... showing us how proteins are created in cells, and helping us to design powerful new materials and drugs." [39]*

The crystals obtained from proteins and protein-inhibitor complexes are very sensitive to even minimal variations of the environmental conditions. Protein crystals contain typically around 50% solvent, mostly in large channels between the stacked macromolecules in the crystal. The protein-protein interactions that maintain adherent molecules are generally weak hydrogen bonds, salt bridges, and hydrophobic interactions supplemented by extensive protein-water and water-water hydrogen bonding. Compared to strong covalent or ionic interactions in crystalline minerals, it is easy to understand why protein crystals are so fragile.

3.3 *Crystals harvesting and data collection.*

Like living creatures and most organic matter, proteins are also susceptible to damage due to X-ray exposure. The absorption of ionizing radiation leads to the formation of free radicals, which subsequently damages most crystallized proteins. For this reason, a method for crystal protection against X-rays has been devised, through the slowing down of the

radical kinetics, using cryogenic cooling. Crystals are harvested using a loop of an appropriate size and then transferred into a cryoprotectant solution before being dipped in liquid nitrogen. The crystals are stored at ~100 K. The cryoprotectant is required since the freezing procedure may otherwise damage the crystals because of ice formation inside the crystal lattice. Ice formation can be visualized because of black rings due to the diffraction of polycrystalline ice. Such rings can mask the diffraction due to the protein-ligand complex and cause partial loss of diffraction data. [21]. The cryoprotective reagents added to the solution to minimize the damage by favoring vitrification rather that crystallization during cryogenic cooling. The cryoprotection allows for longer data collection times and facilitates transport because encased in vitrified solvent the crystal is positionally more stable and less likely to be lost. An optimal cryoprotectant will give an X-ray diffraction pattern free of powder diffraction rings or "ice rings". A poor choice of cryoprotectant can be discerned without X-rays if the drop appears cloudy. Several substances are used as cryoprotectants, including polymers (polethylene glycols), organic acids (malonates), halide salts in high concentration and volatile or non-volatile (isopropanol) organic solvents for biological macromolecular crystals. Such compounds can be used as crystallization additives, but for cryoprotection, their concentration is often higher. Cryoprotectant optimization is a trial and error procedure so that if the ice crystals form, additional agents are added or a different mix of cryoprotectants agents is produced. The cryoprotectant compounds enter the crystal lattice during the soaking step depending on the duration. Longer soaks are used not only to remove the surface layer, but to permit an exchange between the solvent present in the crystal and the one present in the cryoprotectant. For long soaks, the time period must be varied to take into account the characteristics of the cryoprotectant (concentration, molecular mass and diffusion property), the crystal (size, physical stability and hydration state), nature of the crystallization solvent and temperature. Typical soak periods range from minutes to hours depending on the type of solvent used for the crystallization, the type of crystal, the temperature and the type of cryoprotectant [43]. During data collection, the crystal in the loop, is aligned along the line of the X-ray beam maintained frozen by a nitrogen gas flow at 100 K. Modern data collection advances at synchrotron facilities allow for continuous rotation of the frozen crystal around a single axis continuously exposed to X-rays, while previously, data collection required discrete angular oscillations around an axis. The X-rays that pass through the crystal and are scattered are collected by a detector (**Fig.18**). The collected diffraction spot images, called frames, are displayed on a screen for monitoring

the progress and saved for later analysis. The ensemble of these images, recorded from different crystal orientations, are processed (integrated, scaled and merged) into a final list of indexed reflection intensities.

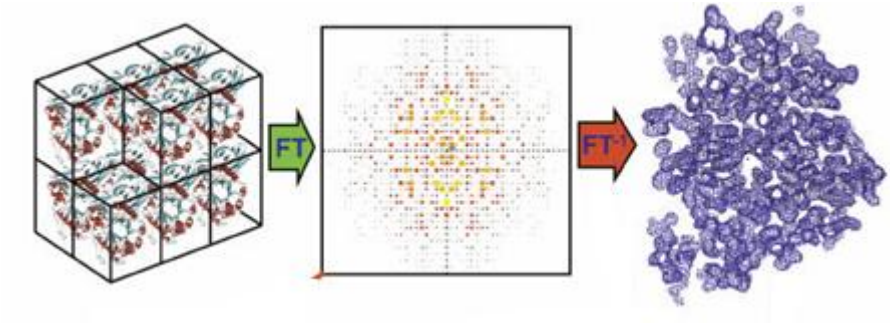

Figure 18. *Transition from the crystal to the electron density map*[13].

The number of images depends on the space group and the resistance of the crystal. The data collection and processing, done by various computer programs, has been automatized extensively so that often a relatively accurate electron density map can be obtained within minutes from the moment the data has been finished collecting (**Fig.18**). The data collection process at third generation synchrotron sources can take less than ten minutes.

3.4 *Structure definition and refinement.*

Depending on the initial model used in molecular replacement, the electron density map can be inaccurate and needs to be improved using a graphic program for model fitting and cycles of structure refinement (REFMAC5). Geometry restraints needed by the refinement programs for synthetic ligand can constructed using the monomer library sketcher from CCP4 program. The generated model coordinates for the molecule allows the ligand to be fitted into the difference electron density (Fo-Fc; green: positive, red: negative) map using COOT. The model was also refined in phenix.refine to obtain at the end, an accurate electron density map of the ligand-protein complex. The the last stages of protein structure refinement involve the interpretation of the electron density for the solvent around the protein which contributes to the diffraction: water molecules and other molecules from the crystallization precipitant or from the cryosolution, typically, glycerol, PEG and other. The positioning of these molecules in the electron density map also follows strict geometrical criteria.

The figure above shows the result in terms of definition, of different resolution values,

[13]Image available at: http://www.ruppweb.org/xray/101index.html.

expressed in Ångstrom. The example shows the same region of the molecule at different resolution settings: 3 Å, 2 Å and 1.2 Å. The ring of phenylalanine is correctly positioned in the resolution with 1.2 Å. This can still be done with confidence in the 2 Å cases, but at 3 Å we observe a deviation of the centroid of the ring from the correct model (**Fig.19**).

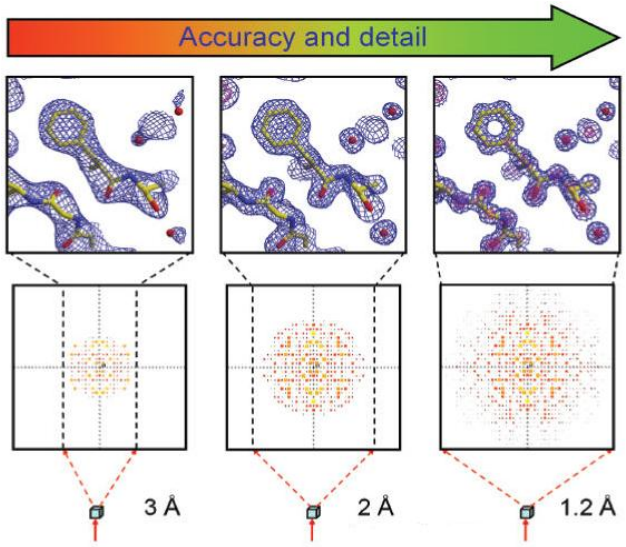

Figure 19. *Data quality determines structural detail and accuracy. The qualitative relation between the extent of X-ray diffraction, the resulting amount of available diffraction data and the quality and detail of the electron density reconstruction and protein structure model, are evident from this figure*[14].

The more and better data, the more accurate and detailed the final structure model will be. An image obtained at a better resolution also contains much more HD data, corresponding to the closest sampling distance in the crystal.

[14]Image available at: http://www.ruppweb.org/xray/resolution.html.

Chapter IV
SYNTHETIC INHIBITORS OF MMPs

4.1 *MMPs inhibitors.*

Initially, the Tissue Inhibitors of Metalloproteinases (TIMPs) were taken into account as potential inhibitors that could be used to control MMPs activity but, given their complexity and large molecular size, were not found as suitable inhibitors. For this reason, in recent years, many studies have turned to the careful design and synthesis of synthetic inhibitors, with defined characteristics, some of which are analyzed in the following paragraphs.

4.2 *First approaches of project and synthesis of possible MMPs inhibitors (MMPi).*

At the very beginning, the first generation of synthetic inhibitors were peptidomimetic substrate-based molecules [44] which were designed on the basis of a knowledge of the amino acid sequence of human triple helical collagen at the site of cleavage by MMP-1. However, the disappointing results discouraged the continuation of this approach. Progressively, with the use of the X-ray crystallography and multidimensional NMR techniques, the early crystal structures of the complexes, between inhibitor and protein, were resolved. On this basis, a new class of inhibitors, designed with computational techniques, was developed: the structure-based inhibitors [47]. Comparing these two classes of inhibitors, it was discovered that the first chemical inhibitors, synthesized in the 90's, still had the same potential as those peptide one, showing no improvement in potency and selectivity towards the metal proteases. Initially, one of the problems that medicinal chemists had to face, was the choice of the inhibition strategy. Indeed, it was possible to direct the synthesis towards broad-spectrum inhibitors or to choose the synthesis of selective inhibitors, turning the interest directly to a specific member of the MMP family [52]. The clinical trial data showed disappointing results for the broad-spectrum inhibitors, where a common problem was represented by the general poor activity. As a consequence of this, the interest was turned to the synthesis of selective inhibitors.

The design of selective inhibitors was developed in accordance to the "structure-based" or "ligand-based" method.

- The structure-based method: the study is based on the careful analysis of the structure of the various MMPs. The intent is to create selective inhibitors, with high affinity, through the use of computational and combinatorial techniques [47].

- The ligand-based approach aims to increase the selectivity of the inhibitor by varying the P1’ portion of the molecule, in particular the one that fits into the S1’ pocket of the MMPs. In fact, this pocket is characterized by high variability among the various metalloproteases.

An effective synthetic MMP inhibitor should have:

- A functional group capable of binding the zinc(II) ion, present in the catalytic site of the enzyme (zinc binding group or ZBG).
- One or more groups able to make hydrogen bonds with the enzyme backbone.
- One or more groups able to establish van der Waals interactions with the enzyme subsites.

The first synthetic inhibitors presented a particular sequence (Gly-Ile) in correspondence of which the human collagen is hydrolyzed by the action of MMP-1. Later on, their structure was improved on the basis of a more specific knowledge of the interaction enzyme-substrate. It should be stated that the standard nomenclature used for the proteases includes:

- S1, S2, S3, S1', S2', S3', to indicate the enzyme subsites.
- P1, P2, P3, P1', P2', P3', to indicate the groups present in the substrate (or in the putative inhibitor) which interact with the corresponding sites of the enzyme, starting from the site of hydrolysis.

These considerations led to design of three classes of compounds:

1. Ligands with amino groups only on the left side of the ZBG
2. Ligands with amino groups only on the right side of the ZBG
3. Ligands with amino groups present on both sides.

In particular, those ligands that carried the amino acid sequence on the right side of the hydrolysis site (P1' and P2') with a hydroxamic acid as ZBG, recorded a greater activity. Moreover, another important factor to consider is how the chemical nature of the various ZBG leads to variations of the inhibitory activity: this decreases starting from the hydroxamate group, up to the minimum value for the carboxylate group (passing by the phosphinate group and amino-carboxylate). The hydroxamate group acts as a bidentate chelator, in which each oxygen is located at an optimal distance compared to the catalytic zinc (1.9-2.3 A): the bond is further enhanced by interactions with specific residues of the

catalytic site, in particular Glu and Ala, which confer rigidity to the geometry. From the study of the various structures obtained by X-rays, it is possible to assume that the nitrogen of the hydroxamate group is protonated: it would thus be capable of forming a hydrogen bond with a carbonyl oxygen of the enzyme. It is clear from the studies [48], that the hydroxamic acid group gives more power to the synthetic ligand. Despite these positive aspects, however, it should be considered that this group has some drawbacks such as:

- a rapid biliary excretion;
- possible hydrolysis to carboxylic acid *in vivo*, and then decreased binding affinity;
- toxicity due to degradation to hydroxylamine in vivo.

The use of groups such as thiol or phosphonate, would lead to the same pharmacokinetic problems whereas, the use of other groups, such as carboxylate, would lead to ligands with reduced side effects but also with lower binding affinity [48].
Experimental studies have led to the design of inhibitors, grouped according to their chemical characteristics, in:

1. peptidic succinyl hydroxamates;
2. non-peptidic succinyl hydroxamates;
3. sulfonamide hydroxamates;
4. non-hydroxamates.

➢ *Peptidic succinyl hydroxamates.*

In this class, it is possible to make some general remarks about the groups P1', P2' and P3'.

- *Group P1'*: This interacts with the S1 pocket, which changes among the MMPs: by varying the group in this position, it is possible to switch from selective inhibitors for gelatinases (with wide P1' group) to broad-spectrum inhibitors (with small P1' group).
- *Group P2'*. After the resulting data from the various X-rays analyses, obtained from the complex MMP_inhibitor, it was possible to observe the real orientation of the P2' group. This is oriented outside from the enzyme, establishing few contacts with the S2' subsite.
- *Group P3'*. The introduction of various chemical groups in this position, leads only to a modest inhibitory effect on the activity.

Two inhibitors, characterized by a broad-spectrum of action, were part of this category:

Batimastat (BB-94, British Biotech) and *Marimastat* (BB-2516) (**Fig.20a-b**).

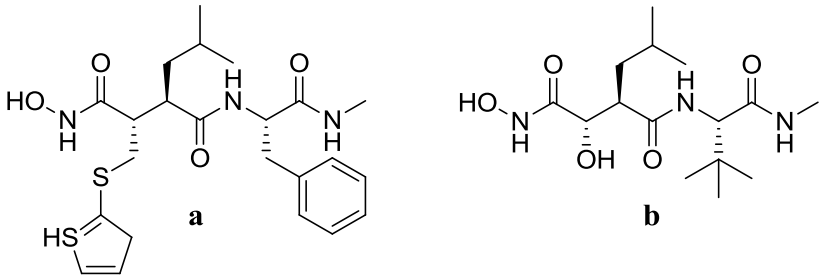

Fig 20. a) *Batimastat*, **b**) *Marimastat*.

Batimastat (**Fig.20a**) has a hydroxamate group as ZBG, whose potential antimetastatic and antiangiogenic activity was studied by carrying out experiments on rats. The effects observed as a result of its use, were: reduction of spontaneous metastasis and inhibition of the appearance of lymphatic metastasis in mice with breast cancer. A limitation of this inhibitor was its solubility: indeed, it is poorly soluble and has poor oral absorption. However, due to strong side effects, its administration was soon interrupted [49].

Also *Marimastat* (**Fig.20b**) has a hydroxamate as ZBG but presents a hydroxyl as substituent positioned in α of the hydroxamic acid, which further increases its water solubility and, in particular, allows this compound to be absorbed orally.

- Introducing some changes in the P1' group of these inhibitors, as in compound **c**, the selectivity increases. Analyzing the case of the insertion of a 3-phenylpropyl group, this has allowed to increase the selectivity towards MMP-2, both in the succinyl hydroxamates, and in carboxylates and phosphonates.

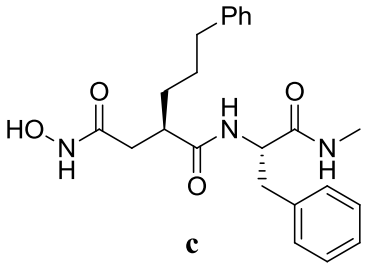

c

- The P2' group has a strong effect on the pharmacokinetic properties of the ligand: the *tert*-butyl in this position, characterizes active compounds orally, just as *Matimastat.* The accredited hypothesis is that an unwieldy group in this position provides the right degree of steric hindrance, thus shielding the adjacent amide bond, by limiting the hydration and favoring the passage of the inhibitor across cell membranes, during the absorption.

- *Non-peptidic succinyl hydroxamates.*

Included in this category, there are compounds that result from rupture of the group P2'-P3' in the pseudo-peptide structure: an example is **Ro 32-3555**, selective for collagenases.

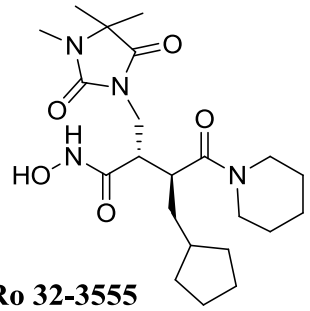

Ro 32-3555

- *Sulfonamide hydroxamates*

Prinomastat (AG 3340), a potent orally active inhibitor, belongs to this class. If compared with other structural analogues, it shows a superior efficacy in the lowering of propagation and development of tumor metastasis in animal models. It is one example of a second-generation inhibitor with selectivity over MMP-1 and -7 [45].

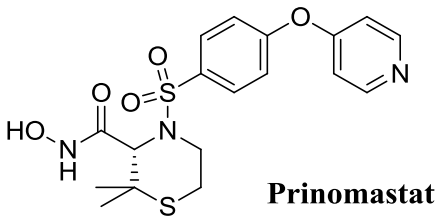

Prinomastat

On the basis of these findings, a series of α-amino-β-solfone hydroxyamates have been designed, such as compounds **d**. These have proved to be potent inhibitors of both MMP-2 and MMP-13. These ligands were allowed to assign:

- more power to the aryl-ether derivatives rather than thioethers
- the disubstitution on the alkyl amine placed in α to the hydroxamate, leads to a loss of power whereas, the inclusion of simple alkyl amines, provides activities both on MMP-2 and MMP-13.

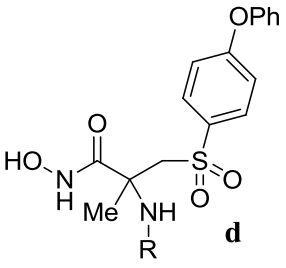

d

- *Non-hydroxamates*

The study of these compounds is aimed at the research of different ZBGs than the hydroxamate group, in order to eliminate or reduce the characteristic toxic effects. The toxicity problems are attributable to the high binding affinity for zinc (II), but also for other transition metals, such as Fe (III), Cu (II), Ni (II). These metals are located within the structure of metalloproteins, variously distributed in the body: therefore the bond to the zinc of MMPs cannot be exclusive. This is the basis of the scarce therapeutic safety of the inhibitors of MMPs with hydroxamate group of first and second generation. A first class object of study is the one represented by di-thiols, as a replacement to the hydroxamic acid group, such as compound **e** [50a].

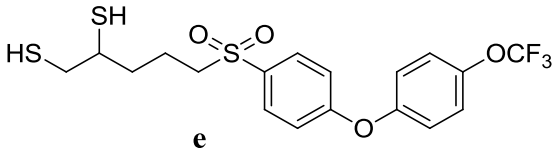

e

It is an inhibitor both of MMP-2 and MMP-9, with Ki in the order of nanomolar. The number of carbon atoms of the side chain do not strongly influence the inhibitor-enzyme binding [50].

4.3 *New selective MMPs inhibitors.*

Despite the various problems associated with hydroxamic acid, and the low-potency related to the carboxylic acid, additional inhibitors have been designed with these two ZBGs, improving the selectivity for the various components of MMPs. Wyeth in 2005 published a series of biphenyl sulfonamide carboxylate MMPi, with a marked selectivity towards MMP-13. Among these, compound **f** showed a high selectivity over MMP-1 (IC_{50}=400 μM), MMP-7 (IC_{50}=1.1 μM), MMP-9 (IC_{50}=7 μM), and MMP-14 (IC_{50}=5 μM), having a carboxylic acid as ZBG [54].

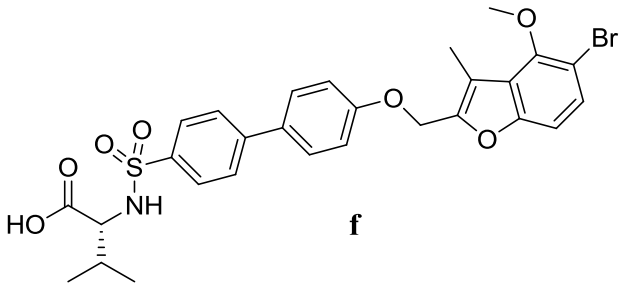

f

Subsequently, other inhibitors [57] were generated by using a fused ring system, trying to obtain a greater selectivity towards MMP-12: an example is compound **g**. It was found that restricting the rotation of the biphenyl group is favored the binding in the less flexible MMP-12 S1' pocket.

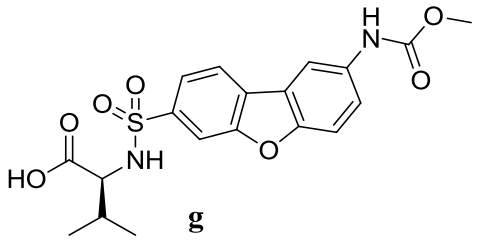

g

Inhibitor **g** showed a 60-fold selectivity for MMP-12 over MMP-13. This inhibitor demonstrated *in vivo* efficacy in a MMP-12-induced mouse model of pulmonary inflammation. In recent years, several research groups have designed molecules with the aim of increasing selectivity. Rossello *et al*. have developed selective hydroxamic acid inhibitors of MMP-2 as potent anti-angiogenic agents [55]. The inclusion of alkyl substituents, at the carbon adjacent to the hydroxamic acid, has increased lipophilicity and therefore, the interactions with the S1 region of the active site, increasing the selectivity of the compound towards the MMP-2 (compound **h**).

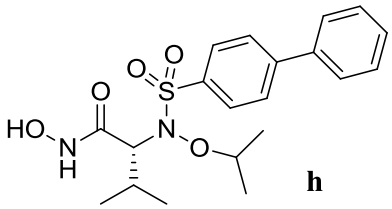

h

In the study of Casalini *et al*, the new fluorinated compound **i**, arylsulfone-based MMP inhibitor**,** containing carboxylate as ZBG was synthesized as radiotracers for positron emission tomography. It showed an IC50 of 16 nM on MMP-2 and an IC50 of 107 nM on MMP-9.

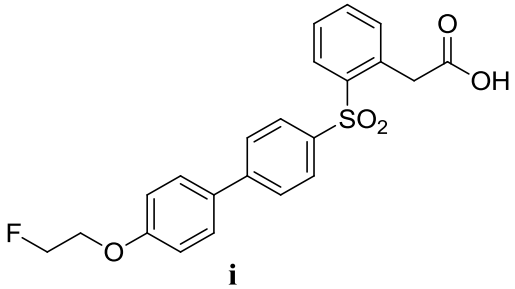

i

These are very good potency data considering the carboxylate nature of the ZBG. It has a good activity for deep S1′ pocket of MMP-2/9/12/13. This compound showed good characteristics of activity and selectivity to be used as a probe in the glioblastoma tumor model. In addition, the concomitant inhibition of MMP-12 and MMP-13 should be beneficial, because also these enzymes have been recently found to be highly expressed in U-87 MG glioblastoma [51]. Now, many research studies are turning their attention to structures having non-hydroxamic groups as ZBG, trying to gradually increase the affinity and selectivity of these ligands to the protein and, at the same time removing its typical side effects.

4.4 *Recent advances in matrix metalloproteinase inhibitor (MMPi) design and development.*

This paragraph shows three recent synthetic approaches, aiming to develop better inhibitors of MMPs, analyzed by Jacobsen *et al*. *[53]*.

1. Research of new zinc-binding groups (ZBG);
2. Study of non-zinc-binding MMPi;
3. Design of MMPi that form covalent adducts with proteins.

4.4.1 *Research of new zinc-binding groups (ZBG).*

The approach adopted with this class of inhibitors is based on the physiological mechanism by which MMPs anchor their endogenous substrate, directly involving the catalytic zinc.
The mechanism initially involves the attachment of the substrate in the catalytic site of the enzyme, which is followed by the zinc-bound water molecule attacks the substrate carbonyl carbon: after the transfer of protons through a conserved Glu residue to the amide nitrogen of the scissile bond, results in peptide cleavage. The purpose of the ZBG in the inhibitor molecule is twofold. This group displaces the zinc-bound water molecule and thus inactivates the enzyme and, moreover, it ensures the anchoring of the ligand to the substrate-binding pockets. As explained in the previous paragraph, all MMPi had one or more group ZBG, such as: hydroxamic acid, carboxylic acid, phosphonic acids and thiols and among them, the hydroxamic acid stood out as the best chelating group of the zinc atom. In particular, the OH group and the NH group of this ZBG, form hydrogen bonds with two aminoacids present in the catalytic site: Glu and Ala, respectively. The need to find other ZBG, derives from its poor bioavailability *in vivo* and from the side effects

common in many hydroxamate MMPi, such as the muskoloskeletal syndrome (MSS), highlighted in clinical trials. Examples of innovative ZBGs are: **ZBG I**, **II**, **III**, **IV**.

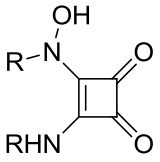

ZBG I

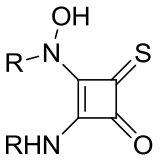

ZBG II

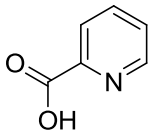

ZBG III

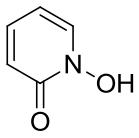

ZBG IV

Squaric acid-based hydroxamic acid analogues (**ZBG I-II**) [58], have been developed to target the MMP-1. These new chelators, form a 6-membered ring upon metal chelation as opposed to the 5-membered ring of hydroxamic acid.

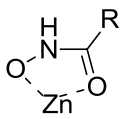

Hydroxamic acid Squaric acid

The compound **l** was reported to have an IC_{50} =15μM on MMP-1, with a 18-fold improvement compared to its carbonyl derivative.

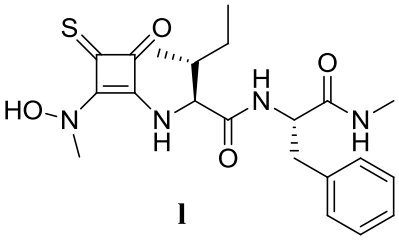

l

The particular bond of squaric acid may provide a viable alternative for the precise positioning of the inhibitor in the various pockets of MMPs. Further developments are still necessary for this new scaffold.

Another example is **ZBG III** [59]: its principal characteristic is the preference binding for late transition metals. It is a bidentate chelator of the zinc ion, through the nitrogen of the pyridine and the oxygen of the carboxylate. This ZBG is 100-fold more potent on MMP-3 compared to acetohydroxamic acid, but also in this case further studies are needed. Another group is represented by heterocyclic bidentate ZBGs, such as **ZBG IV** [60]. They were selected because have common points with the hydroxamic acid, such as: a 5-member

chelate monoanionic, with potentially better biostability and tighter Zn^{2+} binding due to ligand rigidity. The search for new ZBG has led to encouraging results, even if there are still concerns about the use of strong metal chelating groups that may preclude the development of highly selective inhibitors, due to the highly conserved nature of Zn^{2+} in the active site of all MMPs. Many challenges remain for these MMPi, including demonstrations of significant improvements of action on MMPs. Also, more and more studies on the bioavailability and pharmacokinetics of these MMPi are needed to determine if the improvements in these properties are actually conferred by these compounds.

4.4.2 *Non-zinc-binding MMPi.*

These inhibitors are based on the fact that by eliminating or minimizing the interactions with the catalytic zinc, compounds with increased selectivity towards the MMPs could be obtained, because the metal site is well conserved among these proteases. Several of these inhibitors (such as compounds **m**,**n**) show high MMP-13 selectivity and bind deep within the S1' pocket, to induce a specific protein conformation.

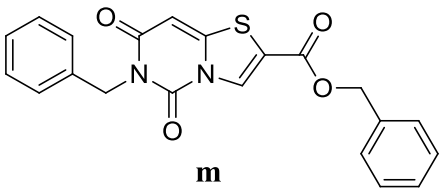

m

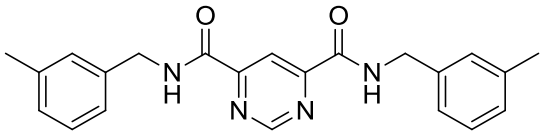

n

Some characteristics are common among members of this class: generally, they are long molecules with linked aromatic or otherwise planar ring structures, have a carbonyl group and N–H groups to offer opportunities for hydrogen bonding interactions with the S1' pocket. A major reason for the selectivity of **m**, is the ability to induce a unique conformation in the S1' specificity loop of MMP-13 that is not accessible in other MMPs. It is still not completely clear whether this selectivity of action is due solely to the absence of ZBG.

4.4.3 *Mechanism-based MMPi.*

The activity of these inhibitors is based on the delay of the protein_inhibitor complex dissociation. The characteristic mode of action requires that the inhibitor acts as a suicide substrate, in which a functional group present on the structure is activated by the zinc atom, leading to a covalent modification in the enzyme structure.

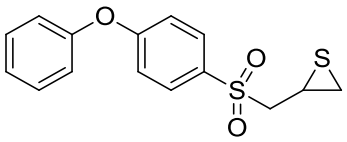

o

The proposed mechanism for the compound **o** is that the thiirane group, activated by coordination with the zinc atom, leads to the opening of the ring as a result of the nucleophile attack on Glu^{404}, giving a covalent bond between the carbon of the thiirane ring and the amminoacid. This bond ensures the inhibitor to the active site leading to low inhibitor dissociation. The use of mechanism-based, slow-binding inhibitors may provide a new approach to gain selectivity in MMPi design.

Chapter V

INTRODUCTION TO THE EXPERIMENTAL PART

In humans, the family of matrix metalloproteinases (MMPs) is composed by 24 closely related proteins that share a catalytic zinc ion, responsible for their catalytic activity and a typical metzincin fold. Their ability to cleave the extracellular matrix (ECM) allows them to remodel the extracellular space, and change connections from cell to cell through the release of ligands present on the cell surface. These changes affect cellular signalization, leading to cellular phenotype modification, extending the role of MMPs far beyond that of mere enzymes. The alteration of MMPs expression is related to the manifestation of a series of severe diseases such as autoimmune pathologies, cancer, myocardial infarction, rheumatoid arthritis and Alzheimer's disease. Moreover, MMPs are involved in the control of physiological processes such as ovulation, wound healing and growth. For these reasons, it is important that their activity at both the transcriptional and post-transcriptional level is finely regulated. The regulatory mechanisms are at several different levels: i) induction or inhibition of the transcription process, mediated by cytokines, hormones, growth factors, and factors which promote tumor growth; ii) secretion and endocytosis of the propeptide; iii) activation of the zymogen by the suitable protease; iv) inhibition by physiological mediators, such as α2-macroglobulin and TIMPs (tissue inhibitors of MMPs).

In recent years, pharmaceutical research has dedicated many efforts to the discovery MMP inhibitors as potential agents for anticancer therapy. In particular, synthetic inhibitors of MMPs have been proposed and tested as potential anti-invasive and anti-angiogenic compounds, characterized by a minor impact on the organism having also minor side effects compared to other drugs commonly used in therapy. Early peptido-mimetic inhibitors such as b*atimastat* and *marimastat,* were subjected to clinical trials which resulted disappointing due to severe side effects. More recently, other non peptido-mimetic compounds were tested in clinical trials. *Prinomastat* is a compound which presents an important turning point in the basic structure of the inhibitors of MMPs: a scaffold carrying a sulfonamide group, capable of forming numerous interactions with various amino acids, present in the sites closest to the enzyme recognition sites. Despite this, the main

limitations of these synthetic ligands are:

- poor selectivity of action, for their inability to distinguish between the various members of the MMP family.
- heavy side effects, such as arthralgia and loss of consciousness, that occur after prolonged therapy and often require the interruption of the latter.

Current knowledge of the three-dimensional structures of these proteins, obtained thanks to the use of X-ray crystallography and the determination of the *in vitro* activity of many synthetic inhibitors tested on MMPs, have allowed the acquisition of further information, necessary for the synthesis of more specific and more active ligands. Indeed, on the basis of recent discoveries, it is known that the pharmacophore should have a zinc-binding group (ZBG) capable of complexing the zinc ion, present in the catalytic site and a non peptidic portion, oriented towards the sites S1, S1', S2' of the enzyme, capable of establishing interactions with those pockets. Important point of selectivity is represented by the S1' pocket, precisely defined "selectivity pocket", because characterized by different shapes and geometries among the members of the MMPs family: it is, therefore, objective of interest for modulating the selectivity of the inhibitors.

In particular, three MMPs have been considered important targets in cancer, cardiovascular and lung diseases: MMP-8, MMP-9 and MMP-12. MMP-8 is the most potent collagenase that degrades collagen type I, which represents the major component of the ECM present in the lung. The main disorders with pathological nature are associated with a high degree of oxidative stress, where again the activity of MMP-8 is correlated: in fact its plays a fundamental role in the activation of reactive oxygen species (ROS) [66-67]. High levels of MMP-8 and MMP-9 were found in lung secretions of patients (adults and children) suffering from acute forms of lung disease. In asthmatic children it was found that eosinophils and macrophages release higher amounts of MMP-8, whereas in healthy persons neutrophils are the main source for MMP-8. Sixty percent of lung transplant patients develop obliterative bronchiolitis (chronic rejection), in which MMP-8 and MMP-9 levels are elevated [74]. Many reports the literature [68–69] describe increased MMP-8 activity during cardiovascular diseases: the serum and plasma MMP-8 concentration is correlated with plaque progression and the severity of coronary disease. Moreover, MMP-8 was demonstrated to be expressed in head and neck squamous carcinoma cells, indicating its important role in carcinoma progression [70]. Other diseases such as rheumatoid

arthritis [71], gastrointestinal disorders [72] are characterized by altered levels expression of MMP-8. [73]. For MMP-9, Rybakoski [75] has analyzed different its involvement as a mediator enzyme in cardiovascular disease, cancer and neuropsychiatric disorders. Welsh *et al* [76] have defined a role for MMP-9 in the incidence of coronary arterial disease. Further involvement of this metalloprotease was defined in coronary artery disease [77], where a high level of MMP-9 expression was detected [78]. In the study by Sakata *et al*. [79] an involvement of this metalloprotease with cancer, has been described. MMP-9 was found over-expressed in an epithelial tumour of the ovary with an involvement in lymph node metastases of the ovarian carcinoma cells, was found. Instead, the attention to MMP-12 is due to its involvement in lung inflammation and remodelling [80]: increased levels of this metalloproteinase were found in the lung of human patients affected by chronic obstructive pulmonary disease (COPD). MMP-12 is the primary elastolytic enzyme of alveolar macrophages [81]. A valid intervention for COPD / emphysema patients could involve the blocking of MMP-12. Clinical studies on MMP-12 deficient mice showed their protection against the development of emphysema induced by cigarette smoke.

The subject of this thesis has been the study of a way of cellular signalization which involves MMPs: the *homodimerization process*. This is important in signal transduction, implicated in many biological processes, both in the homoeostatic regulation and in various processes characterized by a pathological nature. To obtaining structural information for the design of molecules able to control the signalization pathways, the proteins involved will have to be crystallized in complex with ligands that induce dimerization. Therefore, in the first part of my thesis's project I carried out the study of protein-inhibitor complexes, testing ligands previously synthesized by the group of Prof. Rossello (**LC20**, **LC29** and **EN238**) on MMP-9 and MMP-12. In the second part of the thesis, on the basis of the X-ray results, new inhibitors were designed with the aim of increasing the selectivity towards these enzymes.

5.1 *Crystallographic part*

5.1.1 Introduction

This crystallographic study has involved MMP-9 and MMP-12 as model system, to study the protein dimerization process using synthetic inhibitors. Protein-protein subunit interactions play key roles in catalysis and through homo- and heterodimerization events act in concert to functionally tune living systems. Among the vast ensemble of possible molecular interactions, only a few protein dimerization events serve to modulate biological activity. To discover or confirm which interactions are regulatory, various methods can contribute in a sequential manner: predictive *in silico* modeling is a first approach to describe the interaction between sites of folded protein subunits for which primary sequences are available. An efficient crystallization screening method is important in drug design to yield high resolution crystallographic structures of protein-ligand complexes, to understand inhibitor selectivity and potency for various members of an enzyme family. The strategy used in the following analysis begins with a single condition for each protein-ligand complex: progressively, more crystallization conditions to obtain the best possible crystalline form are tested.

In the technique of X-ray crystallography, the X-rays are diffracted by the crystal form a diffraction pattern, from the analysis of this pattern, using the intensities of the reflections (diffraction spots) it is possible to obtain the electron density map corresponding to the protein contained in the unit cell of the crystal. Because the phases are an unknown quantity and need to be "guessed" (probabilistic calculation from heavy atom derivatization or from a model believed to resemble the protein in the crystal) at the very beginning the map is not very accurate, so it is necessary carry out several cycles of refinement with the aid of specific programs that combine general chemical and structural knowledge of proteins with the crystallographically acquired data. Among the unknown components of the unit cell there is the ligand. To create a restraint file for the crystallographic programs to work correctly, the ligand is constructed using the monomer library sketcher from CCP4 program. The result is both a restraints file and a coordinates file. The coordinates of the ligand are fitted at the binding site on the basis of the electron density, using COOT. This first stage is done manually by translating the molecule in the electron density and moving each atom in the appropriate place. The initial draft is refined using COOT and the ligand restraint file, then the protein and ligand structure is further refined with REFMAC5, this completes the first cycle. The model was also improved with

refinement cycles in phenix.refine. After each refinement, COOT is used to analyse the agreement between the model and the electron density end until an accurate electron density map of the ligand-protein complex has been achieved. The final model is used to understand the variety of interactions that characterize the specificity of a protein-substrate or protein-inhibitor interactions. From this analysis synthetic ligands that fit better the topography of the protein catalytic site can be designed characterized so as to achieve greater specificity.

5.1.2 *Inhibitors tested*

The inhibitors used in the crystallization studies have been: **MP24**, **LC20**, **LC29**, **EN238**. All these ligands were synthesized by the research group of Prof. Rossello[15].

- **LC20** and **LC29** are bifunctional ligands (or dual inhibitors) presenting two identical arylsulfonamide scaffolds, able to fit in two pockets of the proteins, linked by a spacer. These ligands have a different zinc-binding group (ZBG) able to coordinate the zinc (II) ion present in the catalytic site of MMPs: a hydroxamic acid for LC29 and a carboxylic acid for LC20.
- **EN238** is a mono-ligand: with a single scaffold and a carboxylic acid as ZBG.
- **MP24** is a bifunctional hydroxamate with a scaffold similar to the previous ones and a spacer longer than the one present in LC20 and LC29 (MP24 has been previously tested by Dr. E. Stura and L.Vera and the results are shown below in order to complete the discussion).

[15]Associated Professor at the Pharmacy Department of the University of Pisa, Scientific Field of Pharmaceutical Chemistry CHIM/08.

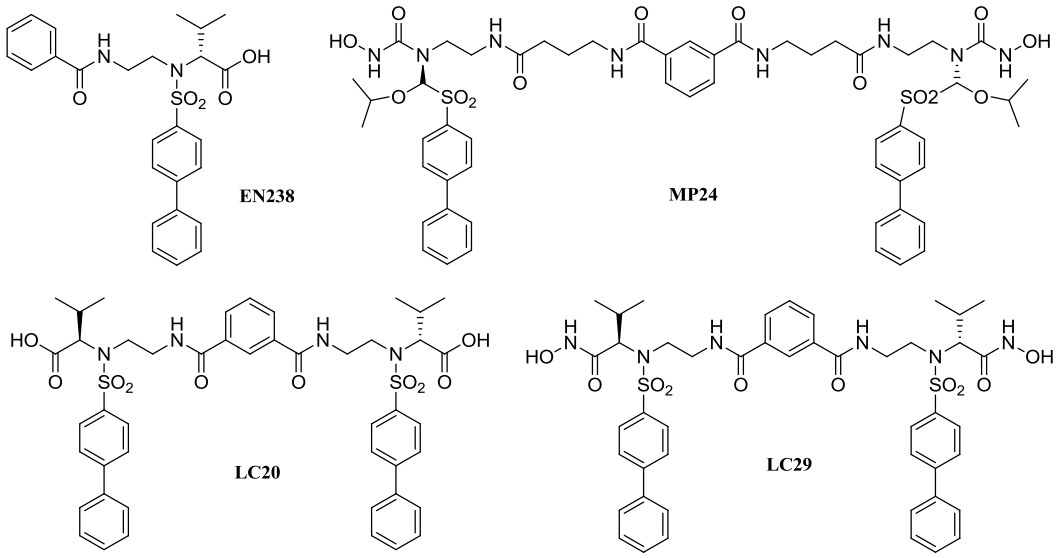

Depending on the different structure of the inhibitor, the stoichiometry of the ligand and the protein used to form the crystals is varied. Ligands bearing two ZBGs and potentially able to interact with two proteins simultaneously, have been tested with a 1 inhibitor : 2 proteins stoichiometry. This stoichiometry facilitates the formation of a homodimeric complex in which two molecule of protein are simultaneously inhibited by a single molecule inhibitor. Otherwise, ligands with only one ZBG are used with a 1 protein : 1 inhibitor stoichiometric ratio. In this case the stoichiometry facilitates the formation of a monomeric complex in which one ligand molecule interacts with one protein molecule.

5.1.3 *Crystallization and structure determination.*

The main difference among all the tested ligands is given by the presence or absence of the linker, different lengths and the nature of ZBG.

Clinical studies have revealed problems of toxicity and poor bioavailability for first and second generation hydroxamates. The toxicity problems are attributable to indiscriminate binding of these compounds due to the high binding affinity of the hydroxamate group for Zn (II) and for other transition metals such as Fe (III), Cu (II) and Ni (II). These metals are distributed throughout the body and are also present inside many metalloproteins. Hydroxamate based inhibitors bind the zinc ion of various MMPs with poor selectivity between family members. This is the main reason why the hydroxamate group, present in the vast majority of MMPs inhibitors, give them low therapeutic safety. The carboxylate group is therapeutically safer than hydroxamates [41].

We have studied whether a linker can confer selectivity to an inhibitor. The linker length

influences the flexibility of inhibitors and their adaptability to different pocket proteins. The assumption is that the linker needs to be long enough, to allow the correct alignment for the two faces of the interacting MMP catalytic domains, without making any steric strains with its groups but eventually, providing additional stabilizing interactions in the formation of the dimer. Selectivity can be achieved because each protein responds differently to the different proposed linkers, irrespective of similar structure of the catalytic domain. The linker distance is an important homodimerization parameter that depends on inter-protein contacts. Since these interactions are difficult to predict, this parameter is difficult to optimize.

- ***Crystallization of MMP-9·MP24.***

For the crystallization of MMP-9·MP24 complex, the stoichiometry was varied. The conditions were: 2 proteins with 1 ligand and in the presence of excess ligand. This compound crystallized readily in complex with MMP-9 (**Fig.21**) but could not be crystallized with a MMP-12 homodimer, inspiriting the design of ligands better suited to obtain crystals that contained the bi-functional ligand in complex with an MMP-12 dimer.

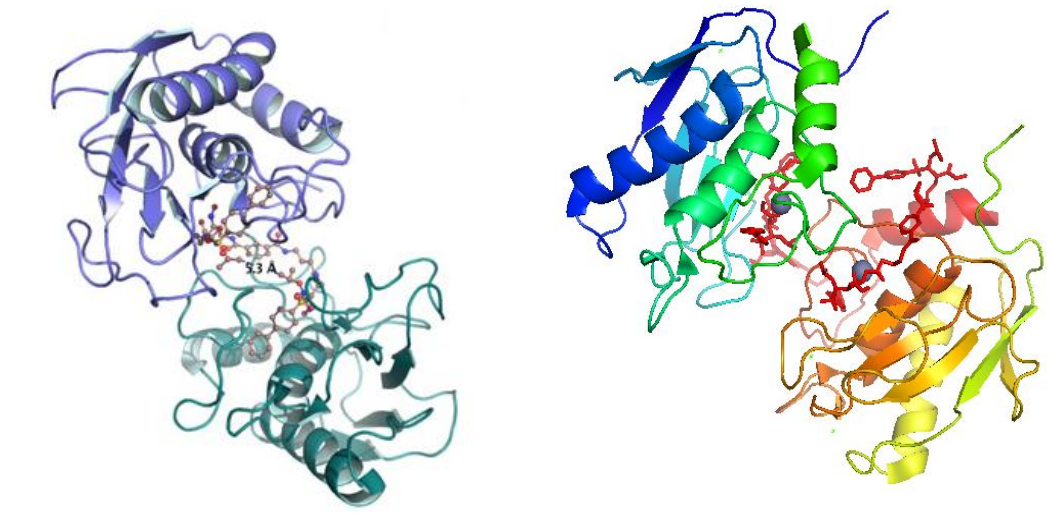

a **b**

Figure 21. ***a)*** *The MMP-9_MP24 homodimer in the asymmetric unit of PDB entry 4H2E. This MMP-9 homodimer is very similar to that obtained for compound LC29.* ***b)*** *MMP-9-MP24 monomer (PBD entry 4H1Q).*

An excess of bi-functional ligand, promotes the attachment of one inhibitor *per* protein (PDB entry 4H1Q), where MP24 behaves therefore as a monofunctional ligand, with a

resolution to 1.59 Å (**Fig.21b**). Instead, with a stoichiometric ratio of 2 proteins for 1 ligand, the formation of a homodimer ensues: one bi-functional inhibitor *per* protein dimer. These crystals diffracted to 2.9 Å (**Fig.21a**).

- ***Crystallization of MMP-9·LC20.***

The X-ray analysis from the crystallization of MMP-9 with the dual inhibitor LC20, shows the formation of a homodimer (**Fig.22**) with space group $P2_12_12$ (PDB entry 4HMA).The crystals had a resolution of 1.94 Å, better than the resolution of MMP-9_MP24 homodimer.

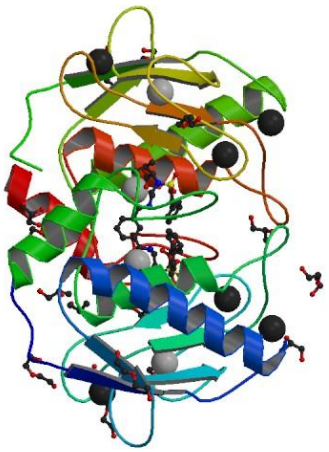

Figure 22. *Homodimer of complex MMP-9·LC20.*

- ***Crystallization of MMP-9·LC29.***

The crystallization of this complex has been carried out both with and without the *streak seeding* method. In the first case, the seeds from the MMP-9-MP24 homodimeric complex were used. The resulting complex crystals diffracted to a resolution of 1.9 Å (**Fig.23**), in space group P1 (PDB entry 4H82). Instead, in the spontaneously nucleated drop, the crystals diffracted to only 2.84 Å. A seed has provided a template on which additional macromolecules were assembled under the proper conditions grow to form a better crystal. Also in this case, crystals with a higher resolution than the homodimeric complex MMP-9·MP24, were obtained [27].

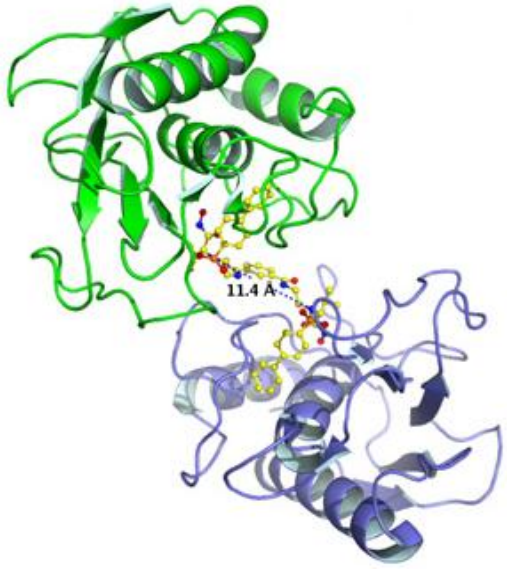

Figura 23*: MMP-9-LC29 homodimer diffracted to 1.9A (PDB entry 4H82).*

❖ ***Comparison between the complex of MMP-9·LC29 and MMP-9·MP24.***

The X-ray crystallographic structure of the complex between LC29 and MMP-9 was superimposed onto the complex between MP24 and MMP-9 (**Fig.24**).

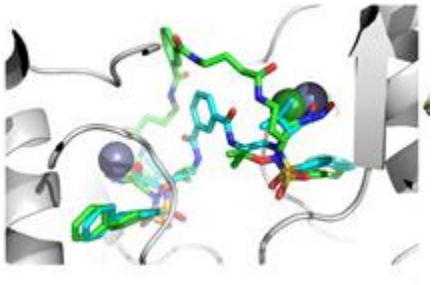

Figure 24. *Superposition of the complex MMP-9·MP24 (inhibitor in green) in complex with MMP-9·LC29 (inhibitor in cyan).*

The crystal structures show that the bivalent ligands superimposed well into the inhibitor part, but this is not valid for the spacer regions. This evidence points out that an alternative linker with a shorter spacer, forms the same homo-dimer but with a different geometry as expected from its design. Studying the superimposition becomes clearly evident that the replacement of the MP24 spacer with a shorter one, gives the correct distance and geometry of the twin inhibitor, capable to homo-dimer formation of MMP-9. Indeed, LC29 with a shorter linker has instead a better affinity than MP24 with a longer linker: shortening the length of the linker, the flexibility decreases but at the same time the affinity increases. The inhibitor MP24 was crystallized with MMP-9, but no condition has allowed the crystallization with MMP-12. This ligand was not properly synthesized for the crystallization, but rather with the aim of promoting the design of best ligands, able to allow the dimerization of MMP-12. Thanks to the study of the structural problems regarding MP24 and its interactions with MMP-9 in both the stoichiometry, it has been possible to design other dual inhibitors with shorter linker, compatible with the crystallization on MMP-12 and MMP-9.

❖ ***Comparison between the complex of MMP-9·LC20 and MMP-9·LC29***.

The biological data (reported below) regarding the affinity of these two inhibitors and the results from X-rays analysis (**Fig.25**), highlights how the hydroxamic acid (present as ZBG) in LC29 is a better chelator, of the zinc ion, compared

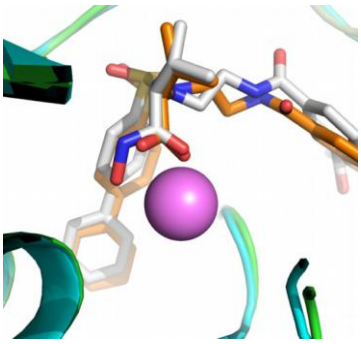

Figure 25. *Superposition of the ligands LC20 and LC29 in their respective complexes with MMP-9, compared at the coordination site with the zinc atom of MMP-9.*

to the carboxylic acid present in LC20.

- ***MMP-9 complex.***

Both compounds LC20 and LC29 have a shorter linker than the original MP24, these ligands are more easily crystallized in complex with MMP-9 and crystals structures at atomic resolution have been obtained for both. Similar homodimers mediated by the bifunctional ligands are present in the asymmetric unit. None of these spacers impose serious restrictions on the formation of MMP-9 homodimers, because of their residual flexibility.

- ***Crystallization of MMP-12·LC20.***

Following the crystallization of this complex in space group $P2_12_12_1$,, a homodimer, was found in the lattice (**Fig. 26**). In this case, micro-crystals appeared spontaneously within a few minutes of mixing the protein-inhibitor complex drop with the precipitant drop from the reservoir (**Fig. 27A**). This allowed rapid optimization of the crystallization conditions, eliminating the needle crystals by controlling the rate of nucleation. Several changes in conditions crystallization were needed to obtain large crystals. Gradually, it was possible to optimize the conditions to reproduce larger crystals (**Fig.27B**). Excessive nucleation was controlled by lowering the inhibitor concentration. Thus 2 MMP for 1 bi-functional ligand was tried and a different crystal form was obtained (**Fig.27C**). This second crystal form is the result of changes in the conditions that improved on initial needles, described in **Fig.27A** [21, 41].

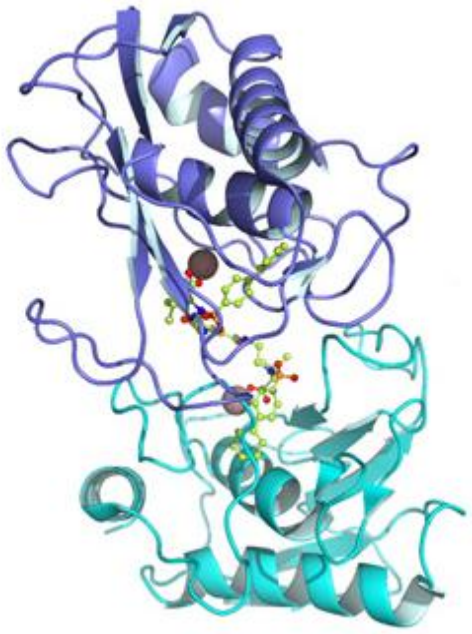

Figure 26. *MMP-12_LC20 complex in homodimers structures with $P2_12_12_1$ space group (PDB entry 4H30).*

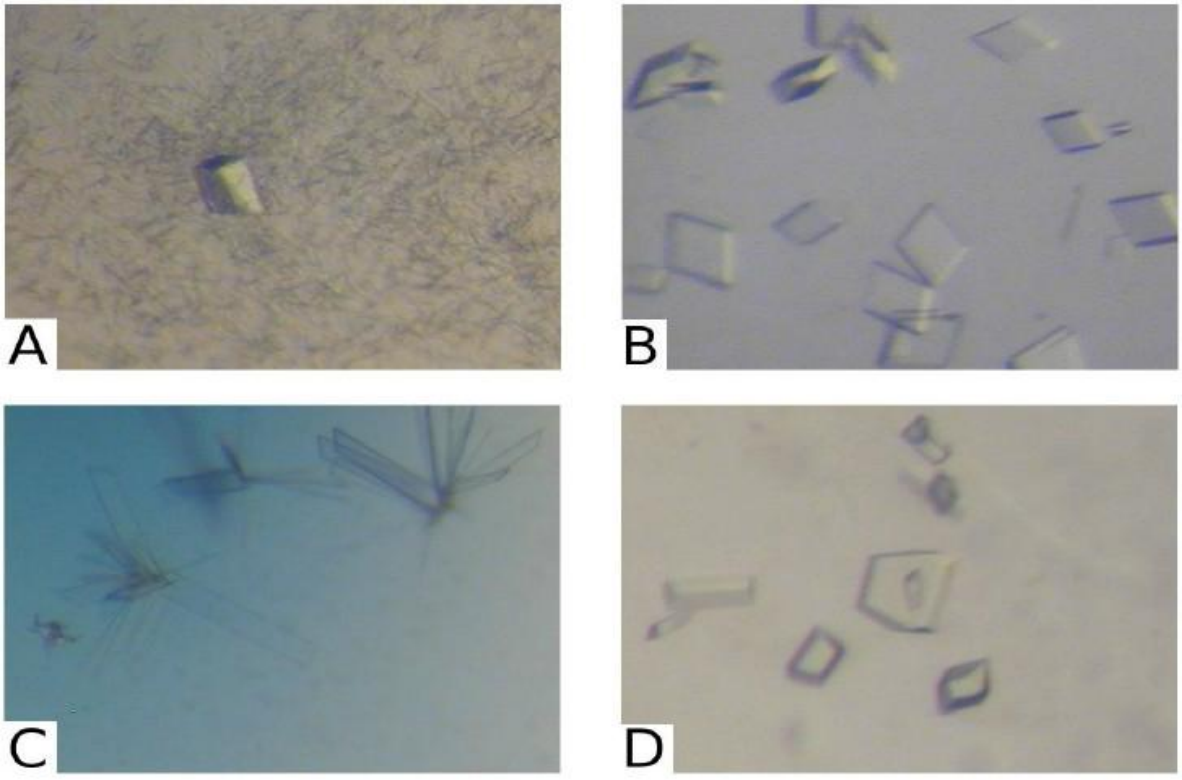

Figure 27. *Crystals of MMP-12 complexe with compounds LC20 and EN238. (**A**) A crystal shower was obtained initially. After a few days larger crystals appeared. (**B**) By refining the reservoir conditions the needle shower was avoided and only the prismatic crystals grew spontaneously. (**C**) The needles were improved and the structure determined. The homodimer in the crystal, is identical to that found in the prismatic crystals in A and B, but there is a small variation in relative orientation in C and D, with poor MMP-12 density for molecule D. (**D**) Crystals of MMP-12 with mono-functional ligand EN238. Morphologically these crystals are similar to those in (B) for ligand LC20. The space groups are the same and the cell parameters similar but the packing is different*[16].

Using two different crystallization conditions MMP-12·LC20 complex crystals were obtained with same protein (MMP-12 wild type F171D, lot 23.3, 364.5 μM with AHA 10 mM) and the same inhibitor in two different crystalline forms characterized by two different space groups ($P2_1$ and $P2_12_12_1$), corresponding to different polymorphs (**Fig.28**).

[16]Antoni, C.; *et al*, Crystallization with bi-functional ligands, *J. Struct. Biol*. 2013, **182**, 246-254 [41].

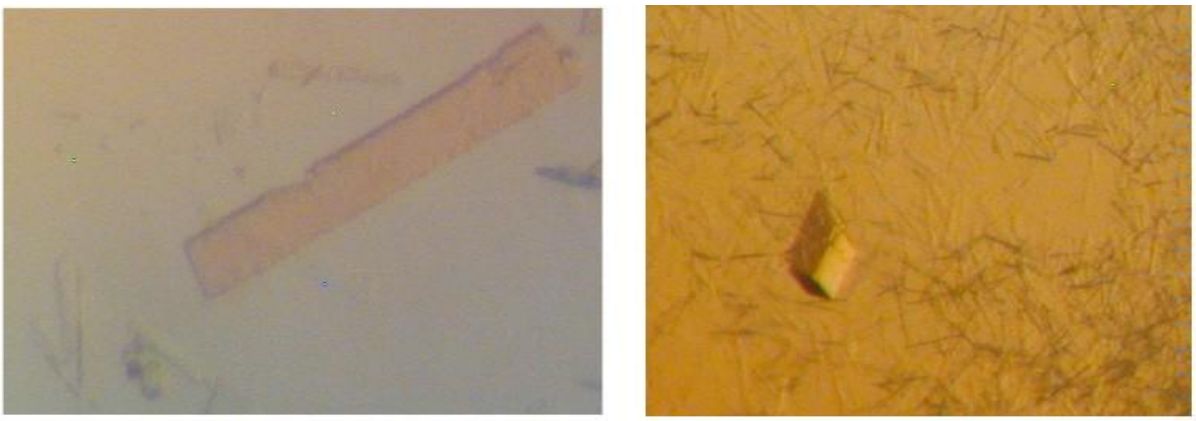

A **B**

Figure 28. *Crystal polymorph of MMP12·LC20 complex. A) space group $P2_1$, B) space group $P2_12_12_1$.*

➢ ***Crystallization of MMP-12·LC29.***

In this case LC29 led to the formation of a homodimeric structure (**Fig. 29**), different from that already described for the same protein with LC20. The crystals belong to space group $P2_1$ (PDB entry 4H49). Both of these inhibitors interact with two protein subunits of MMP-12, forming dimers. Affinity measurements with MMP-12 show a greater potency for the carboxylate based inhibitor than for its hydroxamate counterpart, a fact never reported before. In addition, analyzing the hydroxamate group with respect to the carboxylate one, the ability of the linker to induce dimerization, was not altered.

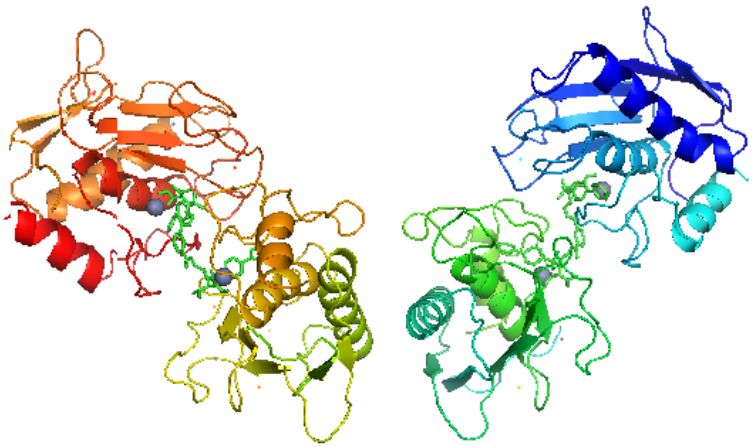

Figura 29. *MMP12 in complex with LC29.*

❖ ***Comparison between the complex of MMP-12·LC20 and MMP-12·LC29.***

Both the biological data regarding the affinity of the two inhibitors and the results from X-rays analysis, highlight how the carboxylic acid (present as ZBG) in LC20 is a better chelator of zinc atom compared to the hydroxamic acid present in LC29 (**Fig.30**), where the distortion of the LC20 in the dimeric complex leads to a closer approach of this group to the zinc, compared hydroxamic acid of LC29. This result is noteworthy, taking in consideration the side effects associated with the use of a hydroxamate group as ZBG.

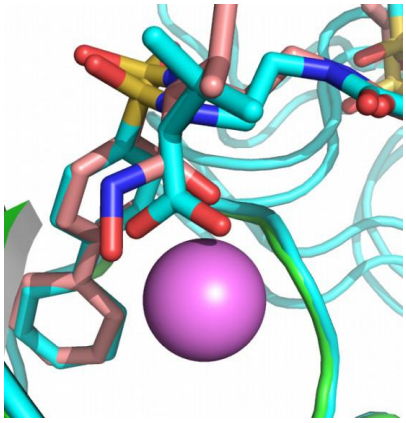

Figure 30. *Superposition of the ligands LC20 and LC29 in their respective complexes with MMP-12, compared to the coordination with the zinc atom of the metalloproteinase.*

❖ ***Comparison between the MMP-12·LC29 and MMP-9·LC29 complexes.***

In order to study induction of homodimerization also on MMP-12, the crystal structure of the complex between LC29 and MMP-9 was superimposed to that of LC29 and MMP-12 (**Fig. 31**). In this case the semi-rigid linker superimposes well in the two structures with the different metalloproteins, but it is not able to give the same homodimerization.

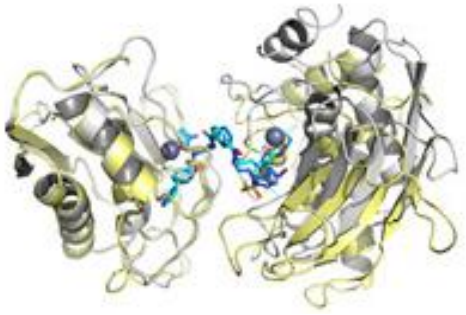

Figure 31. *Superposition of the complexes between LC29 with MMP-9 and MMP12.*

➢ ***Crystallization of MMP-12·EN238.***

EN238 is a carboxylic inhibitor designed to provide monomers on MMPs family. Using the standard crystallization conditions already defined by Dr. E. Stura and L.Vera to obtain MMP-12 complex [12, 27] crystals appeared after few minutes and seeding was not necessary. Afterwards, by working out the electron density map, it was possible to see that the monomeric inhibitor led to a homodimer formation in the $P2_12_12_1$ asymmetric unit, behaving not as a simple monomer, as hypothesized (**Fig.32-B**). EN238 favoured the

formation of a dimer through specific interactions contributed by each individual inhibitor, and each protein subunit of the homodimer (PDB entry 4H84).

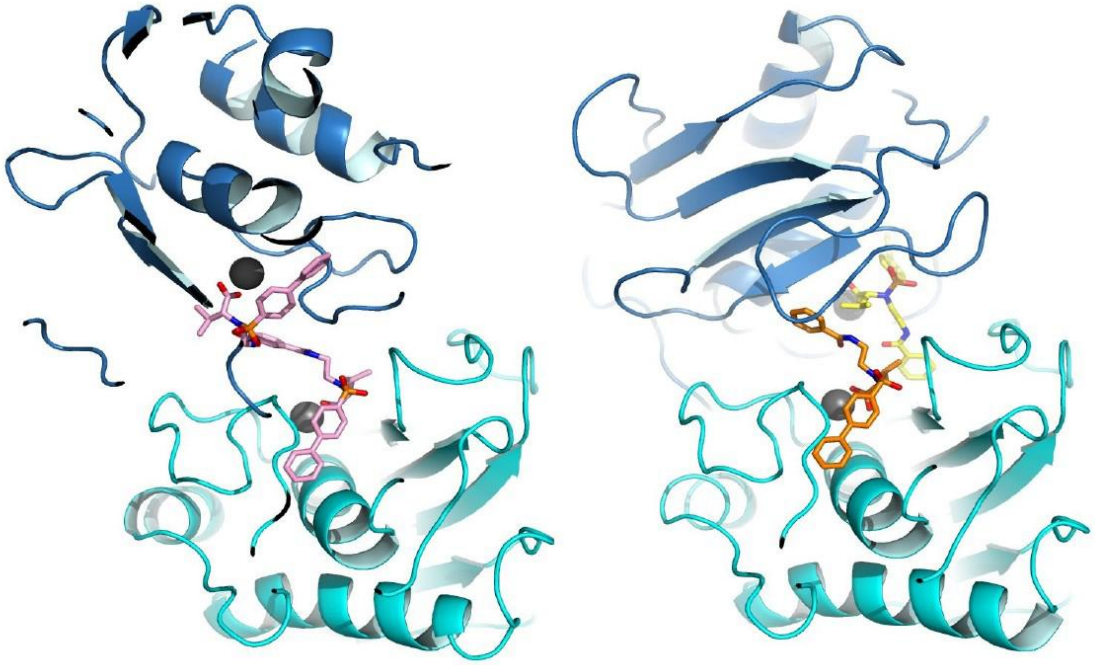

a **b**

Figure 32. *(**a**) Chemical structure of compound LC20 and packing of the MMP-12 induced homodimer in space group $P2_12_12_1$. (**b**) Chemical structure of compound EN238 and MMP-12 homodimer formed with compound EN238 in the same space group, $P2_12_12_1$. This MMP-12 homodimer is different from that formed with compound LC20.*

❖ ***Comparison between the complexes of MMP-12·LC20 and MMP-12·EN238***

Data from crystals of the MMP-12·EN238 complex, have similar cell parameters, but not identical to those for the MMP-12·LC20 complex. Observing the superposition of MMP-12 bound to the monofunctional and bifunctional ligands, it is possible to see that the positioning of the mono-functional ligand matches that for the bi-functional one (**Fig.33**) except regarding the homodimerization mode (**Fig.32a-b)**. It may therefore be hypothesized that MMP-12 imposes strong constraints on ligand

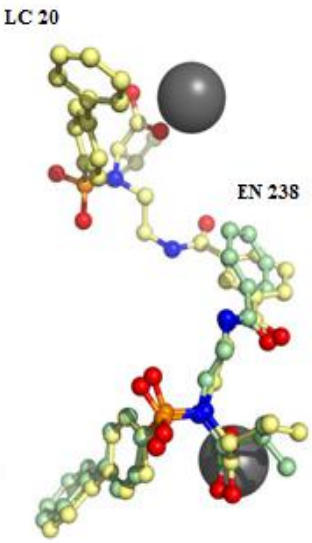

Figure 33. *Superposition of MMP-12 bound to compounds LC20 and EN238, showing good superposition for the ligands.*

positioning, influencing dimerization. In this study of the interaction between a protein and a dual inhibitor, whose ends are joined together by a central linker, dimerization can be affected by the presence of a more or less rigid structure, and when compared with a monovalent ligand by the sole presence of a linker. Comparing mono-functional EN238 with the bi-functional LC20, the mono-functional allows greater flexibility, even if due to a certain structural rigidity it can also induce formation of some homodimers. This limitation could then be used as a variable to deliberately select a defined homodimeric conformation and eliminate unwanted lattice polymorphism. In the homodimer with EN238, the phenyl of the half-linker makes van der Waals interactions within a hydrophobic pocket of the second molecule that composes the MMP-12 dimer in the asymmetric unit.

5.2 *Chemical synthesis section*

5.2.1 *Design and synthesis.*

Initial crystallographic studies conducted on ligands previously synthesized in the laboratory of Prof. Rossello, such as **MP24**, **LC20**, **LC29**, **EN238**, have allowed to acquire the necessary knowledge for the design of new inhibitors. The vision of the real positioning of these ligands, within the pocket of a MMP, has turned the study towards the design of selective inhibitors in which the sulfonamidic scaffold is at the basis of the new compounds structure.

- The first objective was to design and synthesize a new dual carboxylate inhibitor, **SA001,** based on the spontaneously formed dimer obtained between two molecules of EN238 with two molecules of MMP-12, with space group $P2_12_12_1$ (**Fig.32b**). The aim was to insert a linker between the two molecules of EN238 so as to encourage the formation of this homodimer even in presence of the resultant dual inhibitor. The structure of **SA001** was designed by using programs like COOT and CCP4, as previously explained, which allowed the insertion of the linker in the electron density map of the complex EN238·MMP-12. Superimposing the draft of the inhibitor onto the two molecules of EN238 (oriented according to the arrangement dictated by the dimer) structural changes were progressively operated on the new bifunctional ligand. The isopropyl of the original structure of EN238 was removed because, with the insertion of the linker in the new structure, its orientation was changed (if compared to its original position) and the new distances, previously optimal for the interaction with the various boundary amino acids, could cause steric hindrance. Adjustments for achieving the optimal length of the linker were developed with the intent to reproduce precisely the same dimer spontaneously formed with the mono-ligand, suggesting to choose a linker with three carbon atoms. Particular functional groups have not been added on the spacer because the initial assumption was to understand the regulatory mechanism of the dimer formation and therefore we have chosen a spacer with a relatively simple structure (**Synthesis in *Scheme 1***).

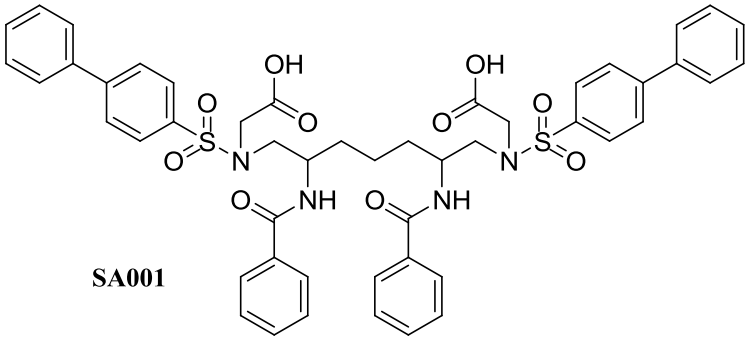

SA001

- A further objective was to synthesize the hydroxamate analogue of EN238 (**LR32**): it has a hydroxamate group as ZBG, in place of the initial carboxylic acid, in order to compare the different affinities of these two ligands for the MMPs. In addition, a further point to test would have been to verify if this derivative was able to form the same dimer as EN238 with MMP-12 (**Synthesis in *Scheme 4***).

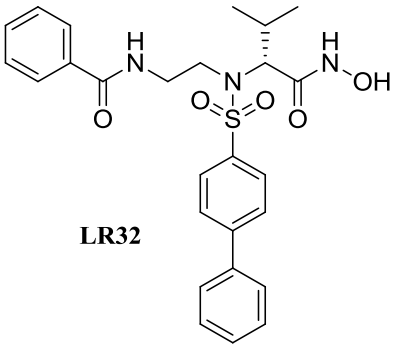

LR32

- Finally, the synthesis of two dual inhibitors (**CA11** and **CA14**) with a short ureidic linker was planned. These had the same sulfonamidic scaffold but a different ZBG (carboxylate and hydroxamate, respectively). The purpose of the synthesis of these inhibitors, was to directly evaluate how the length of the linker could affect the mechanism of homodimer formation among MMPs family members. (**Synthesis in *Schemes 4-5***).

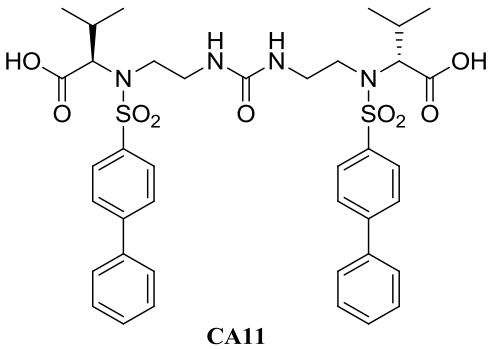

CA11

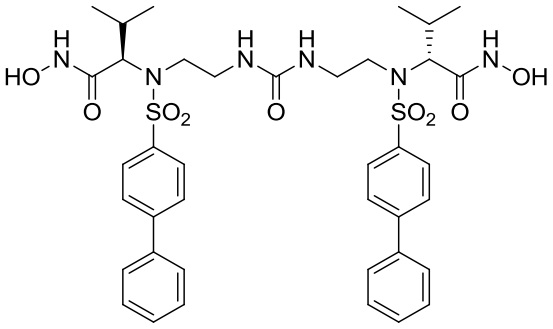

CA14

Scheme 1 shows the retrosynthetic analysis of **SA001**.

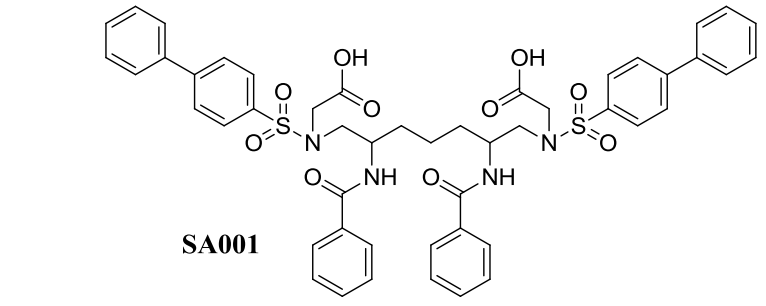

SA001

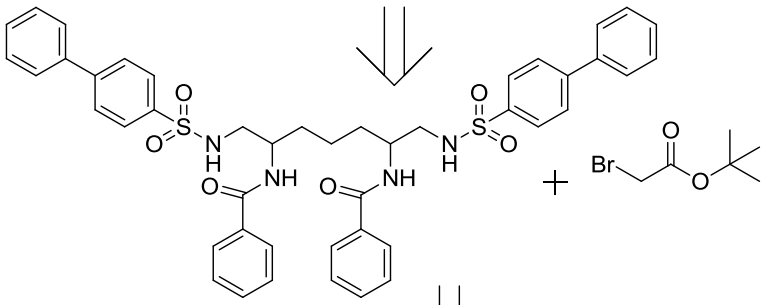

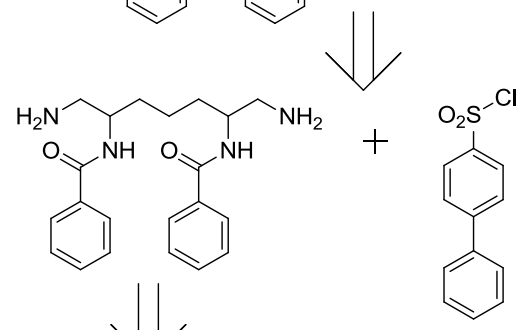

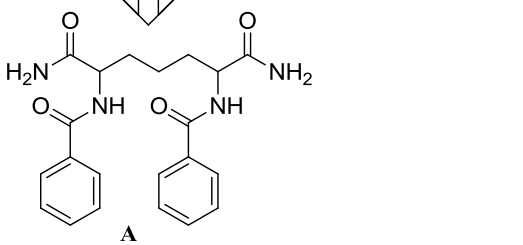

A

Scheme 1

The fundamental synthon was represented by the diamide **A** which could be easily obtained starting from 2,6-diaminopimelic acid (DAP, **1**) in two steps, as reported in Scheme 2.

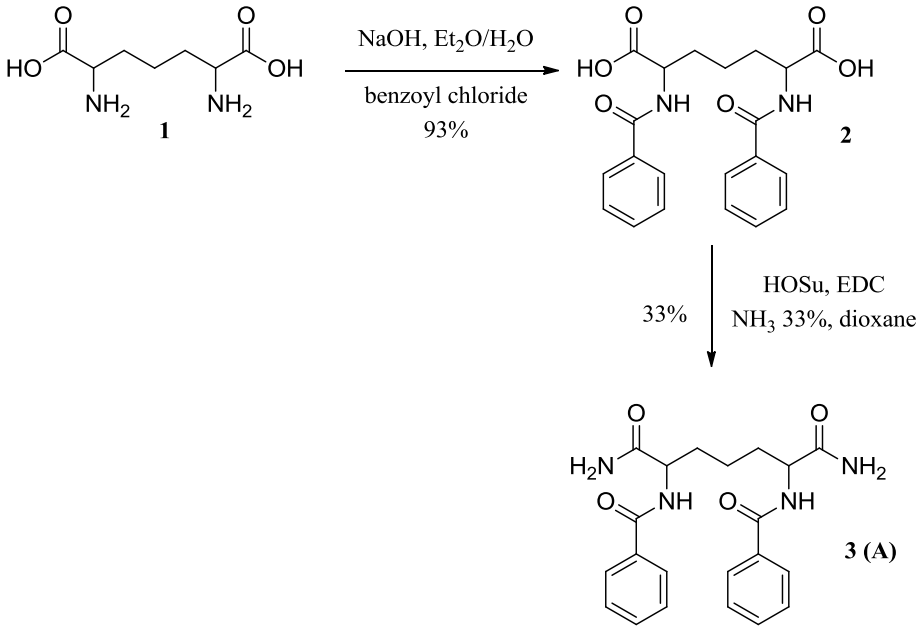

Scheme 2

Our first attempts to obtain diamide **A** (compound **3** in *Scheme 2)* according to this route gave disappointing results, mostly due to the low yield and poor reproducibility of the amidation step using aqueous ammonia solution (33%). Therefore, with the aim to improve the synthetic process of **SA001**, we decided to follow the alternative route described in *Scheme 3*.

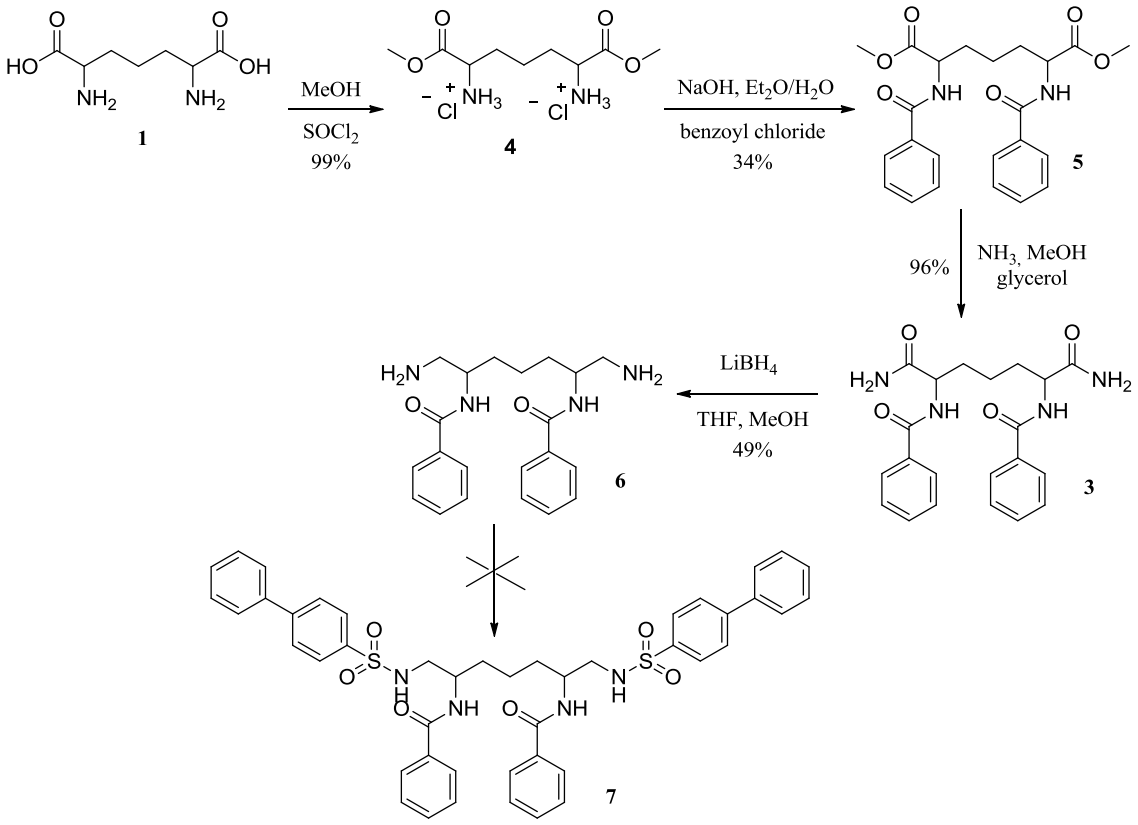

Scheme 3

Diamide **A** (**3**) was obtained starting from DAP, **1**, in three steps with high overall yield. **1** was first converted into methyl ester **4** by treatment with thionyl chloride in MeOH, then *N*-acylated with benzoyl chloride to give ester **5**, which was finally converted into diamide **3** by ammonolysis with dry ammonia gas. Selective reduction of primary amide groups of **3** with lithium borohydride ($LiBH_4$) and MeOH in THF provided the corresponding diamine **6** in good yield, as mixture of two diastereomers. The synthesis was stopped at compound **6**, due to thesis timing and the concomitant other activities linked to the synthesis of the other new dimeric inhibitors (see synthetic Schemes 4 and 5 for LR32, CA11, CA14 and CA15)

Hydroxamic acid **LR32** was prepared as shown in Scheme *4*.

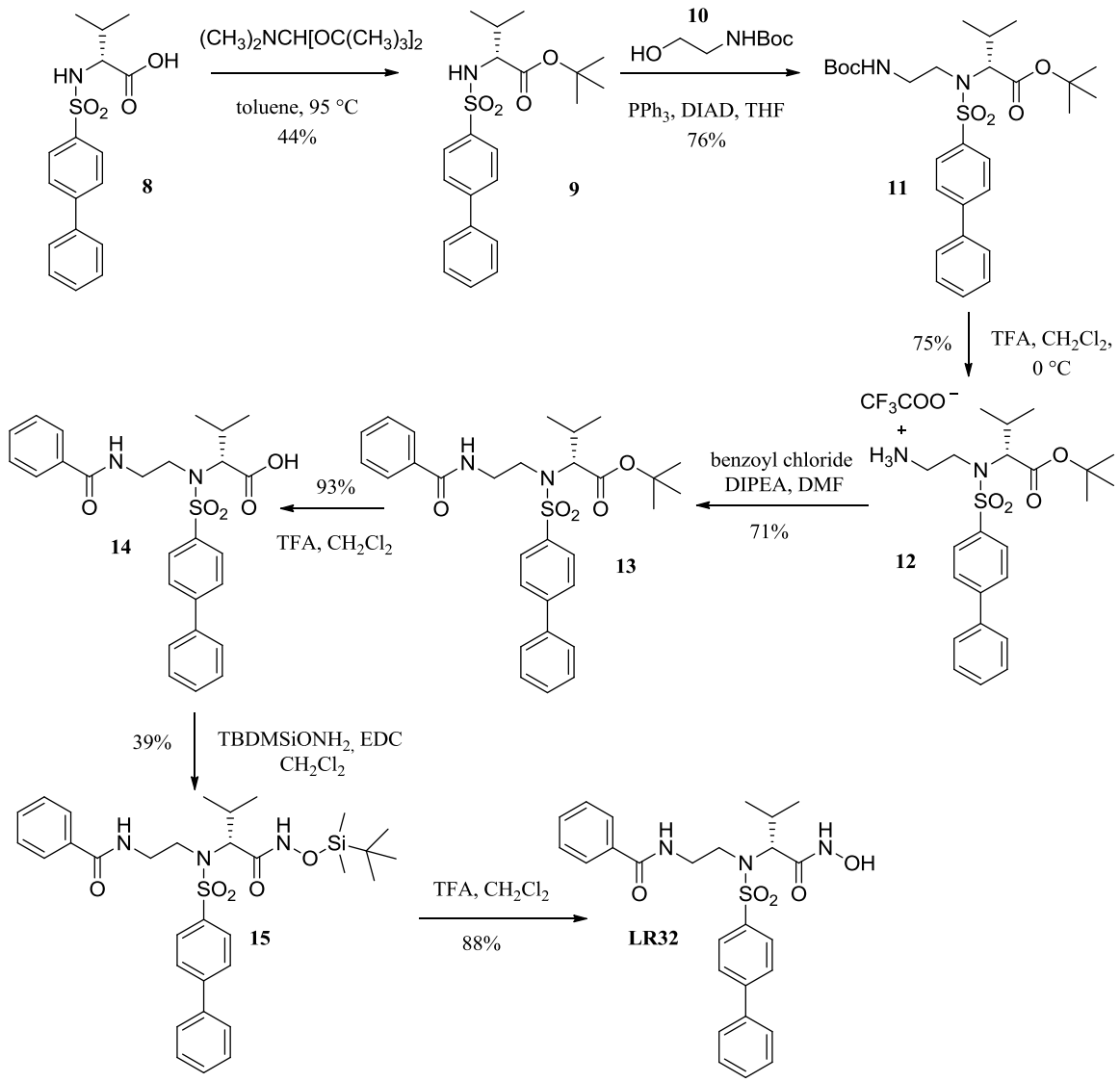

Scheme 4

Compound **8** has been previously synthesized in the laboratory of Prof. Rossello: the carboxylate group was protected as *tert*-butyl ester by treatment with *N*,*N*-dimethylformamide di-*tert*-butyl acetal. Sulfonamide **9** underwent Mitsunobu condensation, in the presence of diisopropylazodicarboxylate (DIAD) and triphenylphophine, with alcohol **10** to give the ester **11**. The latter was subsequently subjected to selective hydrolysis in presence of trifluoroacetic acid (TFA) to remove the NH-Boc protection. *Tert*-butyl ester **13** was obtained by acylation of **12** with benzoyl chloride, using *N*,*N*-diisopropylethylamine (DIPEA) as base. Acid cleavage of ester **13** yielded carboxylate **14** which was finally converted to its corresponding hydroxamate **LR32** by condensation with *O*-(*tert*-butyldimethylsilyl)hydroxylamine followed by acid

hydrolysis with TFA.

The dual inhibitors **CA11** and **CA14** were prepared as shown in Scheme *5*.

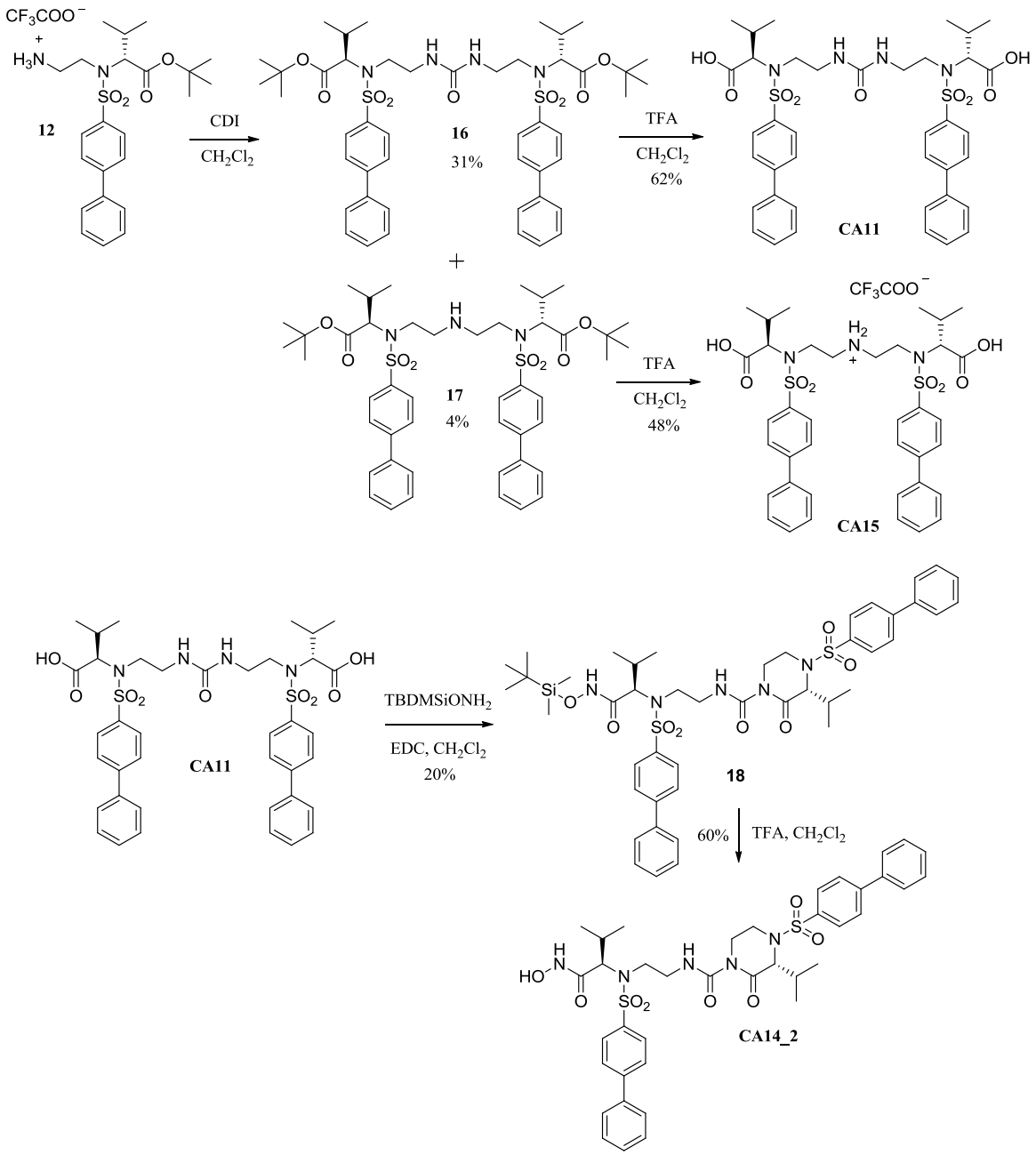

Scheme 5

Compound **12** was treated with 1,1 '-carbonyldiimidazole (CDI) leading to the formation of the desired di-*tert*-butylester, **16**, and the secondary product **17**. After their separation and purification by flash chromatography, both these two esters underwent the same process of

hydrolysis in presence of TFA, thus providing the di-carboxylic acids **CA11** and **CA15**, respectively. **CA11** was then reacted with *O*-(*tert*-butyldimethylsilyl)hydroxylamine in the presence of 1-[3-(Dimethylamino)propyl]-3-ethyl carbodiimide hydrochloride (EDC) as condensing agent, obtaining the cyclic intermediate **18** as principal product instead of the expected di-sylilether. Since the unexpected product was thought to be interesting to be tested and crystallized, **18** was subjected to the mono-silylether hydrolysis with TFA to give the mono-hydroxamate **CA14_2**.

5.3 *Crystallographic investigations of CA11, CA14_2, CA15 binding.*

The derivatives listed above have been crystallized in complex with MMPs. These inhibitors were tested on MMP-8, MMP-9, MMP-12 by Dr. Stura and L. Vera

- *Preliminary X-ray results on CA11.*

  - *CA11·MMP-8 complex.*

    Although CA11 has two ZBG and could potentially promote dimer formation, CA11 can also bind as a monomer on the MMP-8 (**Fig.34**). During crystallization trials both 1:1 and 1:2 inhibitor:MMP ratios are tested but obtaining crystals with both requires several attempts and optimization. The figure shows monovalent binding where one of the two biphenyl sulfonamidic scaffolds penetrates into the pocket of the protein and only one of the two carboxylic acids interacts with the zinc ion of MMP-8.

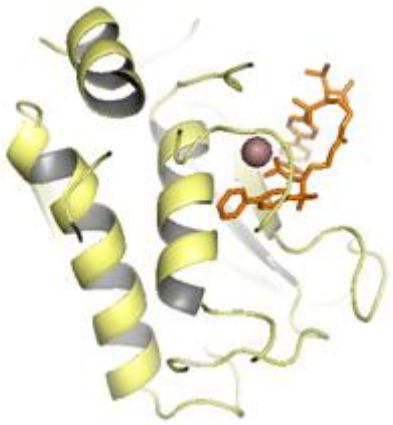

Figure 34 *X-ray structure of the CA11·MMP-8 complex.*

- *Crystallographic CA11·MMP-9 complex.*

  CA11 is a dual inhibitor. Crystals were obtained for the homodimeric complex with MMP-9 (**Fig.35**). This complex was then compared with other complexes formed between CA11 with MMP-8 and MMP-12, discussed below.

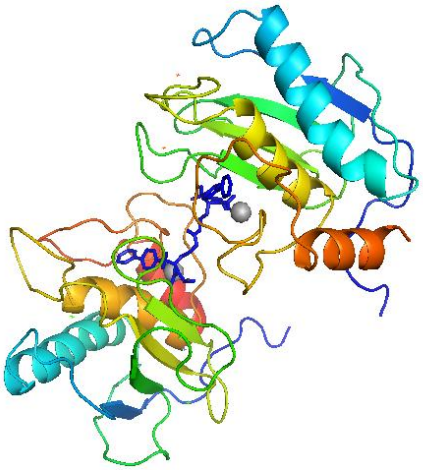

Figure 35. *X-ray structure of the CA11·MMP9 complex.*

- *CA11_MMP-12 complex.*

CA11 can induce a homodimeric MMP-12 complex that is different that previously obtained with the bi-functional inhibitor LC20.

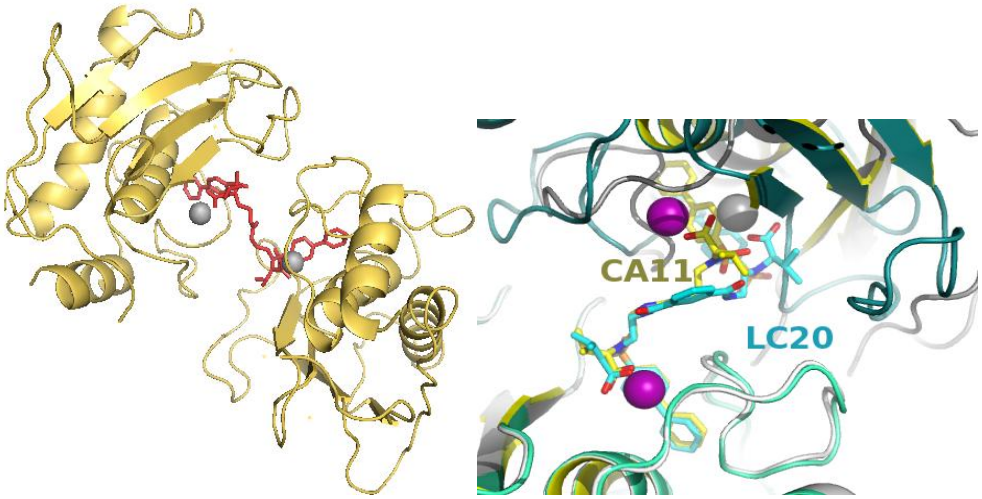

a **b**

Figure 36. ***a)*** *X-ray structure of CA11_MMP12 complex;* ***b)*** *superimposition of CA11 (blue) and LC20 (orange) in their complex with MMP-12.*

The superposition of the CA11·MMP-12 and LC20·MMP-12 homodimers (**Fig 36-b**) clearly shows the different spatial arrangements adopted by the enzyme in the two complexes. The two homodimers are adopting two different orientations relative to each other although the linkers are only slightly staggered. This suggests that linkers shorter than LC20 (11 atoms in total) cannot maintain the same homodimerization mode. Linkers similar as the length of CA11 (with 7 atoms in

total) still allow MMP-12 homodimerization. Homodimeric interactions, different for each MMP, can contribute to increase the selectivity of the inhibitor in favor of MMP-12 (biological data given below).

❖ *Comparison of complexes obtained with CA11.*

Thanks to the superimposition of the images relating to X-ray of the complexes above, it is possible to compare the different positions adopted by CA11 in complex with MMP-8, MMP-9 and MMP-12 (**Fig.37**).

Both crystallographic complexes of MMP-12 and MMP-9 with the inhibitor CA11 are homodimers while monomeric binding for MMP-8 was observed. In the homodimeric complexes CA11 superimposes almost exactly on itself in the MMP-12 and MMP-9 complexes. In both cases, it promotes the formation of homodimers, but the intermolecular orientations of the two proteinases is different in the two cases. In the MMP-8 complex only the monomeric binding was analysed. The orientation of CA11 shows flexibility: one sulfonamidic scaffold overlaps the other two, whereas the second one is redirected towards a secondary pocket on the proteinase.

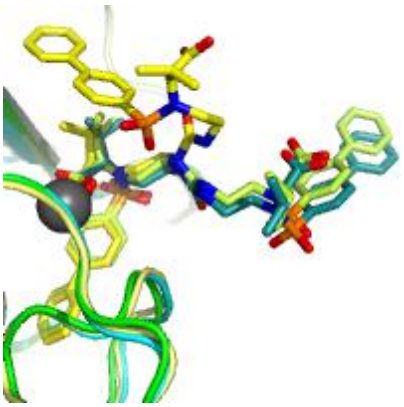

Figure 37. *CA11 overlapping in different complexes with MMP-12 (blue), MMP-9 (green), MMP-8 (yellow).*

➢ *Preliminary X-ray results on CA14_2.*

CA14_2 was tested with MMP-12, MMP-9, MMP-8, but so far crystals have been obtained only in complex with MMP-8.

➢ *CA14·2MMP8 complex.*

The X-ray crystallography structure shows a dimer. In addition to protein-protein interactions, the formation of the homodimer is also mediated by interactions that are established directly between the two molecules of inhibitor (**Fig. 38A-B**).

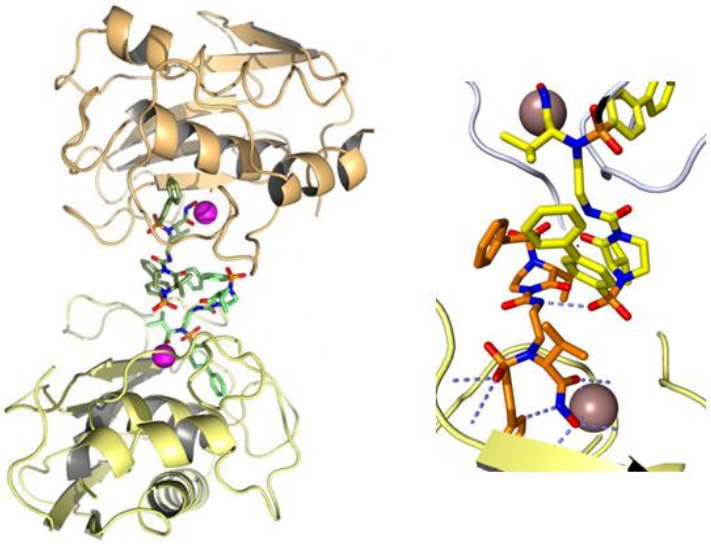

a **b**

Figure 38. ***a)*** *X-ray image of MMP-8·CA14 complex;* ***b)*** *Interaction between the two molecules of CA14, in the complex MMP-8·CA14.*

The analysis of the interactions established between the two molecules of inhibitor aiding to form the MMP-8 homodimer suggest new ways to design selective inhibitors for this metalloprotease.

- *Preliminary X-ray results of CA15.*

  CA15 was used for crystallographic trials with MMP-12, MMP-9, MMP-8, providing at the moment a complex exclusively with MMP-8.

  - *CA15·MMP-8 complex.*

    CA15 has been crystallized with MMP-8 as a monomeric complex (**Fig.39**). In this case, the shortening of the linker up to 5 atoms in total, has not resulted in the

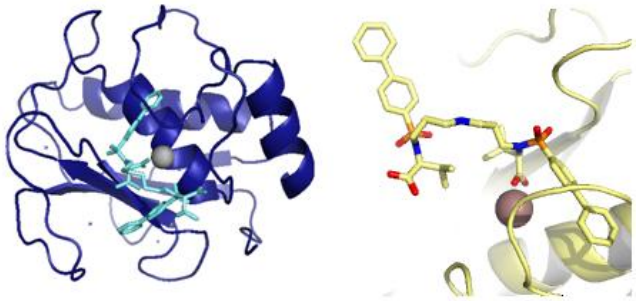

Figure 39.
a) *Monomeric complex between CA15·MMP-8;*
b) *Interaction of the carboxylic acid with the zinc of the MMP-8.*

formation of a homodimer between the metalloproteases analyzed. Further crystallization trials may result in crystal with a dimer the lattice.

5.4 Biological data of CA11, CA14_2, CA15.

All the new inhibitors were tested in vitro on human recombinant MMPs (MMP-1, MMP-2, MMP-8, MMP-9, MMP-12, MMP-13, MMP-14) by fluorometric assay. Results are reported in **Table 1**, together with those obtained for the previously synthesized analogues (EN238, LC20 and LC29).

Table 1. *In vitro* activity (IC_{50}, nM) on MMPs.

Compd	MMP9	MMP12	MMP1	MMP2	MMP8	MMP13	MMP14
EN238	508	35	16000	170	115	152	1830
LR32	2.5	1.5	13	0.16	2.0	0.24	23
LC20	26	1.3	11800	63	89	35	2200
LC29	5.5	7.1	280	10	8.9	8.2	250
CA11	175	4.6	8300	145	134	200	1700
CA14_2	26	15	3100	42	15	9	4900
CA15	430	22	17000	460	116	420	8900

All compounds showed a nanomolar activity against MMP-9 and MMP-12. In general, carboxylates were characterized by a higher selectivity for these proteases over the other MMPs with respect to the corresponding hydroxamates. In fact, hydroxamates such as LR32, LC29 and CA14_2 resulted powerful but unselective MMPs inhibitors. Comparing carboxylate dual-inhibitors with the corresponding monovalent derivatives (i. e. LC20 with EN238) highlights the importance of having a dual ligand. In fact, LC20 displayed an improved activity and selectivity for MMP-12 and MMP-9 with respect to EN238. The newly synthesized carboxylate dual-inhibitor CA11 showed a drop of activity against all tested MMPs with respect to LC20, probably due to the shorter linker. Finally, the mono-hydroxamate cyclic derivative CA14_2 resulted poorly selective like all the other hydroxamates and about 10 times less active than LC20 on MMP-12. Further information about the biological activity of these dual MMPs inhibitors will be provided by cell assays on gliomas that are currently ongoing in Prof. Martini's laboratory.

Chapter VI
EXPERIMENTAL PROCEDURES

6.1 *Crystallization procedures.*

The crystallization experiments were conducted under the supervision of Dr. Stura, in the research laboratory of the CEA, iBiTec-S, Service d' Ingénierie Moléculaire des Protéines (SIMOPRO), Gif-sur-Yvette, France.

6.1.1 *Material and Methods.*

The MMPs were prepared and purified by E. Lajeunesse and L.Vera. The inhibitors **MP24**, **EN238**, **LC20**, **LC29** were synthesized by the research group of Prof. Rossello. The CrysChem sitting drops plates were used for loading the crystallization experimets. The plates were kept at constant temperature of 20 °C, in a thermostat. The precipitant and cryoprotective solutions used were part of the L. Vera and Dr. Stura's kit [12]. The data were collected at the Soleil synchrotron Facility (St. Aubin, France) on beamline Proxima 1 (at 100 K from a single crystal and reduced using XDS and the script "xdsme") and at the European Synchrotron Radiation Facility (ESRF) in Grenoble (France), on beam line ID23–1 (the data processed automatically using XDS). The structure was solved by rigid body refinement using REFMAC5. The inhibitor was built using the monomer library sketcher from CCP4 program suite the model was subsequently optimized with cycles in COOT, followed by cycles of REFMAC5. The structure was solved by molecular replacement using MOLREP. The ligand prepared with the sketcher, the restraints prepared with phenix.elbow and positioned in the binding site with COOT. The model was improved with cycles in phenix.refine and COOT.

6.1.2 *Crystallization experiments.*

Crystallization experiments were carried out in CrysChem sitting drop vapor diffusion plates (**Fig.15**). A volume of 6 μL of protein sample is mixed to a precise volume of inhibitor, defined by the stoichiometry used: 1 μL of the mix is used for single drop. The drop, generally, was composed by 1 μL of protein-inhibitor solution and 1 μL of precipitant solution, taken directly from the reservoir. At this point it is necessary to isolate the experiment from the external environment sealing it with a coverslip. A stoichiometry of 1 protein for 1 ligand was used for monofunctional inhibitors (EN238), whereas a

stoichiometry of 2 proteins *per* ligand was usual for dual inhibitors (LC20, LC29). At the very beginning, the screenings of MMP-9 and MMP-12 were based on pre-established crystallization conditions determined by Dr. E. Stura[17] and L. Vera[18]. The availability of efficient crystallization conditions, made the initial process faster. Using this information it was possible to optimize the yield of crystals. Afterward, new specific strategies were developed. For MMP-9, crystal needles were introduced immediately to facilitate the selection of the optimal working conditions, by streak seeding. This procedure is carried out within 10 minutes after the deposition of the drops of protein-ligand solution and the precipitant solution: after, the coverslip was sealed. The vapor diffusion trays were stored in a cooled incubator at 20°C. For X-ray data collection, the crystals were harvested with a cryo-loop and transferred to a cryo-protective solution and then rapidly plunged in liquid nitrogen to cryo-cool the crystals. [11].

6.1.3 *Crystals of MMP-9·inhibitor complex.*

The MMP-9·E219Q mutant [11] where the catalytic glutamate is mutated to glutamine was used in these experiments. At the beginning, similar conditions for all inhibitors were tested: 14% PEG 20K, 100 mM PCTP 75/25 [sodium propionate, sodium cacodylate, bis-tris-propane (component A pH 4; component B pH 9.5)], 1 M NaCl in 500 µL of reservoir solution.

Drops were composed by 1µL of protein and 1µL of precipitant solution. A few days later the first crystals appeared [41].

- **MMP-9·LC29**: Small crystals of rectangular shape were obtained and no protein precipitation in the drop was observed. The precipitant solution was composed of 10% PEG 20000, 100 mM PCTP 75/25, 1.5 M NaCl in 500 µL of reservoir volume. The structure resolution was 1.9 Å (PDB code 4H82) [**Fig.23**]. Instead, a condition of 12% PEG 20000, 100 mM PCTP 75/25, 1.5 M NaCl in 500 µL gave larger crystals, rectangular in shape and some precipitate.

- **MMP-9·LC20**: In 12% PEG 20000, 100 mM PCTP 75/25, 1.5 M NaCl in 500 µL of reservoir volume, larger crystals with rectangular shape were formed [**Fig.22**]. Instead,

[17]Researchers at CEA, iBiTec-S, Service d'Ingénierie Moléculaire des Protéines (SIMOPRO), Gif-sur-Yvette, France.

[18]Superior technician at CEA, iBiTec-S, Service d'Ingénierie Moléculaire des Protéines (SIMOPRO), Gif-sur-Yvette, France.

composition of 10% M PEG 20000, 100mM PCTP 75/25, 1.5M NaCl in 500 µL of reservoir volume allowed the formation of many smaller crystals.

- **MMP-9·EN238**: Crystals formed spontaneously without the need for seeding with a reservoir solution of 12% PEG 20,000, 140 mM imidazole malate, 175 mM NaCl, pH 8.5

6.1.4 *Crystals of MMP-12-inhibitor complex.*

The MMP-12 wild type was used in these experiments.

- **MMP-12·LC20**: For this crystallization, seeding was not necessary, because the first microcrystals appeared spontaneously on the first attempt. The initial precipitant solution was composed by 17% PEG 20000, 200 mM imidazole malate pH 8.5, 250 mM NaCl : the volume ratio used was 1µL of precipitant solution and 1µL of protein-inhibitor solution. Few minutes later, microcrystals appeared and a few hours afterward, smalls thin needles came out (**Fig.27A**).

  The concentration of precipitant solution was changed to increase the crystals dimension and to try to control the excessive nucleation to 3% PEG 20000, 200 mM imidazole malate pH 8.5, 50 mM NaCl. This condition was better than the previous one because the needle shower formation has been avoided and only prismatic crystals grew spontaneously (**Fig.27B**). The resolution achieved was 1.42 Å (PDB code 4H30).

  Several changes were tried, such as a different volume ratio of mix protein-inhibitor solution and the composition of the working solution: in particular, other different crystals form, using 2 µL of MMP-inhibitor solution added to 0.5µL of precipitant solution, was obtained (**Fig.27C**).

  Crystals obtained for the MMP-12·EN238 complex (**Fig.27D**) are morphologically very similar to those one of the MMP-12·LC20 complex (**Fig.27B)**: the space group is the same, but the packing is different. (**Fig.27D**).

- **MMP-12_LC29**: the first solutions were composed by progressive dilution of a specific working solution, usually used for MMP-12. Dilutions were used at 40%, 30%, of a solution composed by: 17% PEG 20000, 200 mM imidazole malate pH 7.5, 250 mM NaCl. However, all the drops showed small needles. Therefore, the pH of the precipitant solution was changed: a new precipitant solution composed by 17% PEG 20000, 0.2 M imidazole malate pH 6.0, 250 mM NaCl was able to give crystals in form of lamellae

diffracting to 2.16 Å resolution (PDB code 4H49).

- **MMP-12_EN238**; In this case, seeding was not needed as the selected crystallization conditions typically used with MMP-12 gave after few minutes crystals of this complex spontaneously nucleated (**Fig. 27D**). Initially, a specific MMP-12 precipitant solution was tried: 17% PEG 20K, 0.2M imidazole malate pH 8.5, 250mM NaCl. This condition showed smalls square crystals. Subsequently, a dilution of 70% of this mix solution was lead to bigger crystals. A volume of 50 µL, 5 M NaCl was added to the 500 µL reservoir to allow a better crystals growth, by slowly increase the removing of water vapor, accelerating crystal growth (**Fig. 32B**).

6.1.5 *Cryo-protectant condition.*

The freezing of crystals represents a very delicate stage in the diffraction experiment preparation process. The main cryo-protectant condition used, were:

- Cryo-solution MMP-12 _LC20 complex: 27% PEG 8000, 15% MPEG 550, 10% glycerol, 90mM Tris-HCl, pH 8.5.

- Cryo-solution MMP-12_LC29 complex: 10% di-ethylene glycol, 10 % glycerol, 10 % 1,2- propanediol, 25% M PEG 5000, 100mM BES pH 5.5.

- Cryo-solution MMP-12_EN238 complex: 5% Di-ethylene glycol, 10% 1,2-propanediol, 5% glycerol, 5% ethylene glycol, 5% DMSO, 9% PEG 10000, 100mM MMT buffer 75/25 (L-malic acid, 75% component A, pH 4; 25% component B, pH 9), 1 M NaCl.

- Cryo-solution MMP-9_LC29 complex: 10 % di-ethylene glycol, 10 % 1.2-propanediol, 10% glycerol, 1.5 M NaCl, 100 mM PCTP buffer 80/20, 9% PEG 10,000.

The cryoprotection conditions for the crystals reported in this work, were determined by Dr. Stura and L. Vera. A total between 200 and 1000 images for each crystal, were collected during the analysis.

6.2 *Chemistry experiments.*

The chemistry experiments were conducted under the supervision of Dr. E. Nuti and Prof. A. Rossello, in the laboratory of the Dipartimento di Farmacia, Università di Pisa, Pisa, Italy.

6.2.1 *Materials and Methods.*

Melting points were determined on a Kofler hotstage apparatus and are uncorrected. ^{1}H and ^{13}C NMR spectra were determined with a Varian Gemini 200 MHz spectrometer. Chemical shift (δ) are reported in ppm and *J* in Hz. The following abbreviations were used to explain the multiplicities: s=singlet, d=doublet, t=triplet, q=quartet, m=multiplet, dt=double triplet, dd=double doublet. Evaporation was performed under vacuum conditions in rotating evaporator. Chromatographic separations were performed on silica gel columns by flash column chromatography (Kieselgel 40, 0.040–0.063 mm; Merck) or using ISOLUTE Flash Si II cartridges (Biotage). Reactions were followed by thin-layer chromatography (TLC) on Merck aluminum silica gel (60 F254) sheets that were visualized under a UV lamp and hydroxamic acids were visualized with $FeCl_3$ aqueous solution. Anhydrous sodium sulfate was always used as the drying agent. Yields refer to isolated and purified products.

6.2.2 Synthesis

Synthesis of *2,6-bis(benzamido)heptanedioic acid* (2).

2,6-Diaminopimelic acid **1** (5.26 mmol, 1 g) was dissolved in H_2O (8 mL) and the solution was cooled to 0 °C. NaOH (21.04 mmol, 0.8415 g) was added to the solution under magnetic stirring. Benzoyl chloride (10.52mmol, 1.22 mL) in Et_2O (8 mL) was added to the reaction kept at 0 °C. The mixture was stirred overnight at RT. The reaction mixture was diluted with Et_2O (3 mL) and H_2O (3 mL), and the H_2O was separated. The water phase was acidified with 1N HCl (10 mL), until formation of a white solid. This precipitate was extracted with AcOEt (200 mL) and the organic phase was washed with brine (50 mL) and dried over Na_2SO_4. The solvent was evaporated to yield the desired carboxylic acid **2** (0.34 g) as a white crystalline solid.

Yield: 93%

^{1}H-NMR (DMSO) δ: 1.40-1.60 (m, 2H); 1.72-1.95 (m, 4H); 4.31-4.39 (m, 2H); 7.40-7.54 (m, 6H); 7.84-7.88 (m, 4H); 8.59 (dd, J_1=7.7 Hz, J_2=2.9 Hz, 2H).

Synthesis of *2,6-bis(benzamido)heptanediamide* 3 (A)[19].

EDC (6.80 mmol,1.30 g) was added under magnetic stirring to a dioxane solution (34 mL) of compound **2** (3.40 mmol, 1.35 g) and N-hydroxysuccinimide (6.80 mmol, 0.78 g). The reaction was kept under stirring for 1 h and the white precipitate was filtered off. NH_4OH 33% solution (27 mL) was added to the filtrate and the magnetic stirring was maintained overnight. The solvent was evaporated to yield a yellow powder. This precipitate was extracted with AcOEt (250 mL), resulting partially soluble: the organic phase was washed with brine (100 mL) but not dried over Na_2SO_4, given the presence of a suspension. The solvent was evaporated to yield **3** as white-yellow solid (1.11g).

Yield: 33%

^{1}H-NMR (MeOD) δ: 1.55-1.65 (m, 2H); 1.85-1.97 (m, 4H); 4.57 (t, *J*=6.9 Hz, 2H); 7.39-7.52 (m, 6H); 7.77-7.84 (m, 4H).

6.2.2 *Synthesis of 2, 2' - ((2, 6 – bis (benzamido) heptanes - 1, 7 – diyl) bis (([1, 1' – biphenyl] - 4 - ylsulfonyl) azanediyl))diacetic acid (Scheme 3, compound **6**).*

Synthesis of *1,7-dimethoxy-1,7-dioxoheptane-2,6-diaminium chloride* (4)[20].

2,6-Diaminopimelic acid **1** (5.26 mmol, 1 g) was dissolved in MeOH (8.4 mL), under N_2. The suspension was cooled to -5 to -10 °C (ice/acetone bath) and treated dropwise with thionyl chloride (11.57 mmol, 0.85 mL). The mixture was stirred at -5 to -10 °C for 1h, then overnight at room temperature, when TLC monitoring ($CHCl_3$/MeOH/NH_4OH, 4:8:1), indicated completion of the reaction. The solvent was evaporated to yield the amino ester **4** (1.53 g) as white solid.

Yield: 99%

^{1}H-NMR (DMSO) δ: 1.35-1.60 (m, 2H); 1.70-1.85 (m, 4H); 3.74 (s, 6H); 3.94-4.05 (m, 2H); 8.73 (s, 6H).

Synthesis of *dimethyl 2,6-bis(benzamido)heptanedioate* (5).

[19] C. Exon, T. Gallagher, P. Magnus. Indole-2,3-quinodimethanes: A new Strategy for the Synthesis of Tetracyclic Systems of Indole Alkaloids. *J. Am. Chem. SOC.*, ***I983***, 105, *4739-4749* [65].

[20] M. Ilies, L. Di Costanzo, M. L. North, J. A. Scott, D. W. Christianson. 2-Aminoimidazole Amino Acids as Inhibitors of the Binuclear Manganese Metalloenzyme Human Arginase I. *J. Med. Chem.* **2010**, 53, *4266–4276*,[56].

The ester **4** (2.58 mmol, 0.750 g) was dissolved in H_2O (6 mL) and the solution was cooled to 0 °C. To the solution was added NaOH (10.32 mmol, 0.413 g), maintaining the stirring. Benzoyl chloride (5.16 mmol, 0.60 mL) was dissolved in Et_2O (6 mL), and this solution was added to the previous, at 0 °C. The mixture was stirred overnight at RT. The reaction mixture was diluted with EtOAc (100 mL), and separated water. The organic phase was washed once with a saturated solution of $NaHCO_3$ (40 mL) and once with brine (40 mL) and dried over Na_2SO_4. The solvent was evaporated to give **5** as a yellow crystalline solid (383 mg).

Yield: 35%

^{1}H-NMR ($CDCl_3$) δ: 1.51-1.68 (m, 2H); 1.82-2.03 (m, 4H); 3.73 (s, 3H); 3.75 (s, 3H); 4.69-4.85 (m, 2H); 6.96 (d, *J*=8.0 Hz, 1H); 7.01 (d, *J*=8.0 Hz, 1H); 7.29-7.54 (m, 6H); 7.73-7.85 (m, 4H).

Synthesis of *2,6-bis(benzamido)heptanediamide* (3)[21].

Dry ammonia gas was bubbled for 20 min into a solution containing the methyl ester **5** (0.89 mmol, 0.38 g) and glycerol (4.4 g) in MeOH (15 mL) at 4 °C. Dry ammonia gas was obtained by dropping NH_4OH 33% solution (10 mL) on KOH solid (4 g). The vial was tightly closed and left at RT overnight. MeOH and ammonia were removed by evaporation and the residual liquid was dissolved in water (80 mL). After acidification with 1N HCl, the solution was extracted with EtOAc (2x150 mL). The combined organic layers were washed with brine (2x50 mL). The solvent was evaporated to yield diamide **3** as white crystalline solid (0.34 g).

Yield: 96%

^{1}H-NMR (MeOD) δ: 1.55-1.65 (m, 2H); 1.85-1.97 (m, 4H); 4.57 (t, *J*=6.9 Hz, 2H); 7.39-7.52 (m, 6H); 7.77-7.84 (m, 4H).

Synthesis of *N,N'-(1,7-diaminoheptane-2,6-diyl)dibenzamide* (6)[22].

To a solution of amide **3** (0.605 mmol, 0.240 g) and $LiBH_4$ (3.63 mmol, 0.079 g) in

[21] Y. Yamazaki, M. Savva, H. K. Kleinman, S. Oka, M. Mokotoff. Enhanced cleavage of diaminopimelate - containing isopeptides by leucine aminopeptidase and matrix metalloproteinases in tumors: application to bioadhesive peptides. J. Peptide Res., **1999**, 53, *177-187* [61].

[22] K.Soai, A.Ookawa. Mixed Solvents Containing Methanol as Useful Reaction Media for Unique Chemoselective Reductions with Lithium Borohydride. *J. Org. Chem*. **1986**, 51, *4000-4005* [62].

THF(2.5 mL), was added MeOH (0.3 mL). The mixture was refluxed for 4h, under Argon. After quenching the reaction by adding MeOH, was added oxalic acid (0.726 mmol, 0.065 g). The solvent was evaporated under reduced pressure and the crude was purified by flash chromatography to obtain di-amine **6** as a mixture of two diastereomers.

Chromatographic conditions: Eluent $CHCl_3$ 20 : 1 MeOH. Flash column: h = 21 cm; d = 3 cm.

Yield: 49%

^{1}H-NMR (MeOD) δ: 1.20-1.49 (m, 6H); 3.30 (d, *J*=5.8 Hz, 4H); 3.78-3.84 (m, 2H); 7.05-7.23 (m, 6H); 7.46-7.52 (m, 4H).

6.2.3 *Synthesis (R)-N-(2-(N-(1-(hydroxyamino)-3-methyl-1-oxobutan-2-yl)-[1,1'-biphenyl]-4-ylsulfonamido)ethyl)benzamide (Scheme 4, compound **LR32**).*

Synthesis of *(R)-tert-butyl 2-([1,1'-biphenyl]-4-ylsulfonamido)-3-methylbutanoate* (9).

A solution of carboxylic acid **8** (7.85 mmol, 2.62 g) in anhydrous toluene (15 mL) containing *N*,*N*-dimethylformamide di-*tert*-butyl acetal (31.4 mmol, 7.53 mL) was heated to 95 ºC for 3 h. The solvent was then evaporated and the crude product was purified by flash chromatography on silica gel (*n*-hexane/EtOAc 4:1) to give **9** as a white solid.

Yield: 44%

^{1}H-NMR ($CDCl_3$) δ: 0.86 (d, *J*= 6.7 Hz, 3H); 1.02 (d, *J*= 6.7 Hz, 3H); 1.19 (s, 9H); 1.98-2.14 (m, 1H); 3.63-3.70 (dd, *J*= 4.6 Hz, *J*= 10.0 Hz, 1H); 5.15 (d, *J*= 9.8 Hz, 1H); 7.41-7.58 (m, 5H); 7.66-7.70 (m, 2H); 7.88-7.92 (m, 2H).

Synthesis of *(R)-tert-butyl 2-(N-(2-((tert-butoxycarbonyl)amino)ethyl)-[1,1'-biphenyl]-4-ylsulfonamido)-3-methylbutanoate* (11).

Diisopropyl azodicarboxylate (DIAD) (4.39 mmol, 0.864 mL) was added dropwise to a solution containing the alcohol **10** (1.26 mmol, 0.20 g), the sulfonamide **9** (1.88 mmol, 0.733 g) and triphenylphosphine (4.39 mmol, 1.152 g) in anhydrous THF (21 mL) under argon atmosphere at 0 ºC. The resulting solution was stirred overnight at RT and evaporated under reduced pressure to afford a crude product, which was purified by flash chromatography on silica gel (*n*-hexane/EtOAc 8:1) (Rf= 0.3) to yield **11** as a yellow oil.

Yield: 76%

^{1}H-NMR ($CDCl_3$) δ: 0.92 (d, *J*=6.4 Hz, 6H); 1.04 (d, *J*= 6.4 Hz , 3H); 1.22 (s, 9H); 1.41 (s, 9H); 2.01-2.17 (m, 1H); 3.22-3.46 (m, 3H); 3.73-3.83 (m, 1H); 3.96 (d, *J*= 9.6 Hz, 1H); 5.15 (t, 1H); 7.38-7.56 (m, 5H); 7.64-7.68 (m, 2H); 7.87-7.91 (m, 2H). **^{13}C-NMR** ($CDCl_3$) δ: 19.34; 20.07; 27.83; 28.47; 29.30; 41.30; 44.73; 66.69; 79.19; 82.05; 127.25; 127.61; 128.08; 128.47; 129.05; 183.34; 189.28; 145.60; 155.83; 169.60.

Synthesis of *(R)-tert-butyl 2-(N-(2-aminoethyl)-[1,1'-biphenyl]-4-ylsulfonamido)-3-methylbutanoate* (12).

Trifluoroacetic acid (57 mmol, 4.4 mL) was added dropwise to a stirred solution of *tert*-butyl ester **11** (0.93 mmol, 0.50 g) in dry CH_2Cl_2 (20 mL) under argon atmosphere, cooled to 0 °C. The solution was stirred for 2 h at 0 °C and the solvent was removed in vacuo. The crude product was purified by flash chromatography on silica gel ($CHCl_3$/MeOH 15:1) to yield **12** as a yellow oil.

Yield: 75%

^{1}H-NMR ($CDCl_3$) δ: 0.93 (d, *J*= 6.4, 3H); 1.02 (d, *J*= 6.4 Hz, 3H); 1.24 (s, 9H); 1.97-2.12 (m, 1H); 2.89-3.01 (m, 2H); 3.21-3.35 (m, 1H); 3.51-3.66 (m, 1H); 3.98 (d, *J*= 9.6 Hz , 1H); 7.40-7.57 (m, 5H); 7.63-7.68 (m, 2H); 7.87-7.93 (m, 2H). **^{13}C-NMR** ($CDCl_3$) δ: 19.36; 19.80; 27.83; 29.27; 42.60; 48.24; 66.49; 82.00; 127.23; 127.54; 127.99; 128.41; 129.03; 139.01; 139.30; 145.44; 169.65.

Synthesis of *(R)-tert-butyl 2-(N-(2-benzamidoethyl)-[1,1'-biphenyl]-4-ylsulfonamido)-3-methylbutanoate* (13).

A solution of **12** (0.499 mmol, 0.273 g) in dry DMF (7 mL) was treated with benzoyl chloride (0.599 mmol, 0.07 mL) and *N*,*N*-diisopropylethylamine (0.998 mmol, 0.2 mL) under nitrogen atmosphere. The reaction mixture was stirred at RT for 18 h, then was diluted with EtOAc, washed with H_2O, dried over Na_2SO_4 and evaporated. The crude was purified by flash chromatography (*n*-hexane/EtOAc 8:1) using a Isolute Flash Si II cartridge to give **13** as a yellow oil (0.190 g).

Yield: 71%

^{1}H-NMR ($CDCl_3$) δ: 0.96 (d, *J*= 6.4 Hz, 3H); 1.04 (d, *J*= 6.4 Hz, 3H); 1.26 (s, 9H); 2.06-2.25 (m, 1H); 3.50-3.62 (m, 1H); 3.70-3.76 (m, 2H); 4.01-4.09 (m, 2H); 7.37-7.69 (m, 10H); 7.84-7.93 (m, 3H); 8.09-8.13 (m, 1H).

Synthesis of (R)-2-(N-(2-benzamidoethyl)-[1,1'-biphenyl]-4-ylsulfonamido)-3-

methylbutanoic acid (14).

Trifluoroacetic acid (57 mmol, 1.5 mL) was added dropwise to a stirred solution of *tert*-butyl ester **13** (0.354 mmol, 0.190 g) in freshly distilled CH_2Cl_2 (6 mL), cooled to 0 °C. The solution was stirred for 5 h at 0 °C and the solvent was removed *in vacuo*. The crude product was purified by trituration with *n*-hexane/Et_2O to give **14** as a white solid.

M.p.: 63 °C

Yield: 93%

^{1}H-NMR ($CDCl_3$) δ: 0.91 (d, *J*= 6.2 Hz, 6H); 2.01-2.16 (m, 1H); 3.34-3.53 (m, 1H); 3.58-3.83 (m, 3H); 4.11 (d, *J*= 10.4 Hz, 1H); 5.67 (br s, 1H); 7.33-7.55 (m, 9H); 7.60-7.64 (m, 2H); 7.78-7.88 (m, 4H). **^{13}C-NMR** ($CDCl_3$) δ: 19.71; 20.09; 28.89; 40.67; 44.51; 66.19; 127.19; 127.41; 127.67; 128.14; 128.70; 129.16; 131.73; 133.97; 137.64; 139.15; 146.06; 168.03; 172.86.

Synthesis of *(R)-N-(8-([1,1'-biphenyl]-4-ylsulfonyl)-7-isopropyl-2,2,3,3-tetramethyl-6-oxo-4-oxa-5,8-diaza-3-siladecan-10-yl)benzamide* (15).

To a solution of the carboxylic acid **14** (0.329 mmol, 0.158 g,), in anhydrous CH_2Cl_2 (13.2 mL), was added *O*-(tert-butyldimethyl-sylil) hydroxylamine (0.658 mmol, 0.097 g). The reaction mixture was cooled in an ice bath and gradually EDC (0.658 mmol, 0.126 g) was added. The reaction mixture was left under stirring at RT overnight. The reaction mixture was diluted with CH_2Cl_2 (8 mL) and evaporated at RT, obtaining a yellow-brown oil. The crude was purified by chromatography, providing 0.079 g of compound **15,** as brown oil.

Chromatographic conditions: Eluent Exane 4: 1 EtOAc. Isolute column (Si II) 10 g.

Yield: 39%

Synthesis of *(R)-N-(2-(N-(1-(hydroxyamino)-3-methyl-1-oxobutan-2-yl)-[1,1'-biphenyl]-4-ylsulfonamido)ethyl)benzamide* (LR32).

Silyl precursor **15** (0.354 mmol, 0.190 g) was dissolved in dry CH_2Cl_2 (6 mL) and TFA (57 mmol, 1.5 mL) was added dropwise at 0 °C. After 5 h of stirring the solvent was evaporated and the crude product was purified by trituration with *n*-hexane/Et_2O to afford **LR32** as a white solid.

M.p. 80-85 °C

Yield: 88%

^{1}H-NMR (DMSO-d_6) δ: 0.87-0.94 (m, 6H); 2.16-2.22 (m, 1H); 3.22-3.29 (m, 1H); 3.64-3.76 (m, 3H); 3.99-4.06 (m, 1H); 7.47-7.59 (m, 6H); 7.77-7.99 (m, 8H); 8.64 (s, 1H); 10.88

(s, 1H). **^{13}C-NMR** (acetone-d_6) δ: 19.52; 20.05; 41.06; 44.67; 64.46; 127.97; 128.21; 128.68; 129.01; 129.17; 129.77; 131.76; 135.60; 139.66; 139.95; 145.98; 167.14.

6.2.5 *Synthesis of (2R,12R)-3,11-bis([1,1'-biphenyl]-4-ylsulfonyl)-2,12-diisopropyl-7-oxo-3,6,8,11-tetraazatridecane-1,13-dioic acid (Scheme 4, compound CA11) and (2R,2'R)-2,2'-((azanediylbis(ethane-2,1-diyl))bis(([1,1'-biphenyl]-4-ylsulfonyl)azanediyl))bis(3-methylbutanoic acid) (Scheme 5, compound CA15).*

Synthesis of *(2R,12R)-di-tert-butyl 3,11-bis([1,1'-biphenyl]-4-ylsulfonyl)-2,12-diisopropyl-7-oxo-3,6,8,11-tetraazatridecane-1,13-dioate* (16) and *(2R,2'R)-di-tert-butyl 2,2'-((azanediylbis(ethane-2,1-diyl))bis(([1,1'-biphenyl]-4-ylsulfonyl)azanediyl))bis(3-methylbutanoate)* (17)[23].

Compound **12**, as free base (0.745 mmol, 0.0.322 g), was dissolved in anhydrous CH_2Cl_2 (6.4 mL) and 1,1'-carbonyldiimidazole (0.410 mmol, 0.066 g) was added to the solution. The reaction mixture was left under stirring at RT overnight. The crude was diluted with CH_2Cl_2 (15 mL) and the organic phase was washed with H_2O (2x5 mL), with brine (1x4 mL) and dried over Na_2SO_4. The crude was purified by flash chromatography, providing compounds **16** and **17**.

Chromatographic conditions: Eluent Exane 2: 1 EtOAc. Flash column: h = 17 cm; d = 2 cm.

Yield: 16 (31%); **17** (4%).

^{1}H-NMR ($CDCl_3$) δ: **16**: 0.95 (d, *J*= 6.4 Hz, 6H); 1.02 (d, *J*= 6.4 Hz, 6H); 1.25 (s, 18H); 2.04-2.17 (m, 2H); 3.30-3.50 (m, 6H); 3.75-3.85 (m, 2H); 3.97 (d, *J*= 10.4 Hz, 2H); 5.32 (br s, 2H); 7.40-7.58 (m, 10H); 7.65-7.69 (m, 4H); 7.88-7.92 (m, 4H). **^{13}C-NMR** ($CDCl_3$) δ: 19.54; 20.20; 28.05; 29.87; 41.52; 45.27; 66.94; 82.27; 127.39; 127.77; 128.28; 128.54; 129.14; 138.66; 139.52; 145.80; 158.00; 169.94.

^{1}H-NMR ($CDCl_3$) δ: **17**: 0.98 (d, *J*= 6.6 Hz, 12H); 1.30 (s, 18H); 2.00-2.20 (m, 2H); 3.43-3.57 (m, 4H); 3.64-3.73 (m, 4H); 4.03 (d, *J*= 10.1 Hz, 2H); 7.41-7.57 (m, 10H); 7.65-7.70 (m, 4H); 7.78 (br s, 1H); 7.85-7.89 (m, 4H). **^{13}C-NMR** ($CDCl_3$) δ: 20.24; 20.96; 28.72;

[23] K.Kaur, M.Jaina, S.I.Khanc, M.R. Jacobc, B.L. Tekwani c,S.Singhb, P.Singhb, R.Jaina. Amino acid, dipeptide and pseudodipeptide conjugates of ring-substituted 8-aminoquinolines: Synthesis and evaluation of antiinfective, b-haematininhibition and cytotoxic activities. J.Med. Chem. **2012,** 52**,** *230-241* [64].

30.23; 42.29; 44.73; 65.58; 83.77; 128.03; 128.56; 128.67; 129.41; 129.85; 138.79; 139.83; 146.95; 171.60.

Synthesis of *(2R,12R)-3,11-bis([1,1'-biphenyl]-4-ylsulfonyl)-2,12-diisopropyl-7-oxo-3,6,8,11-tetraazatridecane-1,13-dioic acid* (CA11*).*

To a solution of the *tert*-butyl ester **16** (0.100 mmol, 0.089 g,), in anhydrous CH_2Cl_2 (2 mL), at 0 °C in a H_2O/ice bath, under Argon, trifluoroacetic acid (11.4 mmol, 0.8 mL,) was added dropwise. The reaction mixture was left under stirring at 0 °C for 5h. The crude was diluited with CH_2Cl_2 (5 mL) and the organic solvent was evaporated at r.p.. The crude was triturated with Hexane and Et_2O, to give **CA11** as a white solid.

Yield: 62%

^{1}H-NMR ($CDCl_3$) δ: 0.75 (d, *J*= 5.5 Hz, 6H); 0.86 (d, *J*= 5.5 Hz, 6H); 1.85-2.10 (m, 2H); 3.15-3.49 (m, 6H); 3.50-3.70 (m, 2H); 3.99 (d, *J*= 10.4 Hz, 2H); 6.29 (br s, 2H); 7.39-7.45 (m, 6H); 7.52-7.55 (m, 4H); 7.61-7.65 (m, 4H); 7.83-7.87 (m, 4H). **^{13}C-NMR** ($CDCl_3$) δ: 19.67; 19.93; 29.89; 40.98; 44.85; 66.25; 127.39; 127.67; 128.12; 128.65; 129.14; 138.03; 139.19; 145.86; 159.51; 174.10.

Synthesis of (2R,2'R)-2,2'-((azanediylbis(ethane-2,1-diyl))bis(([1,1'-biphenyl]-4-ylsulfonyl)azanediyl))bis(3-methylbutanoic acid) (CA15).

To a solution of the *tert*-butyl ester **17** (0.0248 mmol, 0.021 g), in anhydrous CH_2Cl_2 (1 mL), at 0 °C in a H_2O/ice bath, under Argon, trifluoroacetic acid (2.82 mmol, 0.22 mL) was added dropwise. The reaction mixture was left under stirring at 0 °C for 5h. The crude was diluited with CH_2Cl_2 (5 mL) and the organic solvent was evaporated. The crude was triturated with Hexane and Et_2O to give a white solid.

Yield: 48%

^{1}H-NMR ($CDCl_3$) δ: 0.98 (d, *J*= 6.6 Hz, 12H); 2.00-2.20 (m, 2H); 3.43-3.57 (m, 4H); 3.64-3.73 (m, 4H); 4.03 (d, *J*= 10.1 Hz, 2H); 7.41-7.57 (m, 10H); 7.65-7.70 (m, 4H); 7.85-7.89 (m, 4H).

6.2.6 *Synthesis of (R)-4-([1,1'-biphenyl]-4-ylsulfonyl)-N-(2-(N-((R)-1-(hydroxyamino)-3-methyl-1-oxobutan-2-yl)-[1,1'-biphenyl]-4-ylsulfonamido)ethyl)-3-isopropyl-2-oxopiperazine-1-carboxamide (Scheme 5, compound CA14_2).*

Synthesis of *(R)-4-([1,1'-biphenyl]-4-ylsulfonyl)-N-((R)-8-([1,1'-biphenyl]-4-ylsulfonyl)-7-isopropyl-2,2,3,3-tetramethyl-6-oxo-4-oxa-5,8-diaza-3-siladecan-10-yl)-3-isopropyl-2-oxopiperazine-1-carboxamide* (18).

CA11 (0.113 mmol, 0.088 g) was dissolved in anhydrous CH_2Cl_2 (3 mL) and *O*-(*tert*-butyldimethyl-silyl) hydroxylamine (0.226 mmol, 0.033 g) and EDC (0.339 mmol, 0.065 g) were added to the solution. The reaction mixture was left under stirring at RT overnight. The crude was diluted with CH_2Cl_2 (5 mL) and the organic phase was washed with H_2O (2x4 mL) and dried over Na_2SO_4. The crude was purified by chromatography, obtaining the cyclic intermediate **18** as a yellow oil.

Chromatographic conditions: Eluent Exane 3: 1 EtOAc. Isolute column (Si II) 10 g.

Yield: 20%

^{1}H-NMR ($CDCl_3$) δ: 0.16 (s, 3H); 0.18 (s, 3H); 0.83-0.87 (m, 6H); 0.96 (s, 9H); 1.05 (d, *J*= 6.8Hz, 3H); 1.16 (d, *J*= 6.8 Hz, 3H); 2.04-2.20 (m, 2H); 3.10-3.24 (m, 1H); 3.36-3.74 (m, 7H); 4.11 (d, *J*= 8.8 Hz, 1H); 4.16-4.30 (m, 1H); 7.42-7.48 (m, 6H); 7.57-7.61 (m, 4H); 7.69-7.73 (m, 4H); 7.81-7.86 (m, 4H); 8.53 (s, 1H); 8.88 (t, 1H).

Synthesis of *(R)-4-([1,1'-biphenyl]-4-ylsulfonyl)-N-(2-(N-((R)-1-(hydroxyamino)-3-methyl-1-oxobutan-2-yl)-[1,1'-biphenyl]-4-ylsulfonamido)ethyl)-3-isopropyl-2-oxopiperazine-1-carboxamide* (CA14_2).

The compound **18** (0.0193 mmol, 0.020 g), was dissolved in anhydrous CH_2Cl_2 (1 mL), at 0 °C in a H_2O/ice bath, under Argon and trifluoroacetic acid (2.20 mmol, 0.17 mL) was added dropwise to the solution. The reaction mixture was left under stirring at 0 °C for 5h. The crude was diluited with CH_2Cl_2 (5 mL) and the organic solvent was evaporated. The crude product was triturated with Hexane and Et_2O, obtaining **CA14_2** as a white solid.

Yield: 60%

^{1}H-NMR (CD_3CN) δ: **^{1}H-NMR** (CD_3CN) δ: 0.68 (d, *J*= 6.8 Hz, 3H); 0.80 (d, *J*= 6.8 Hz, 3H); 0.99 (d, *J*= 6.8 Hz, 3H); 1.00 (d, *J*= 6.8 Hz, 3H); 2.01-2.19 (m, 2H); 3.14-3.36 (m, 2H); 3.40-3.47 (m, 2H); 3.51-3.61 (m, 3H); 3.73-3.97 (m, 1H); 4.05 (d, *J*= 9.1 Hz, 1H); 4.09-4.15 (m, 1H); 7.39-7.54 (m, 6H); 7.64-7.69 (m, 4H); 7.71-7.91 (m, 8H); 8.67 (t, *J*= 4.6 Hz; 1H); 9.27 (s, 1H). **^{13}C-NMR** (CD_3CN) δ: 19.31; 19.58; 19.79; 20.45; 28.64; 30.30;

31.92; 39.33; 41.30; 42.74; 44.23; 64.12; 67.15; 78.39; 79.10; 128.18; 128.44; 128.75; 128.93; 129.57; 130.07; 137.39; 139.15; 139.72; 139.83; 146.12; 146.64; 154.30; 167.44; 171.80.

Bibliography

[1] A.Pischinger,The Extracellular Matrix and Ground regulation. Basis for a Holistic Biological Medicine.**2007**. Edited by H.Heine.

[2] R.P.Mecham Editor. The extracellular Matrix: an overview.**2011**

[3] H. Nar, K.Werle, M.Bauer, H.Dollinger, B.Jung. Crystal structure of human macrophage elastasee in complex with a hydroxamic acid inhibitor. **2001**.

[4] R.A.Williamson, F.A. Marston, S. Angal, P. Koklitis, M. Panico, H.R. Morris, A.F. Carne, B.J.Smith, T.J. Harris, R.B. Freedman Disulphide bond assignment in human tissue inhibitor of metalloproteinases (TIMPS). *Biochemistry*, **1993**, 32. *4330–4337*.

[5] H. Nagase, J.F. Woessner. Matrix Metalloproteinases, *Jr. J Biol Chem*. **1999** Jul 30 ;274 (31): *21491-4*.

[6] R. Visse, H. Nagase. Matrix Metalloproteinases and Tissue Inhibitors of Metalloproteinases. Structure, Function and Biochemistry, *Circ. Res.* **2003**, 92, *827-839.*

[7] V.W. Yong, C. Power, P. Forsyth, D.R. Edwards, Metalloproteinases in biology and pathology of the nervous system, *Macmillan Magazines Ltd*, **2001**, *502-511*.

[8] P.J.Burke, P.D.Senter, D.W.Meyer, J.B.Miyamoto, M.Anderson, B.E.Toki, G.Manikumar, M.C.Wani, D.J.Kroll, S.C.Jeffrey. Design, Synthesis, and Biological Evaluation of Antibody-Drug Conjugates Comprised of Potent Camptothecin Analogues. *Bioconjugate Chem.* **2009,** 20, *1242–1250.*

[9] E.S. Olson, T. Jiang, T.A. Aguilera, Q.T. Nguyen, L.G. Ellies, M. Scadeng, R.Y. Tsien. Activatable cell penetrating peptides linked to nanoparticles as dual probes for *in vivo* fluorescence and MR imaging of proteases. www.pnas.org/cgi/doi/10.1073/pnas.0910283107

[10] C.R.Robinson, R.T.Sauer. Optimizing the stability of single-chain proteins by linker length and composition mutagenesis. *Proc. Natl. Acad. Sci.* **1998**. 95, *5929-5934*.

[11] L.Vera, C. Antoni, L. Devel, B. Czarny, E.C. Lajeunesse, A. Rossello, V. Dive, E.A. Stura. Screening using polymorphs for the crystallization of protein-ligand complexes. *Cryst. Growth & Des*. **2013**, 13, *1878-1888.*

[12] Vera, L.; Stura, E. A. Strategies for protein cryocrystallography. Cryst. Growth & Des. 2012.

[13] N.E.Chain, E.Saridakis, Protein crystallizzation: from purified protein to diffraction-quality crystal", *Nature Methods*, **2008**, 5, n.2, *147-153*.

[14] G Murphy, F. Willenbrock, R.V. Ward, M.I Cockett; D. Eaton, A. J.Docherty. The terminal domain of 72 kDa gelatinase A is not required for catalysis, but is essential for membrane activation and modulates interactions with tissue inhibitors of metalloproteinases. *Biochem J* **1992**, 238, *637-41*.

[15] L. Chung, D. Dinakarpandian, N. Yoshida, J.L.Lauer-Fields, G. B.Fields, R.Visse, H. Nagase, Collagenase unwinds triple-helical collagen prior to peptide bond hydrolysis. *Embo. J.* **2004**, 23, (15), *3020-30*.

[16] C. Fernandez-Catalan, W. Bode, R.Huber, D.Turk, J.J. Calvete, A.Lichte, H.Tschesche, K.Maskos, Crystal structure of the complex formed by the membrane type 1-matrix metalloproteinase with the tissue inhibitor of metalloproteinases-2, the soluble progelatinase A receptor. *Embo J* **1998**, 17, (17), *5238-48.*

[17] M.Whittaker,. C. D.Floyd, P. Brown, A. J.Gearing. Design and therapeutic application of matrix metalloproteinase inhibitors. *Chem Rev* **1999**, 99, (9), *2735-76.*

[18] Y. Herouy, D. Trefzer, U. Zimpfer, E. Schöpf, W. Vanscheidt, J. Norgauer. Matrix metalloproteinases and venous leg ulceration. N. *Eur. J.Dermatol*. **2000**, 10, *173-180*.

[19] Y. Herouy, A. E. May, G. Pornschlegel, C. Stetter, H. Grenz, K. T Preissner, E. Schöpf, J. Norgauer, W. Vanscheidt. Lipodermatosclerosis is characterized by elevated expression and activation of matrix metalloproteinases: implication for venous ulcer formation. J Invest Dermatol. **1998**, 111, *822-827*.

[20] Pontieri. Fisiopatologia generale, seconda edizione, PICCIN.

[21] Vera, L., Czarny, B., Georgiadis, D., Dive, V., Stura, E.A. (2011) Practical Use of Glycerol in Protein Crystallization. *Cryst. Growth & Des*. **2011**, 11, *2755–2762*.

[22] J.Numata, A.Juneja, J.D.Diestler, E.W.Knapp. Influence of Spacer–Receptor Interactions on the Stability of Bivalent Ligand–Receptor Complexes. J. Phys. Chem. B, **2012**, 116, *2595−2604.*

[23] A. McPherson. Preparation and analysis of protein crystals. **1982**. Krieger publ. Company.

[24] M. Kunitz, Crystalline inorganic pyrophosphatase isolated from bakers yeast. *J Gen Phys*, **1952**, 35 (3), *423-450*.

[25] W.B.J., Methods Enzymology, volume 511.

[26] The Stura CryoScreen KitTM MD1–61, “get better results from your crystals”, A novel multicomponent cryoprotectant kit. Developed and formulated by Dr. E. Stura & L.Vera at CEA Saclay, France to improve the diffraction of protein crystals by using mixtures of cryoprotectants. moleculardimensions.com

[27] S. Nénan, E. Boichot, V. Lagente, C. P. Bertrand, Macrophage elastase (MMP-12): a pro-inflammatory mediator?, *Mem Inst Oswaldo Cruz,* **2005**. 100, *167-172*.

[28] G. Kleina, E. Vellengab, M.W. Fraaijec, W.A. Kampsa, E.S.J.M. de Bonta. de Bont. The possible role of matrix metalloproteinase (MMP)-2 and MMP-9 in cancer, e.g. acute leukemia. Critical Reviews in Oncology/Hematology. **2004,** *5087–100*.

[29] G.R. Andersen, T.J. Koch, K. Dolmer, L. Sottrup-Jensen, J. Nyborg. Low resolution X-ray structure of human methylamine-treated alpha 2-macroglobulin. *J. Biol. Chem*. 1995, 270 (42), *25133–41*.

[30] A.W. Dodds, S.K. Law, The phylogeny and evolution of the thioester bondcontaining proteins C3, C4 and alpha 2-macroglobulin. *Immunol. Rev*. **1998**, 166: *15–26.*

[31] M.D. Sternlicht, Z. Werb, How matrix metalloproteinases regulate cell behavior. *Annu Rev Cell Dev Biol*. **2001**, 17*, 463–516.*

[32] V. Pelmenschikov, P.E.M. Siegbahn, Catalytic Mechanism of Matrix Metalloproteinases: Two-Layered ONIOM Study, *Inorg. Chem*. **2002**, 41, *5659-5666*.

[33] M.Whittaker, C.D.Floyd, P.Brown, A.J.H. Gearing, Design and Therapeutic Application of Matrix Metalloproteinase Inhibitors *Chem. Rev*. **1999**, 99, *2735-2776*.

[34] H.Nagase, R.Visse, G.Murphy, Structure and function of matrix metalloproteinases and TIMPs. *Cardiovasc. Res*., **2006**, 69, *562-573.*

[35] M.D Carrithersl, M.R Lerner.Synthesis and characterization of bivalent peptide ligands targeted to G-protein-coupled receptors. *Chem Biol*. **1996,** 7, *537-42*.

[36] G. Loidl, M. Groll, H-Ju. Bivalency as a principle for proteasome inhibition *Biochemistry*. **1999**. 96, *5418–5422*.

[37] A.Rossello, E.Nuti, C.Antoni, L.Vera, L.Rosalia, E.Da Pozzo, C.Giacomelli, B.Costa,E.A. Stura, E.Orlandini, S.Nencetti, C.Martini V.Dive. Powerful twin carboxylic inhibitors for MMP homodimerization. Gordon Research Conference on Matrix Metalloproteinases: Crucial Components of Molecular Networks and Disease Pathways, Renaissance Tuscany. Il Ciocco Resort, Barga (LU), Italy, May 19-24, **2013**.

[38] R.Chirco, X. W. Liu, K. K. Jung, H. R. Choi Kim. Novel functions of TIMPs in cell signaling. *Cancer Metastasis Rev*, **2006**, *25*, 99-13.

[39] http://www.iycr2014.org/

[40] E. Nuti, T. Tuccinardi, A. Rossello, Matrix Metalloproteinase Inhibitors: New Challenges in the Era of Post Broad-Spectrum Inhibitors. *Current Pharmaceutical Design*, **2007**, 13, *2087-2100*.

[41] C. Antoni, L.Vera, M. P Catalani, B.Czarny, E. Cassar-Lajeunesse, E.Nuti, A.Rossello,

V.Dive, E. A. Stura, Crystallization with bi-functional ligands. *J. Struct. Biol.* **2013**, 182, *246-254.*

[42] F. Manello. What does matrix metalloproteinase-1 expression in patients with breast cancer really tell us?. *BMC Medicine*, **2011**.

[43] http://hamptonresearch.com/documents/product/hr003056_2-132_user_guide.pdf

[44] B.G. Rao. Recent developments in the design of specific matrix metalloproteinase inhibitors aided by structural and computational studies. *Curr. Pharm. Des*. **2005**, 11, *295–322*.

[45] D.R. Shalinsky, J. Brekken, H. Zou, C.D. McDermott, P. Forsyth, D. Edwards, S. Margosiak, S. Bender, G. Truitt, A. Wood, N.M. Varki, K. Appelt, Broad antitumor and antiangiogenic activities of AG3340, a potent and selective MMP inhibitor undergoing advanced oncology clinical trials, *Ann. N.Y. Acad. Sci*. **1999** , 878, *236–270*.

[47] N.G.Li, Z.H.Shi, Y.P Tang, Z.J. Wang, S.L.Song, L.H.Qian, D.W.Qian, J.A. Duan. New hope for the treatment of osteoarthritis through selective inhibition of MMP-13. *Curr. Med. Chem.* **2011**, 18, *977-1001*.

[48] *a)* Fujisawa, T.; *et al*. Design and Synthesis of Carboxylate Inhibitors for Matrix Metalloproteinases, *Chem.Pharm. Bull*. **2001**, 49, *1272-1279*. b) Hajduk, P.J. *et al*. NMR-Based Modification of Matrix Metalloproteinase Inhibitors with Improved Bioavailability, *J. Med. Chem.* **2002**, 26, *5628-5639*.

[49] Jacobsen, F. E.; *et al*. The Design of Inhibitors for Medicinally Relevant Metalloproteins, *Chem. Med. Chem.* **2007**, 2, *152 –171*.

[50] *a)* Bernardo, M.M.; *et al*. Enzyme catalysis and regulation**,** *J.Biol. Chem*.**2002**, 277, *11201-11207*. *b)* Rosenblum, G.; *et al*. Protein Structure and Folding , *J. Biol. Chem*., **2003**, 278, *27009-27015*.

[51] Casalini, F.; *et al.* Synthesis and Preliminary Evaluation in Tumor Bearing Mice of New ^{18}F-Labeled Arylsulfone Matrix Metalloproteinase Inhibitors as Tracers for Positron emission Tomography, *J. Med. Chem.* **2013**, 56, *2676−2689.*

[52] Schröder, J. *et al* Structure-Based Design and Synthesis of Potent Matrix Metalloproteinase Inhibitors Derived from a 6H-1,3,4-Thiadiazine Scaffold. *J. Med. Chem*. **2001,** 44, *3231-3243*.

[53] J.A. Jacobsen, Jody L. Major Jourden, Melissa T. Miller, Seth M. Cohen. To bind zinc or not to bind zinc: An examination of innovative approaches to improved metalloproteinase inhibition. *Biochimica et Biophysica Acta*, **2010,** 1803**,** *72–94.*

[54] Y. Hu, J.S. Xiang, M.J. DiGrandi, X. Du, M. Ipek, L.M. Laakso, J. Li, W. Li, T.S.

Rush, J. Schmid, J.S. Skotnicki, S. Tam, J.R. Thomason, Q. Wang, J.I. Levin. Potent, selective, and orally bioavailable matrix metalloproteinase-13 inhibitors for the treatment of osteoarthritis, *Bioorg.Med. Chem*. **2005**, 13, *6629–6644*.

[55] A. Rossello, E. Nuti, P. Carelli, E. Orlandini, M. Macchia, S. Nencetti, M. Zandomeneghi, F. Balzano, G.U. Barretta, A. Albini, R. Benelli, G. Cercignani, G. Murphy, A. Balsamo. N-i-Propoxy-N-biphenylsulfonylaminobutylhydroxamic acids as potent and selective inhibitors of MMP-2 and MT1-MMP, *Bioorganic Med. Chem. Lett*. **2005**, 15 *1321–1326*.

[56] M. Ilies,L. Di Costanzo, M.L. North, J.A. Scott, D. W. Christianson. 2-Aminoimidazole Amino Acids as Inhibitors of the Binuclear Manganese Metalloenzyme Human Arginase I. *J. Med. Chem.* **2010**, 53, *4266–4276.*

[57] W. Li, J. Li, Y. Wu, J. Wu, R. Hotchandani, K. Cunningham, I. McFadyen, J. Bard, P.Morgan, F. Schlerman, X. Xu, S. Tam, S.J. Goldman, C. Williams, J. Sypek, T.S.Mansour, A selective matrix metalloprotease 12 inhibitor for potential treatmentof chronic obstructive pulmonary disease (COPD): discovery of (S) -2- (8-ethoxycarbonylamino) dibenzo [b,d] furan-3-sulfonamido) -3-methylbutanoic acid (MMP408), *J. Med. Chem.* **2009**, 52, *1799–1802.*

[58] M.B. Onaran, A.B. Comeau, C.T. Seto, Squaric acid-based peptidic inhibitors of matrix metalloprotease-1, J. Org. Chem. **2005**, 70, *10792–10802*.

[59] F.E. Jacobsen, J.A. Lewis, S.M. Cohen, A new role for old ligands: discerning chelators for zinc metalloproteinases, *J. Am. Chem. Soc*. **2006**, 128, *3156–3157*.

[60] D.T. Puerta, J.A. Lewis, S.M. Cohen, New beginnings for matrix metalloproteinase inhibitors: identification of high-affinity zinc-binding groups, *J. Am. Chem. Soc*. **2004**, 126, *8388–8389*.

[61] Y. Yamazaki, M. Savva, H.K. Kleinman, S. Oka, M. Mokotoff. Enhanced cleavage of diaminopimelate - containing isopeptides by leucine aminopeptidase and matrix metalloproteinases in tumors: application to bioadhesive peptides. J. Peptide Res. **1999**, 53, *177-187*.

[62] K.Soai, A.Ookawa. Mixed Solvents Containing Methanol as Useful Reaction Media for Unique Chemoselective Reductions with Lithium Borohydride. *J. Org. Chem*. **1986**, 51, *4000-4005*.

[63] A.Carotti, A.Carrieri, S.Cellamare, F.P. Fanizzi, E.Gavuzzo, F.Mazza. Extended Form of a Retro–Inverso Peptide Stabilized by _-Sheet Unidirectional H-Bonds: Crystallographic and NMR Evidence. *Biopol.(Peptide Science)*, **2001,** 60, *322–332*.

[64] K.Kaur, M.Jaina, S.I.Khanc, M.R. Jacobc, B.L. Tekwani c,S.Singhb, P.Singhb, R.Jaina. Amino acid, dipeptide and pseudodipeptide conjugates of ring-substituted 8-aminoquinolines: Synthesis and evaluation of antiinfective, b-haematininhibition and cytotoxic activities. J.Med. Chem. **2012,** 52**,** *230-241*.

[65] C.Exon, T.Gallagher, P.Magnus. Indole-2,3-quinodimethanes: A new Strategy for the Synthesis of Tetracyclic Systems of Indole Alkaloids. *J. Am. Chem. SOC.,* ***I983***, 105, *4739-4749.*

[66] Prikk K, Maisi P, Pirila E, Sepper R, Salo T, Wahlgren J, et al. In vivo collagenase 2 (MMP-8) expression by human bronchial epithelial cells and monocytes/macrophages in bronchiectasis. J *Pathol.***2001**, 8, *194-232*.

[67] Kong MY, Gaggar A, Li Y, Winkler M, Blalock JE, Clancy JP. Matrix metalloproteinase activity in pediatric acute lung injury. *Int J Med Sci.* **2009**, 6, *9-17*.

[68] Djuric T, Zivkovic M, Stankovic A, Kolakovic A, Jekic D, Selakovic V. Plasma levels of matrix metalloproteinase-8 in patients with carotid atherosclerosis.*J Clin Lab Anal* **2010**, 24, *246–251*.

[69] Turu MM, Krupinski J, Catena E, Rosell A, Montaner J, Rubio J, et al. Intraplaque MMP-8 levels are increased in asymptomatic patients with carotid plaque progression on ultrasound. *Atherosclerosis*. **2006**, 18, *161–9*.

[70] Pirila E, Ramamurthy NS, Sorsa T, Salo T, Hietanen J, Maisi P. Gelatinase A (MMP-2), collagenase-2 (MMP-8), and laminin-5 gamma2-chain expression in murine inflammatory bowel disease (ulcerative colitis). *Digest Dis Sci* **2003**, 48, *93–8*.

[71] Akhavani MA, Madden L, Buysschaert I, Sivakumar B, Kang N, Paleolog EM. Hypoxia upregulates angiogenesis and synovial cell migration in rheumatoid arthritis. *Arthritis Res Ther* **2009**, *11*, *64*.

[72] Rautelin HI, Oksanen AM, Veijola LI, Sipponen PI, Tervahartiala TI, Sorsa TA, et al. Enhanced systemic matrix metalloproteinase response in Helicobacter pylori gastritis. *Ann Med* **2009**, 41, *208–15*.

[73] E.Dejonckheere, R.E.Vandenbroucke, C.Liber Matrix metalloproteinase8 has a central role in inflammatory disorders and cancer progression. *Cytokine & Growth Factor Reviews*, **2011**, 22, *73–81*.

[74] Jr GN.Smith, E.A .Mickler, KK .Payne, J. Lee, M.Duncan, J.Reynolds, et al. Lung transplant metalloproteinase levels are elevated prior to bronchiolitis obliterans syndrome. *Am J Transplant* **2007**, 7, *1856–61*.

[75] J.K.Rybakoski. MatrixMetalloproteinase-9 (MMP9) - A Mediating Enzyme in

Cardiovascular Disease, Cancer, and Neuropsychiatric Disorders**.** *Cardiovascular Psychiatry and Neurology*, **2009**, *7 pages*.

[76] P. Welsh, P. H. Whincup, O. Papacosta, et al., Serum matrix metalloproteinase-9 and coronary heart disease: a prospective study in middle-aged men, *QJM,* **2008**, 101 n.10, *785-791*.

[77] P. Garvin, L. Nilsson, J. Carstensen, L. Jonasson, and M. Kristenson, Plasma levels of matrix metalloproteinase-9 are independently associated with psychosocial factors in a middle-aged normal population, *Psychosomatic Medicine,* **2009**, 71, *292–300*.

[78] M. L. Muzzio, V. Miksztowicz, F. Brites, et al. Metalloproteases 2 and 9, Lp-PLA(2) and lipoprotein profile in coronary patients. *Archives of Medical Research,* **2009**. 40, *48-53*.

[79] K. Sakata, K. Shigemasa, N.Nagai, and K.Ohama, Expression of matrix metalloproteinases (MMP-2, MMP-9, MT1-MMP) and their inhibitors (TIMP-1, TIMP-2) in common epithelial

tumors of the ovary, *International Journal of Oncology*, **2000**, 17, n. 4, *673-681*.

[80] W.Li, J.Li, Y.Wu, J.Wu, R.Hotchandani, K.Cunningham, I.McFadyen, J. Bard, P.Morgan, F.Schlerman, X.Xu, S.Tam, S.Goldman, C.Williams, J.Sypek, T.S. Mansour. A Selective Matrix Metalloprotease 12 Inhibitor for Potential Treatment of Chronic Obstructive Pulmonary Disease (COPD): Discovery of (*S*)- 2-(8-(Methoxycarbonylamino)dibenzo[*b*,*d*]furan- 3-sulfonamido)-3-methylbutanoic acid (MMP408). *J. Med. Chem.* **2009,** 52, *1799–1802.*

[81] Shapiro, S. D.; Kobayashi, D. K.; Ley, T. J. Cloning and characterization of a unique elastolytic metalloproteinase produced by human alveolar macrophages. *J. Biol. Chem.* **1993**, 26, *23824–23829*.

[82] http://atlasgeneticsoncology.org/Genes/MMP9ID41408ch20q11.html

[83] K. Sakata, K. Shigemasa, N.Nagai, and K.Ohama. Expression of matrix metalloproteinases (MMP-2, MMP-9, MT1-MMP) and their inhibitors (TIMP-1, TIMP-2) in common epithelial tumors of the ovary. *International Journal of Oncology*, **2000**. 17, *673–681*.

[84] N. Odajima, T. Betsuyaku, Y. Nasuhara, H. Inoue, K. Seyama, and M. Nishimura, Matrix metalloproteinases in blood from patients with LAM. *Respiratory Medicine*, **2009**, 103, *124–129*.

[85] V.W. Yong, R. K. Zabad, S. Agrawal, A. Goncalves DaSilva, L. M. Metz. Elevation of matrix metalloproteinases (MMPs) in multiple sclerosis and impact of immunomodulators,

Journal of the Neurological Sciences, vol. 259, no. 1-2, pp. 79–
84, 2007.

[86] Y. Benesova, A. Vasku, H. Novotna, *et al*. Matrix metalloproteinase-9 and matrix metalloproteinase-2 as biomarkers of various courses in multiple sclerosis. *Multiple Sclerosis,* **2009**, 15, *316–322*.

[87] P. Garvin, L. Nilsson, J. Carstensen, L. Jonasson, and M. Kristenson. Circulating matrix metalloproteinase-9 is associated with cardiovascular risk factors in a middle-aged normal population. *PLoS ONE,* **2008**, article e1774.

[88] P. Garvin, L. Nilsson, J. Carstensen, L. Jonasson, and M. Kristenson. Plasma levels of matrix metalloproteinase-9 are independently associated with psychosocial factors in a middle-aged normal population. *Psychosomatic Medicine,* **2009**, 71, *292-300*.

[89] G. Murphy, V. Knauper. Relating matrix metalloproteinase structure to function: why the ‘‘hemopexin’’ domain? *Matrix Biol* **1997**, 15, *511–8*.

[90] C.A. Owen, Z. Hu, C. Lopez-Otin, S.D. Shapiro. Membrane-bound matrix metalloproteinase- 8 on activated polymorphonuclear cells is a potent, tissue inhibitor of metalloproteinase-resistant collagenase and serpinase. *J Immunol*, **2004**, 172, *7791–803*.

[91] Devarajan P, Mookhtiar K, Van Wart H, Berliner N. Structure and expression of the cDNA encoding human neutrophil collagenase. *Blood,* **1991**, 77, *2731–8*.

[92] P. Van Lint, C. Libert. Matrix metalloproteinase-8: cleavage can be decisive. *Cytokine Growth Factor Rev.* **2006,** 17, *217–23*.

[93] K.A. Hasty, J.J. Jeffrey, M.S. Hibbs, H.G. Welgus. The collagen substrate specificity of human neutrophil collagenase. *J Biol Chem* **1987**, 262, *10048–52*.

[94] H. Saari, T. Sorsa, O. Lindy, K. Suomalainen, S. Halinen, Y.T. Konttinen. Reactive oxygen species as regulators of human neutrophil and fibroblast interstitial collagenases. *Int J Tissue React* **1992**, 14, *113–20*.

[95] S.E. Fligiel, T. Standiford, H.M. Fligiel, D. Tashkin, R.M. Strieter, R.L. Warner, *et al*. Matrix metalloproteinases and matrix metalloproteinase inhibitors in acute lung injury. *Hum Pathol* **2006**, 37, *422–30.*

[96] M.P Herman, G.K. Sukhova, P. Libby, N. Gerdes, N. Tang, D.B. Horton, *et al*. Expression of neutrophil collagenase (matrix metalloproteinase-8) in human atheroma: a novel collagenolytic pathway suggested by transcriptional profiling. *Circulation,* **2001**, 104, *1899–904*.

[97] K.J. Molloy, M.M. Thompson, J.L. Jones, E.C. Schwalbe, P.R. Bell, A.R. Naylor, et *al*. Unstable carotid plaques exhibit raised matrix metalloproteinase-8 activity. *Circulation*

2004, 110, *337–43*.

[98] J.A. Curci, S. Liao, M.D. Huffman, S.D. Shapiro, R.W. Thompson. Expression and localization of macrophage elastase (matrix metalloproteinase-12) in abdominal aortic aneurysms. J *Clin Invest***, 1998**, 102, *1900-1910.*

[99] U. Saarialho-Kere, E. Kerkela, L. Jeskanen, T. Hasan, R. Pierce, B. Starcher, R. Raudasoja, A. Ranki, A. Oikarinen, M. Vaalamo. Accumulation of matrilysin (MMP-7) and macrophage metalloelastase (MMP-12) in actinic damage. *J Invest Dermatol*, **1999**, 113, *664-672*.

[100] S. Matsumoto, T. Kobayashi, M. Katoh, S. Saito, Y. Ikeda, M. Kobori, Y. Masuho, T. Watanabe. Expression and localization of matrix metalloproteinase-12 in the aorta of cholesterol-fed rabbits: relationship to lesion development. Am J Pathol **1998**, 153, *109-119.*

[101] E. Kerkela, T. Bohling, R. Herva, J.A. Uria, U. Saarialho-Kere. Human macrophage metalloelastase (MMP-12) expression is induced in chondrocytes during fetal development and malignant transformation. *Bone* **2001**, 29, *487-493*.